Contents

1. Introduction: Conservation equations, material properties

Consider a material element $d^3\underset{\sim}{x}$ whose position vector in a Cartesian inertial frame is $\underset{\sim}{x}(t)$, where t is the time. (Restrict discussion to nonrelativistic effects). The material element is deformable and experiences stresses that may be related to e.g. the rate of deformation. Let the velocity field be $\underset{\sim}{u}(\underset{\sim}{x},t)$. The infinitesimal motion of a fluid element may be decomposed into a translation, a rotation and a deformation. In fluids the frictional stresses depend most strongly on the rate of deformation which may be expressed as

$$\underset{\approx}{D} = \frac{1}{2}\left[\text{grad}\,\underset{\sim}{u} + (\text{grad}\,\underset{\sim}{u})^T\right]$$

$$= \begin{bmatrix} \frac{\partial u}{\partial x} & \frac{1}{2}\left(\frac{\partial u}{\partial y}+\frac{\partial v}{\partial x}\right) & \frac{1}{2}\left(\frac{\partial u}{\partial z}+\frac{\partial w}{\partial x}\right) \\ \frac{1}{2}\left(\frac{\partial u}{\partial y}+\frac{\partial v}{\partial x}\right) & \frac{\partial v}{\partial y} & \frac{1}{2}\left(\frac{\partial v}{\partial z}+\frac{\partial w}{\partial y}\right) \\ \frac{1}{2}\left(\frac{\partial u}{\partial z}+\frac{\partial w}{\partial x}\right) & \frac{1}{2}\left(\frac{\partial v}{\partial z}+\frac{\partial w}{\partial y}\right) & \frac{\partial w}{\partial z} \end{bmatrix} \quad (1)$$

where $\underset{\sim}{u} = (u, v, w)$ and $\underset{\sim}{x} = (x, y, z)$ are the Cartesian components of $\underset{\sim}{u}$ and $\underset{\sim}{x}$

Note that the deformation rate is symmetric. Restrict discussion to situations where the fluid behaves to a good approximation like a Newtonian one. I.e. the frictional stress depends linearly and homogeneously on the deformation rate. Dividing the stress tensor $\underset{\approx}{S}$ into the isotropic pressure and the frictional stress $\underset{\approx}{T}$

$$\underset{\approx}{T} = \underset{\approx}{S} + \underset{\approx}{I}\, p = \begin{bmatrix} \sigma_x & \tau_{xy} & \tau_{xz} \\ \tau_{xy} & \sigma_y & \tau_{yz} \\ \tau_{xz} & \tau_{yz} & \sigma_z \end{bmatrix}, \qquad (2)$$

this linear dependence of $\underset{\approx}{T}$ on $\underset{\approx}{D}$ implies that

$$\underset{\approx}{T} = 2\eta \underset{\approx}{D} + \left(\eta_d - \tfrac{2}{3}\eta\right) \underbrace{\operatorname{div} \underset{\sim}{u}}_{(=\operatorname{tr}\underset{\approx}{D})}\, \underset{\approx}{I} \qquad (3)$$

which is the constitutive equation of the Newtonian fluid model. The constants η and $\eta_v = \eta_d - \frac{2}{3}\eta$ are called shear viscosity and bulk viscosity. Note that the stress in equation (2) has been written as a symmetric matrix, which is consistent with (1) and (3).

<u>Example</u> : <u>Simple shear flow</u>

$$\underset{\sim}{u} = (u, 0, 0) = (ky, 0, 0), \quad \operatorname{div} \underset{\sim}{u} = 0$$

Potential vortex:

$$v_\theta = \frac{\Gamma}{2\pi r}$$

$$u = -\frac{\Gamma}{2\pi r}\sin\theta = -\frac{\Gamma}{2\pi}\frac{y}{x^2+y^2}$$

$$v = \qquad\qquad + \frac{\Gamma}{2\pi}\frac{x}{x^2+y^2}$$

$$\underset{\sim}{D} = \frac{\Gamma}{2\pi(x^2+y^2)^2}\begin{bmatrix} 2yx & y^2-x^2 & 0 \\ y^2-x^2 & -2yx & 0 \\ 0 & 0 & 0 \end{bmatrix}$$

if friction not zero:

$$\underset{\sim}{T} = 2\eta \underset{\sim}{D} = \frac{\eta\Gamma}{\pi(x^2+y^2)^2}\begin{bmatrix} & & \\ & & \\ & & \end{bmatrix}$$

note: $\mathrm{tr}\,\underset{\sim}{D} = 0$ continuity

$$\underset{\approx}{D} = \begin{bmatrix} 0 & \frac{k}{2} & 0 \\ \frac{k}{2} & 0 & 0 \\ 0 & 0 & 0 \end{bmatrix}$$

$$\underset{\approx}{T} = 2\eta \underset{\approx}{D} = \begin{bmatrix} 0 & \eta k & 0 \\ \eta k & 0 & 0 \\ 0 & 0 & 0 \end{bmatrix}$$

i.e. $\tau_{xy} = \tau_{yx} = \eta \frac{\partial u}{\partial y} = \eta k$.

The conservation of momentum may be written as

$$\rho \frac{D\underset{\sim}{u}}{Dt} = \operatorname{div} \underset{\approx}{S} + \rho \underset{\sim}{f} \qquad (4)$$

where $\rho(\underset{\sim}{x}, t)$ is the density field, and $\underset{\sim}{f}$ is the body force per unit mass. With the above constitutive equation (3) it becomes

$$\rho \frac{D\underset{\sim}{u}}{Dt} = -\operatorname{grad} p + \operatorname{div}\left\{2\eta \underset{\approx}{D} + \eta_v \operatorname{div} \underset{\sim}{u} \underset{\approx}{I}\right\} + \rho \underset{\sim}{f} \qquad (5)$$

(Navier-Stokes equation)

If the fluid may be considered to be in local thermodynamic equilibrium everywhere, at the temperature $T(\underset{\sim}{x}, t)$, the quantities η_v and η may be written

as state variables

$$\eta = \eta(p, \rho) \quad , \quad \eta_v = \eta_v(p, \rho)$$

just like $$T = T(p, \rho) . \qquad (6)$$

The thermodynamic equilibrium state is defined by the thermal (6) and caloric equations of state

$$h = h(p, \rho) \qquad (7)$$

where h is the specific enthalpy. In most of the discussion, these two equations will be considered in the form they take for an ideal gas, i.e.

$$T = \frac{p}{\rho R} \qquad (8)$$

$$h = \frac{c_p}{R} \cdot \frac{p}{\rho} \qquad (9)$$

If temperature gradients are significant in the flow, heat transfer may not be neglected. In the following we restrict discussion to situations where the rate of heat transfer per unit area (heat flux vector) is given by the Fourier law

$$\underset{\sim}{q} = -k \operatorname{grad} T , \qquad (10)$$

where k is the thermal conductivity.

These quantities are needed in the general form of the equation for the conservation of energy

$$\rho \frac{Dh_0}{Dt} = \frac{\partial p}{\partial t} + \operatorname{div}(\underset{\approx}{T} \cdot \underset{\sim}{u}) + \rho(\underset{\sim}{u} \cdot \underset{\sim}{f}) - \operatorname{div} \underset{\sim}{q} \qquad (11)$$

where $h_0 = h + u^2/2$. Equation (11) may be rewritten in the form

$$T\rho \frac{Ds}{Dt} = \Phi - \operatorname{div} \underset{\sim}{q} \qquad (12)$$

where s is the specific entropy and Φ is the dissipation function

$$\Phi = \operatorname{tr}(\underset{\approx}{T} \cdot \underset{\approx}{D}) \qquad (13)$$

$\nabla(\underset{\sim}{u} \cdot \underset{\approx}{T}) - (\underset{\sim}{u} \cdot \nabla \underset{\approx}{T})$

by invoking the Gibbs relation

$$T ds = dh - \frac{1}{\rho} dp.$$

The equation for the conservation of mass may be written ~~for~~ in the absence of relative species diffusion as

$$\frac{\partial \rho}{\partial t} + \operatorname{div}(\rho \underset{\sim}{u}) = 0. \qquad (14)$$

In terms of the discussion so far, we may summarize:

Equations:

$$\frac{\partial \rho}{\partial t} + \operatorname{div}(\rho \underset{\sim}{u}) = 0 \qquad \text{C}$$

$$\rho \frac{D\underset{\sim}{u}}{Dt} = \operatorname{div} \underset{\approx}{T} - \operatorname{grad} p + \rho \underset{\sim}{f} \qquad \text{M}$$

$$T\rho \frac{Ds}{Dt} = \Phi - \operatorname{div} \underset{\sim}{q} \qquad \text{E}$$

$$T\,ds = dh - \frac{1}{\rho}\,dp \qquad \text{G}$$

$$\Phi = \operatorname{tr}(\underset{\approx}{T}\,\underset{\approx}{D})$$

$$\left.\begin{aligned} T &= p/(\rho R) \\ h &= \frac{c_p}{R}\frac{p}{\rho} \end{aligned}\right\} \text{S}$$

$$\underset{\sim}{q} = -k \operatorname{grad} T \qquad \text{F}$$

$$\underset{\approx}{T} = 2\eta \underset{\approx}{D} + \eta_v (\operatorname{div} \underset{\sim}{u}) \underset{\approx}{I} \qquad \text{N}$$

$$\underset{\approx}{D} = \frac{1}{2}\left(\operatorname{grad} \underset{\sim}{u} + (\operatorname{grad} \underset{\sim}{u})^T\right)$$

Material properties

ρ, mass density $[ML^{-3}]$
R, specific gas constant $[L^2T^{-2}\theta^{-1}]$
c_p, spec. heat constant pr. $[L^2T^{-2}\theta^{-1}]$
η, shear viscosity $[ML^{-1}T^{-1}]$
η_v, bulk viscosity $[ML^{-1}T^{-1}]$
k, thermal conductivity $[ML^3T^{-3}\theta^{-1}]$

2. Introduction: Dimensionless numbers, the simplest case.

In the case of the simplest nontrivial geometry of the boundaries of the flow, these boundaries may be characterized by a single length scale L. The kinematics of the flow field may, in the simplest case, be described in terms of a characteristic velocity U and a characteristic time t_0, typefying the movement of the boundaries. In the simple case when the gas is thermally and calorically perfect, the reservoir enthalpy h_0 and the enthalpy of the boundaries may be characterized by the reservoir temperature T_0 and the boundary temperature T_W. With the addition of the material properties listed on p 6, any ~~materi~~ quantity Q may be expressed formally as a function of the independent variables:

$$Q = Q\Big(\underbrace{L}_{\text{geometry b.c's}}, \underbrace{U, t_0}_{\text{kinematic b.c's}}, \underbrace{T_0, T_W}_{\text{thermo b.c's}}, \underbrace{\rho, \eta, \eta_v, R, C_p, k}_{\text{material}}\Big) \quad (2.1)$$

If, for example, Q is the length of

a separation bubble behind a sphere we may use dimensional analysis to reduce the list of dimensional variables to a shorter list of dimensionless

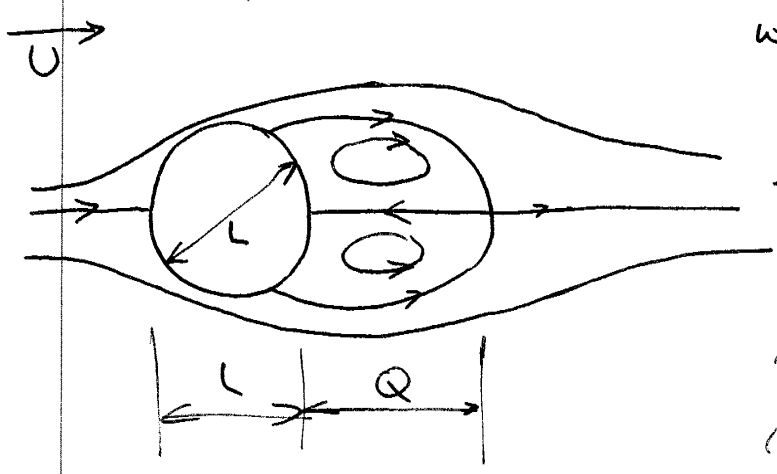

variables:

$$\frac{Q}{L} = f\left(\frac{\rho L U}{\eta}, \frac{\eta}{\eta_v}, \frac{U}{a}, \gamma, \frac{L}{U t_0}, \frac{T_w}{T_0}, \frac{\eta C_p}{k}\right) \quad (2.2)$$

where $a = \sqrt{\frac{\gamma p}{\rho}}$, $\gamma = \frac{C_p}{C_p - R}$

or

$$\frac{Q}{L} = f\left(Re, \frac{\eta_v}{\eta}, M, \gamma, St, \frac{T_w}{T_0}, Pr\right) \quad (2.3)$$

where (2.3) and (2.2) define the Reynolds number Re, Mach number M, Strouhal number St and Prandtl number Pr. As may be seen, even in this simple case, seven independent dimensionless variables enter the problem. We therefore restrict the discussion even further, by restricting to steady flow at constant density and temperature with $U \ll a$.

In this degenerate case $M=0$, $\eta_\infty/\eta = \text{const}$. $\gamma = \text{const}$, $St = 0$, $T_W/T_0 = 1$, $Pr = \text{const}$ and (2.3) reduces to

$$\frac{Q}{L} = f_1(Re). \qquad (2.4)$$

The function f_1 may, for example, be determined experimentally if our assumptions are valid in a reasonable range.

Let us illustrate this process by considering photographs of flow over a circular cylinder at small Reynolds number. (see next pages) These photographs have been copied from the book of Milton vanDyke: "An album of fluid motion" which is an extremely useful reference for many fields of fluid mechanics.

The photos show that at $Re \to 0$, $Q/L = 0$; in fact there is a threshold of $Re \doteq 5$ below which $Q/L = 0$; as Re is increased beyond 5, Q/L increases approximately linearly, so that the function f_1 may be described roughly by

$$\frac{Q}{L} = 0, \quad 0 < Re < 5; \quad \frac{Q}{L} = 0.06(Re-5), \quad Re > 5$$

At very large Re, the flow is not steady, (even if the boundaries are steady)

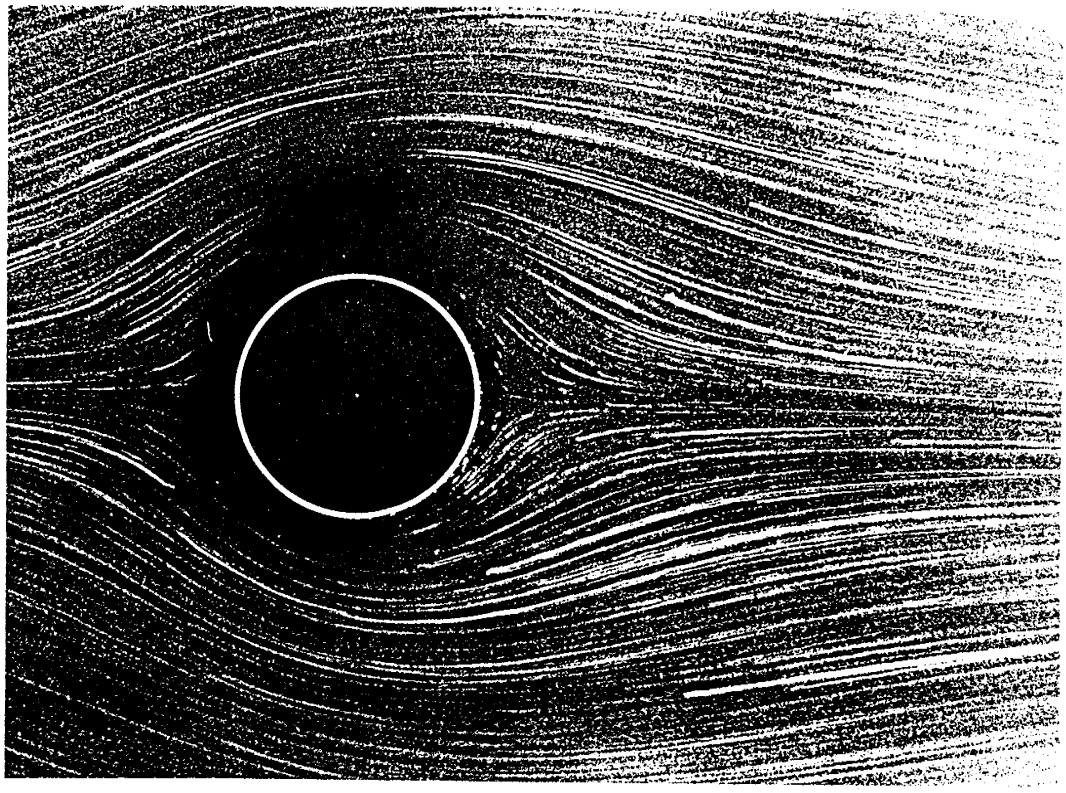

24. Circular cylinder at $R=1.54$. At this Reynolds number the streamline pattern has clearly lost the fore-and-aft symmetry of figure 6. However, the flow has not yet separated at the rear. That begins at about $R=5$, though the value is not known accurately. Streamlines are made visible by aluminum powder in water. *Photograph by Sadatoshi Taneda*

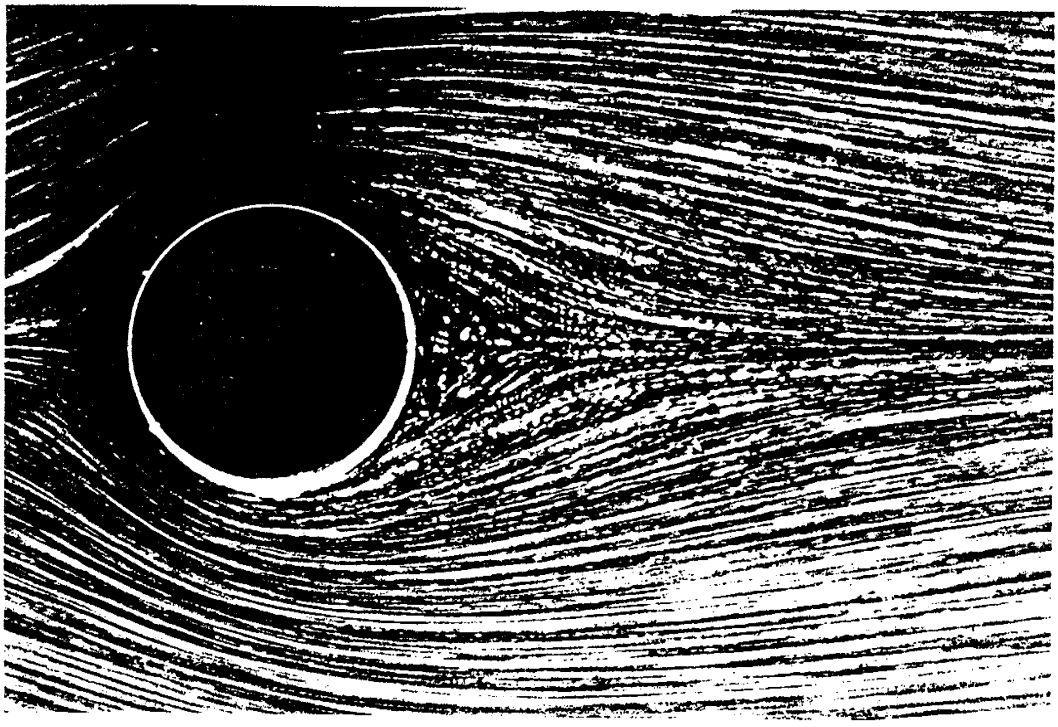

40. Circular cylinder at $R=9.6$. Here, in contrast to figure 24, the flow has clearly separated to form a pair of recirculating eddies. The cylinder is moving through a tank of water containing aluminum powder, and is illuminated by a sheet of light below the free surface. Extrapolation of such experiments to unbounded flow suggests separation at $R=4$ or 5, whereas most numerical computations give $R=5$ to 7. *Photograph by Sadatoshi Taneda*

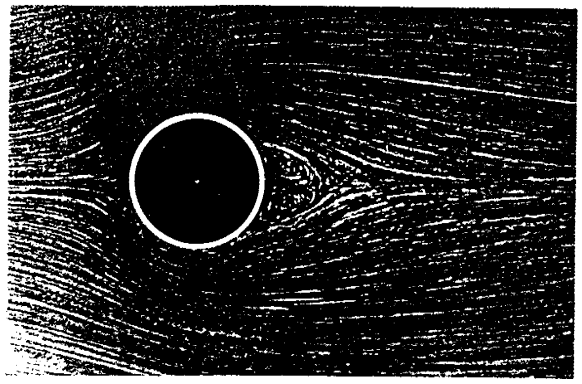

41. **Circular cylinder at $R=13.1$.** The standing eddies become elongated in the flow direction as the speed increases. Their length is found to increase linearly with Reynolds number until the flow becomes unstable above $R=40$. *Taneda 1956a*

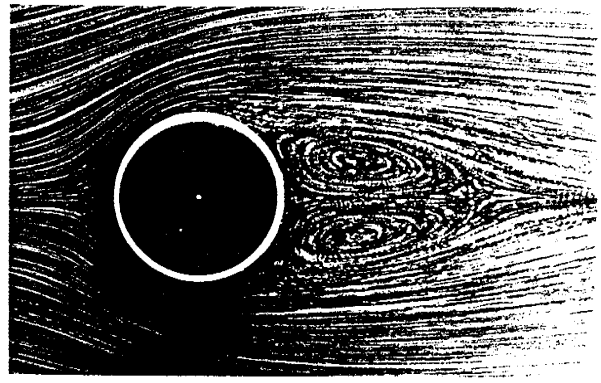

42. **Circular cylinder at $R=26$.** The downstream distance to the cores of the eddies also increases linearly with Reynolds number. However, the lateral distance between the cores appears to grow more nearly as the square root. *Photograph by Sadatoshi Taneda*

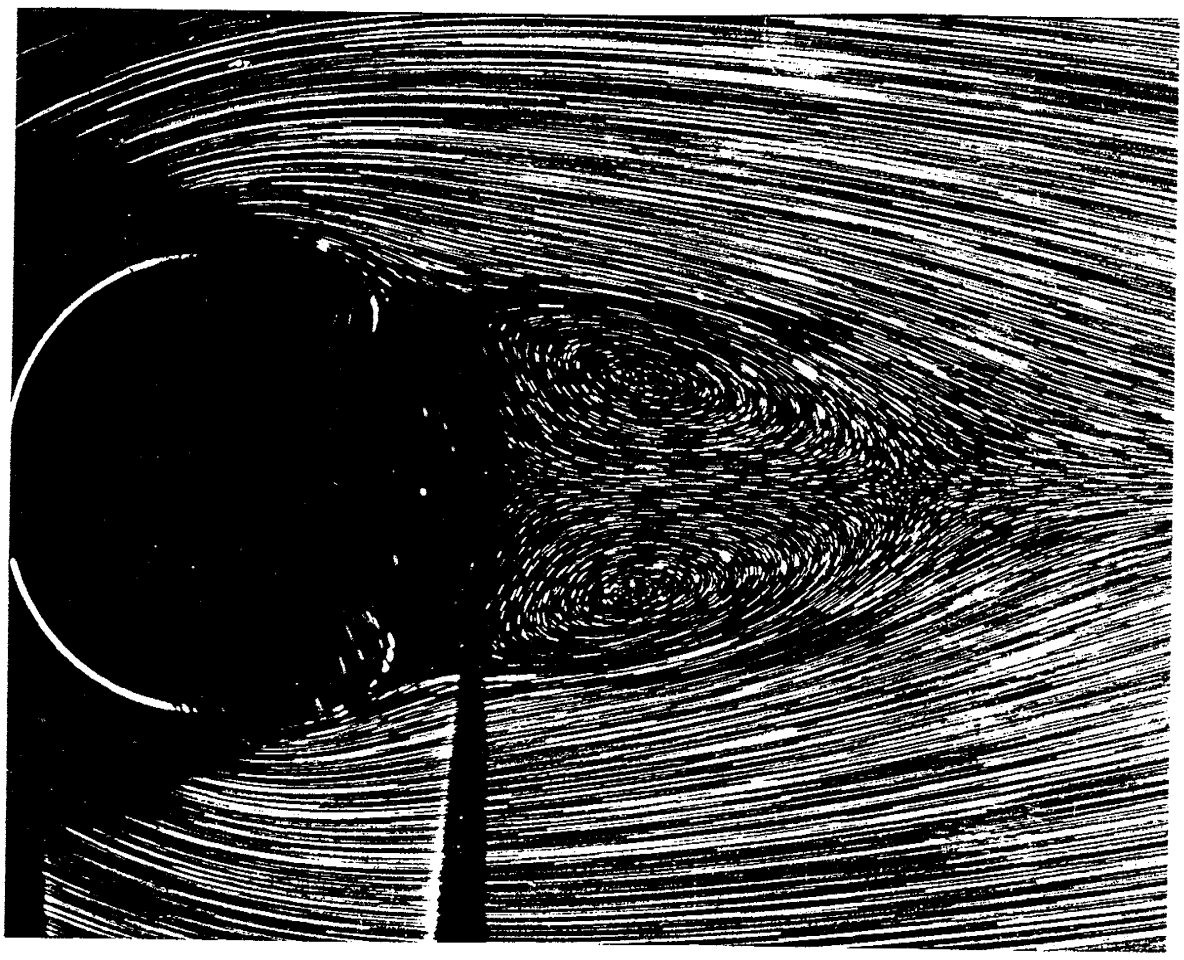

43. **Circular cylinder at $R=24.3$.** A different view of the flow is obtained by moving a cylinder through oil. Tiny magnesium cuttings are illuminated by a sheet of light from an arc projector. The two dark wedges below the circle are an optical effect. The lengths of the particle trajectories have been measured to find the velocity field to within two per cent. *Coutanceau & Bouard 1977*

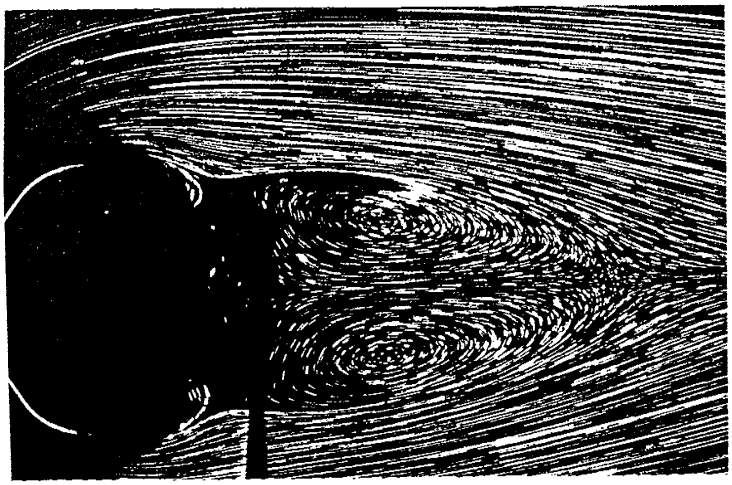

44. Circular cylinder at $R=30.2$. The flow is here still completely steady with the recirculating wake more than one diameter long. The walls of the tank, 8 diameters away, have little effect at these speeds. *Photograph by Madeleine Coutanceau and Roger Bouard*

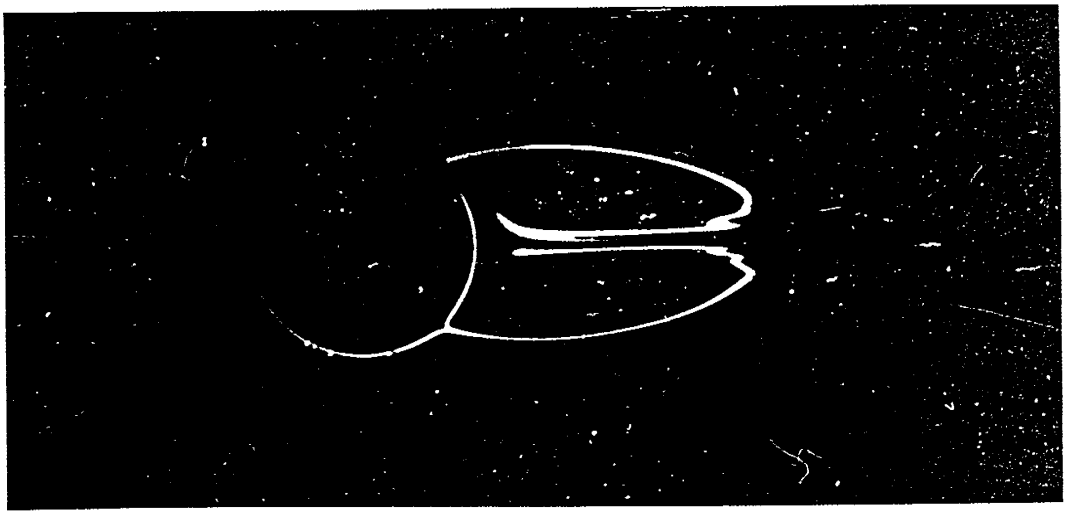

45. Circular cylinder at $R=28.4$. Here just the boundary of the recirculating region has been made visible by coating the cylinder with condensed milk and setting it in motion through water. *Taneda 1955*

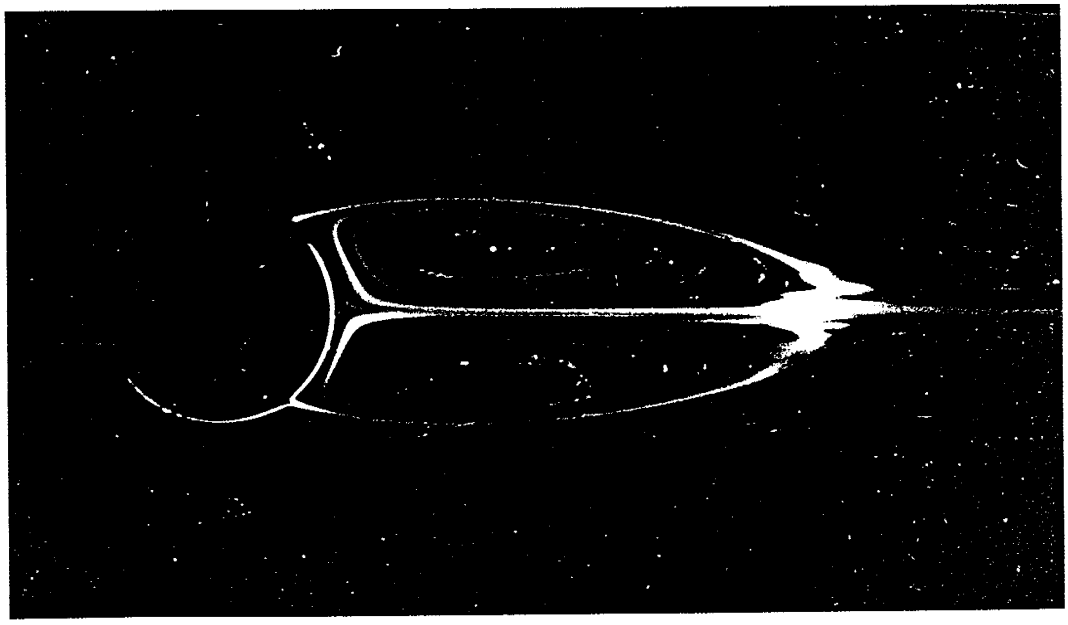

46. Circular cylinder at $R=41.0$. This is the approximate upper limit for steady flow. Far downstream the wake has already begun to oscillate sinusoidally. Tiny irregular gathers are appearing on the boundary of the recirculating region, but dying out as they reach its downstream end. *Taneda 1955*

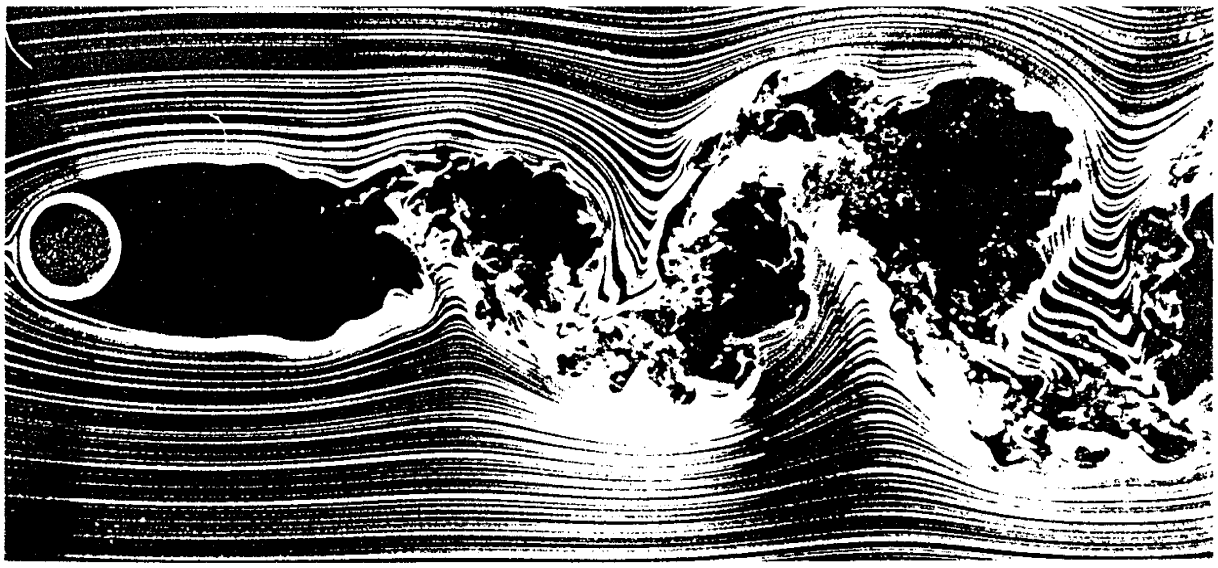

48. **Circular cylinder at R=10,000.** At five times the speed of the photograph at the top of the page, the flow pattern is scarcely changed. The drag coefficient consequently remains almost constant in the range of Reynolds number spanned by these two photographs. It drops later when, as in figure 57, the boundary layer becomes turbulent at separation. *Photograph by Thomas Corke and Hassan Nagib*

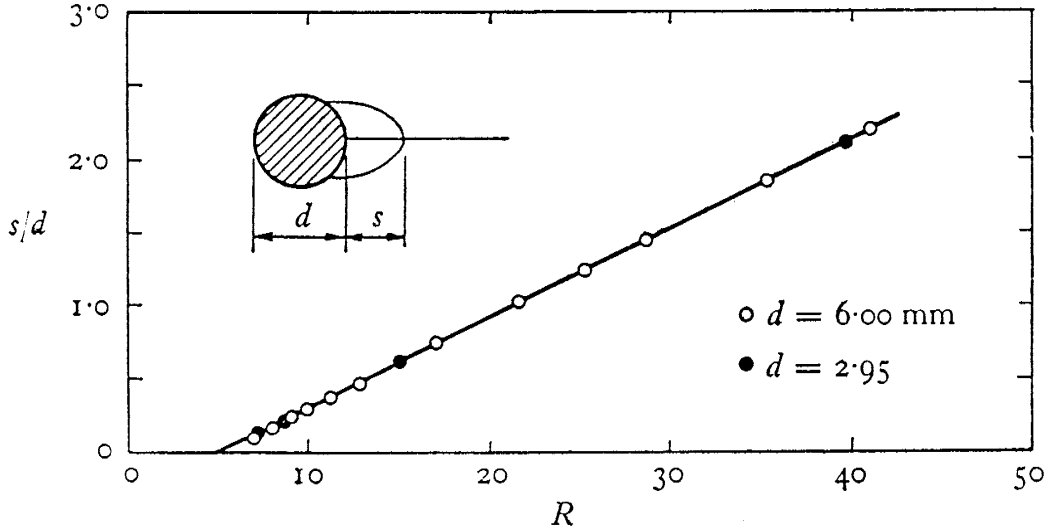

Figure 4.12.5. Observed lengths of the region of closed streamlines behind a circular cylinder (from Taneda 1956*a*).

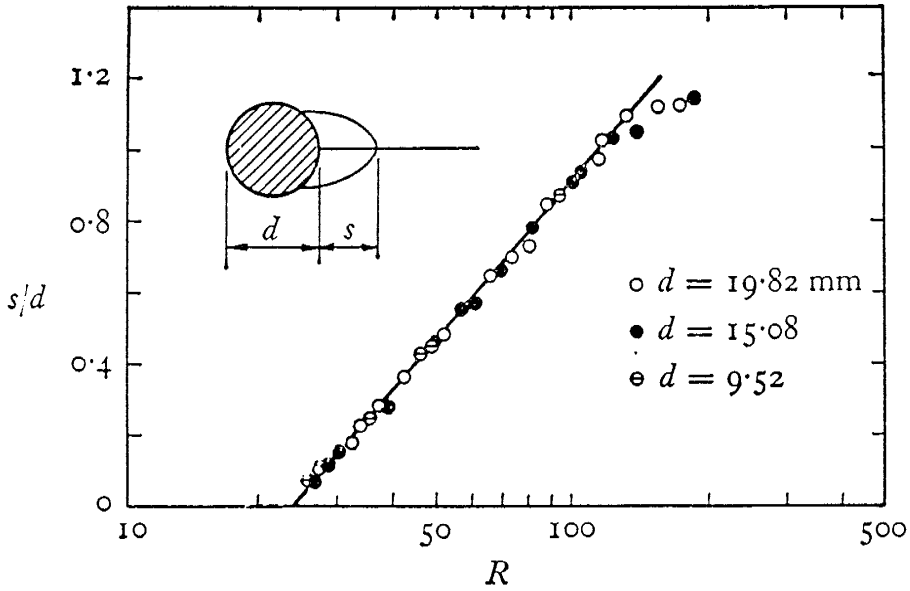

Figure 4.12.9. Observed lengths of the region of closed streamlines behind a sphere (from Taneda 1956*b*).

3. Impulsive start of a body to constant speed

(constant density)

Consider a fluid bounded along the xy-plane by a rigid wall. The wall is accelerated to a constant speed U along the x-direction at time $t=0$. The velocity field is then given by

$$u = U f(z,t), \qquad (3.1)$$

since $\underset{\sim}{u} = (u, 0, 0)$ gives $\frac{D\underset{\sim}{u}}{Dt} = \frac{\partial u}{\partial t}$.

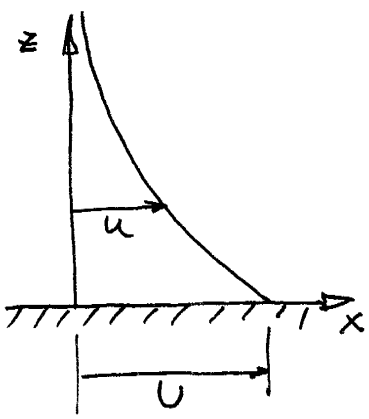

With $v = 0 = w$, the streamlines are straight and parallel. Hence $\frac{\partial p}{\partial z} = 0$. Since the components in x-direction of all gradients are zero, $\frac{\partial p}{\partial x} = 0$

so $p = \text{const.}$ (M) reduces to

$$\frac{\partial u}{\partial t} = \nu \frac{\partial^2 u}{\partial z^2} \qquad \left[\nu = \frac{\eta}{\rho}\right. \qquad (3.2)$$

With the boundary conditions

$u = U$ at $z = 0$ for all $t > 0$

$u = 0$ at $t = 0$ for all $z > 0$

$$\boxed{\frac{\partial f}{\partial t} = \nu \frac{\partial^2 f}{\partial z^2}, \quad \text{with} \quad \begin{array}{l} f(z,0) = 0 \\ f(0,t) = 1 \end{array}} \qquad (3.3)$$

Although this diffusion equation can be solved easily we can also just observe that: f being dimensionless can only depend on dimensionless numbers. The only other dimensionless number is

$$\eta = z/\sqrt{\nu t}, \qquad (3.4)$$

hence

$$f = f(\eta) = f\left(\frac{z}{\sqrt{\nu t}}\right). \qquad (3.5)$$

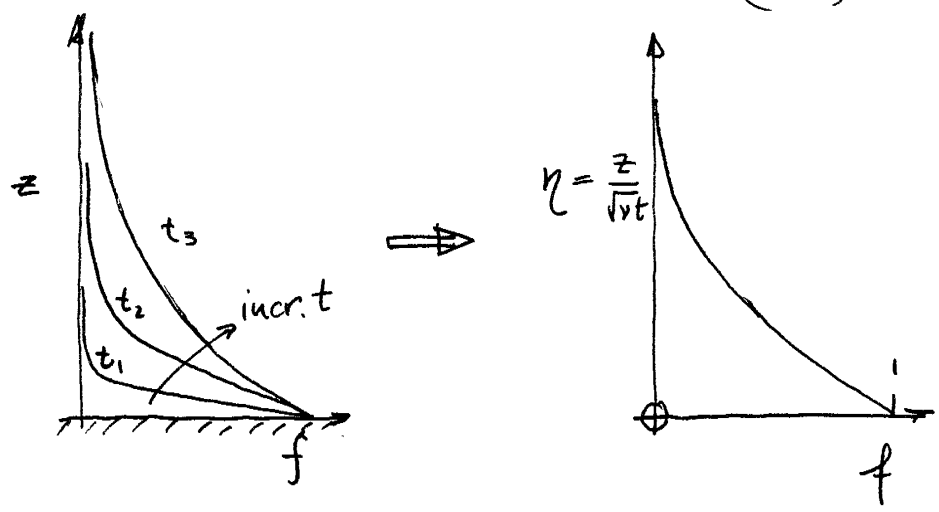

Hence the region affected significantly by the movement of the wall extends to

$$z = \delta \sim \sqrt{\nu t} \qquad (3.6)$$

The kinematic viscosity ν acts as a diffusivity of momentum, or of vorticity $\underset{\sim}{\omega} = \text{curl}\, \underset{\sim}{u} = \frac{\partial u}{\partial z}$ in this geometry. The diffusion of vorticity causes a transport of vorticity <u>across</u> the streamlines in this flow.

Transport of vorticity is also possible by convection. This may be shown by taking the curl of the momentum equation

$$\frac{D\underset{\sim}{u}}{Dt} = \frac{1}{\rho}\,\mathrm{div}\,\underset{\approx}{S}$$

using the identity

$$\mathrm{curl}\,\frac{D\underset{\sim}{u}}{Dt} = \frac{D\underset{\sim}{\omega}}{Dt} - (\mathrm{grad}\,\underset{\sim}{u})\underset{\sim}{\omega} - \underset{\sim}{u}\,\mathrm{div}\,\underset{\sim}{\omega} + \underset{\sim}{\omega}\,\mathrm{div}\,\underset{\sim}{u}$$

and $\mathrm{div}\,\underset{\sim}{\omega} = 0$:

$$\mathrm{curl}\,\frac{D\underset{\sim}{u}}{Dt} = \rho\,\frac{D\underset{\sim}{\omega}/\rho}{Dt} - (\mathrm{grad}\,\underset{\sim}{u})\underset{\sim}{\omega} + \frac{\underset{\sim}{\omega}}{\rho}\left\{\cancelto{0}{\frac{\partial\rho}{\partial t} + \mathrm{div}\,\rho\underset{\sim}{u}}\right\}$$

Hence

$$\frac{D(\underset{\sim}{\omega}/\rho)}{Dt} = \frac{1}{\rho}(\mathrm{grad}\,\underset{\sim}{u})\underset{\sim}{\omega} + \overbrace{\frac{1}{\rho}\,\mathrm{grad}\,\frac{1}{\rho}\times\mathrm{div}\,\underset{\approx}{S}}^{\text{baroclinic torque}} + \frac{1}{\rho^2}\,\mathrm{curl}\,\mathrm{div}\,\underset{\approx}{T} \qquad (3.7)$$

In the special case of constant density flow of a Newtonian fluid, this vorticity transport equation reduces to

$$\frac{D\underset{\sim}{\omega}}{Dt} = (\mathrm{grad}\,\underset{\sim}{u})\underset{\sim}{\omega} + \nu\,\mathrm{div}\,\mathrm{grad}\,\underset{\sim}{\omega} \qquad (3.8)$$

or

$$\frac{D\underset{\sim}{\omega}}{Dt} = (\mathrm{grad}\,\underset{\sim}{u})\underset{\sim}{\omega} - \mathrm{div}\,\overbrace{(-\nu\,\mathrm{grad}\,\underset{\sim}{\omega})}^{\text{diffusive vorticity flux}}$$

The last form gives a physical explanation of the vorticity transport. On the left is the convective term. On the right the first term is the change of vorticity due

to stretching of the fluid along the direction of $\underset{\sim}{\omega}$, the second term is in the form of the divergence of a flux of vorticity proportional to the vorticity gradient. The baroclinic torque is absent if ρ = constant.

If the flow is plane, $(\text{grad}\,\underset{\sim}{u})\underset{\sim}{\omega} = 0$ and $\underset{\sim}{\omega} = (0,\omega,0)$ is a scalar, only one component normal to the flow plane is nonzero. Hence (3.8) becomes

$$\frac{D\omega}{Dt} = \nu \,\text{div}\,\text{grad}\,\omega$$

I.e. deformation of vortex lines is only possible in 3-d or axisymmetric flow.

Clearly, diffusion transports ω in the direction of $-\text{grad}\,\underset{\sim}{\omega}$ and convection transports it in the direction of $\underset{\sim}{u}$.

This allows us to form a qualitative picture of the <u>impulsive start of a two-d. body</u>: Consider the case when the motion of the body follows the sketch with $t_0 \to 0$.

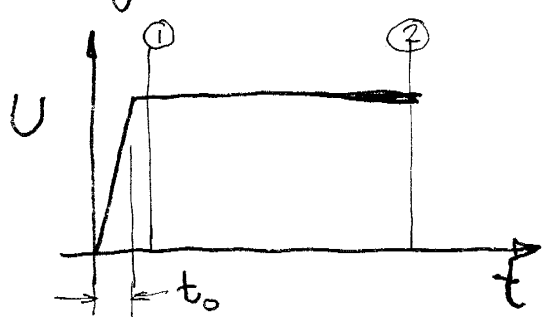

We take two snapshots of the flow. One at $t = t_1$, immediately after the start:

$\underline{\underline{t = t_1}}$

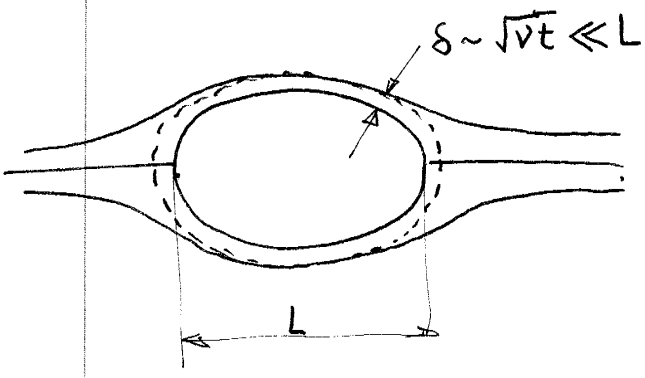

A thin layer at the wall (no-slip condition $\underset{\sim}{u} = 0$ at wall) is rotational, the remainder of the flow is irrotational. The source of vorticity is the wall and it has only been transported away from the wall by diffusion (since convection distance $\sim Ut_1 \ll \sqrt{\nu t_1}$, the diffusion distance).

The second snapshot we take at a much later time. Here it is necessary to distinguish two cases

a) $\frac{UL}{\nu} = O(1)$ b) $\frac{UL}{\nu} \gg 1$.

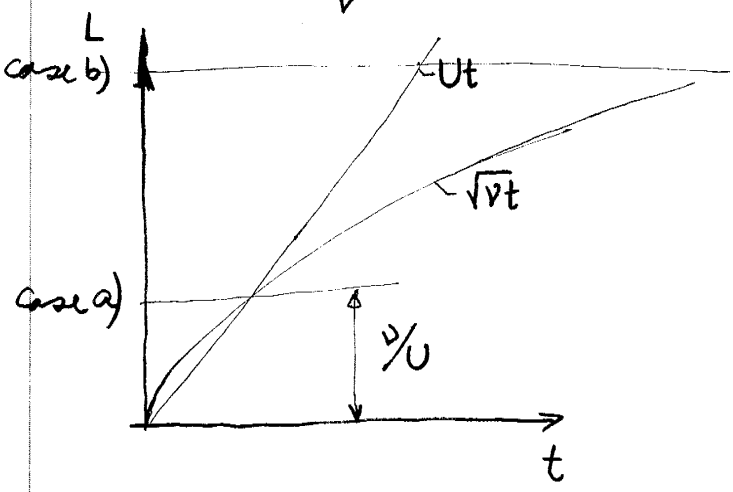

This is because the two functions of time Ut and $\sqrt{\nu t}$ show that when $L \sim \nu/U$ i.e. case a) is clearly different from what happens when $L \gg \nu/U$, case b) In case a) the diffusion length and the convection length become equal to L at

approximately the same time. In case b) the diffusion length is much smaller than the convection length when the latter has reached L.

<u>$t = t_2$, case a)</u>

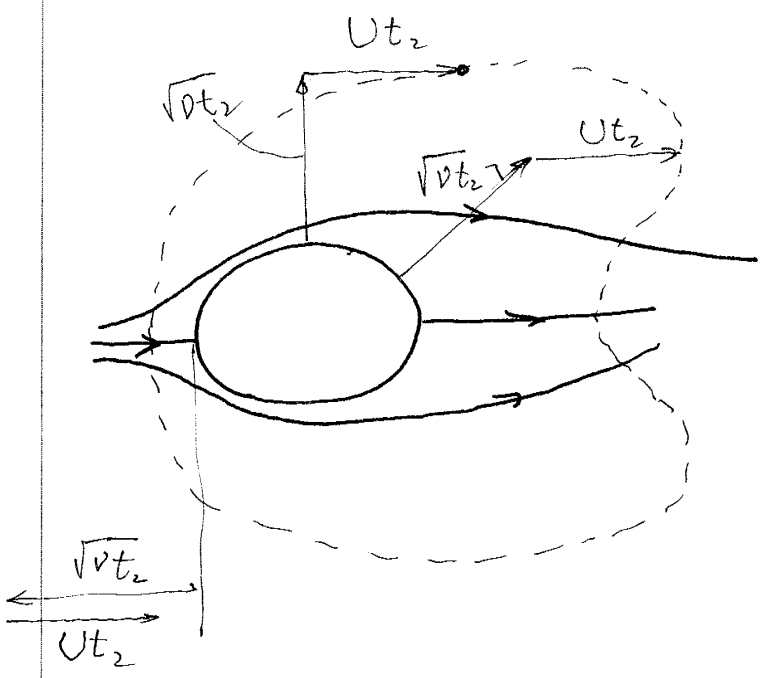

Diffusion and convection length approx = L. Since their directions relative to the flow vary, get distortion of the line of constant |vorticity| as shown. On the lower side, the vorticity has opposite sign to that on the upper side. Hence get some cancellation near the symmetry plane by gradients

<u>case b)</u> Diffusive transport weak compared with convection. (except at very small times). Hence get narrow streamwise extended loops of rotational region with sufficient accumulation of rotating flow to cause a region of closed stream lines to appear on the lee side.

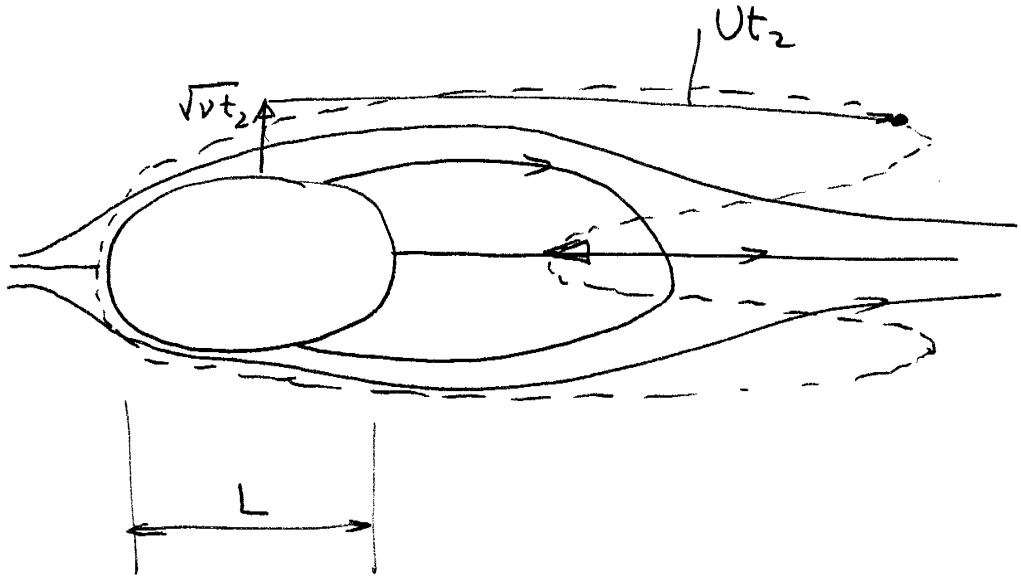

At even higher Re the separated region at the rear opens up and becomes unsteady. The photographs show portions of these processes quite clearly.

After a sufficiently long time $\frac{Ut}{L} \gg 1$ the boundary of the rotational region depends only on the Reynolds number, and a steady state is reached, provided that Re is not too large.

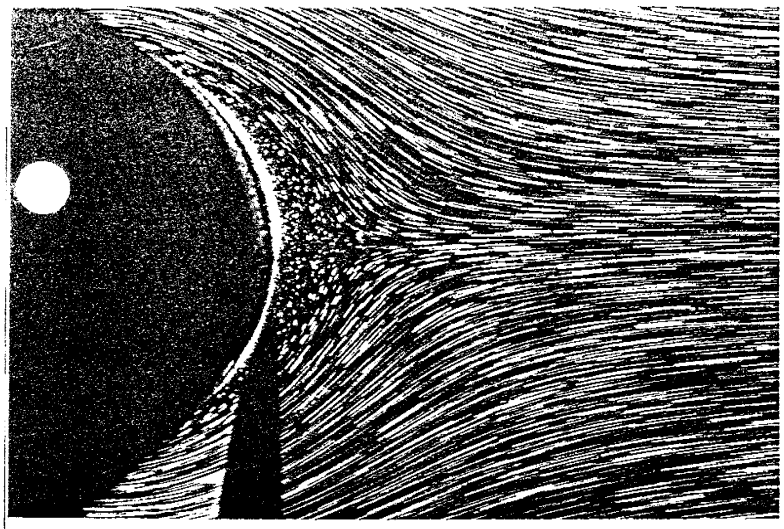

$R=50$, $Ut/d=0.5$

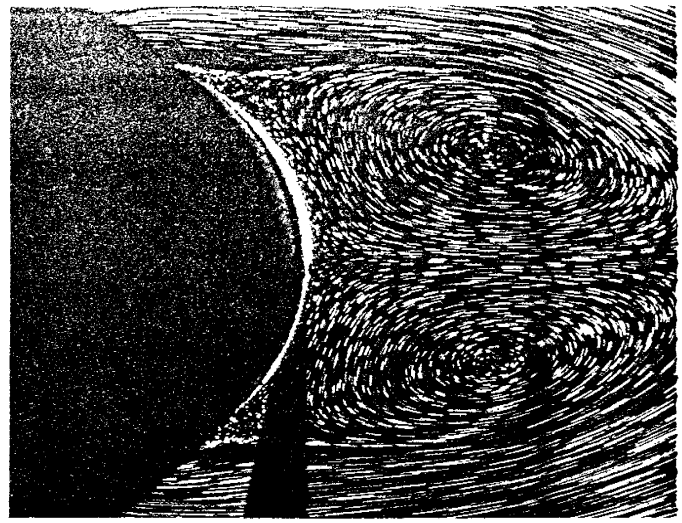

$R=50$, $Ut/d=2.5$

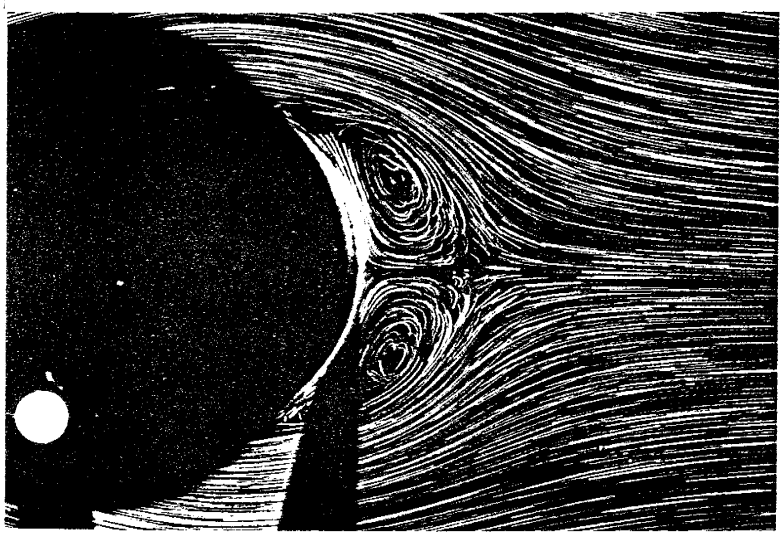

$R=500$, $Ut/d=1.0$

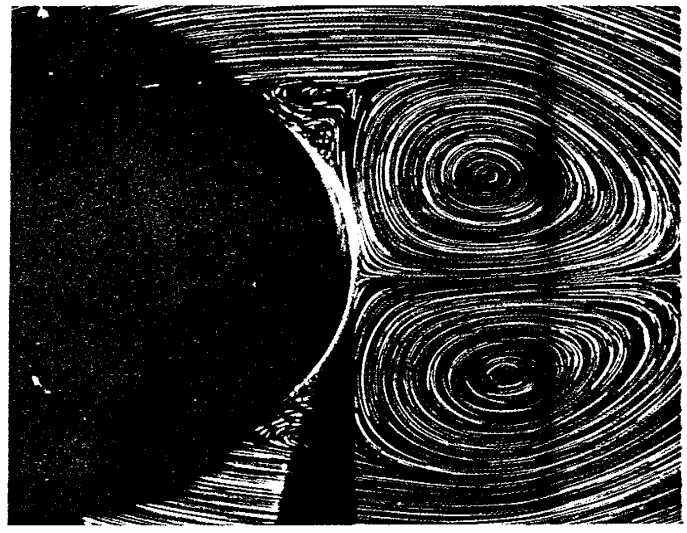

$R=500$, $Ut/d=3.0$

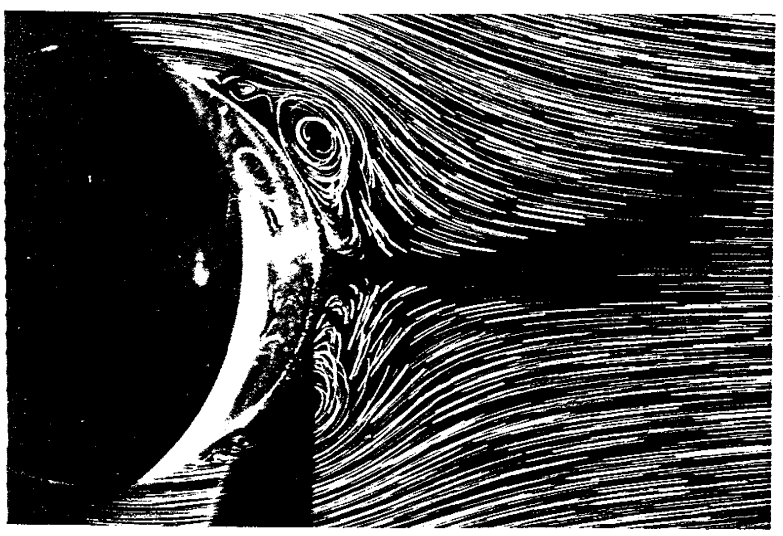

$R=5000$, $Ut/d=1.0$

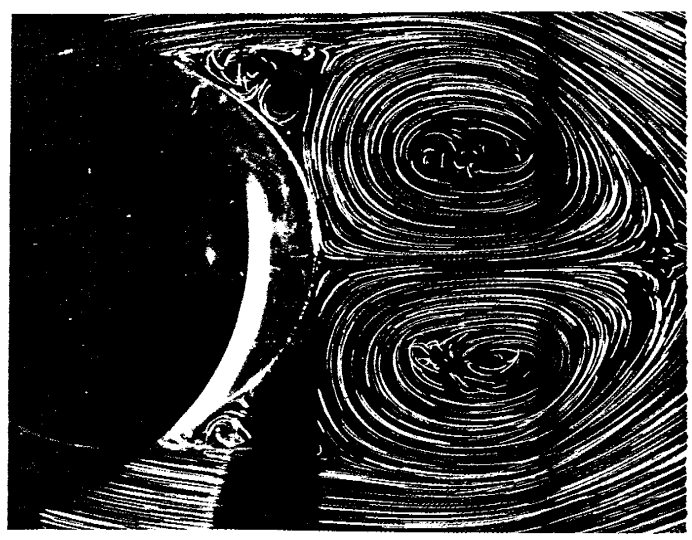

$R=5000$, $Ut/d=3.0$

59. Impulsive start of a circular cylinder. The camera moves with the cylinder, of which only the lighted rear surface is seen. The dark angle below results from a difference in refractive index of the Plexiglas cylinder and the oil through which it is set in motion. The tracer particles are fine magnesium cuttings. *Photograph by Madeleine Coutanceau and Roger Bouard*

FIGURE 5. $Re = 3000$, $t^* = 2{\cdot}5$.

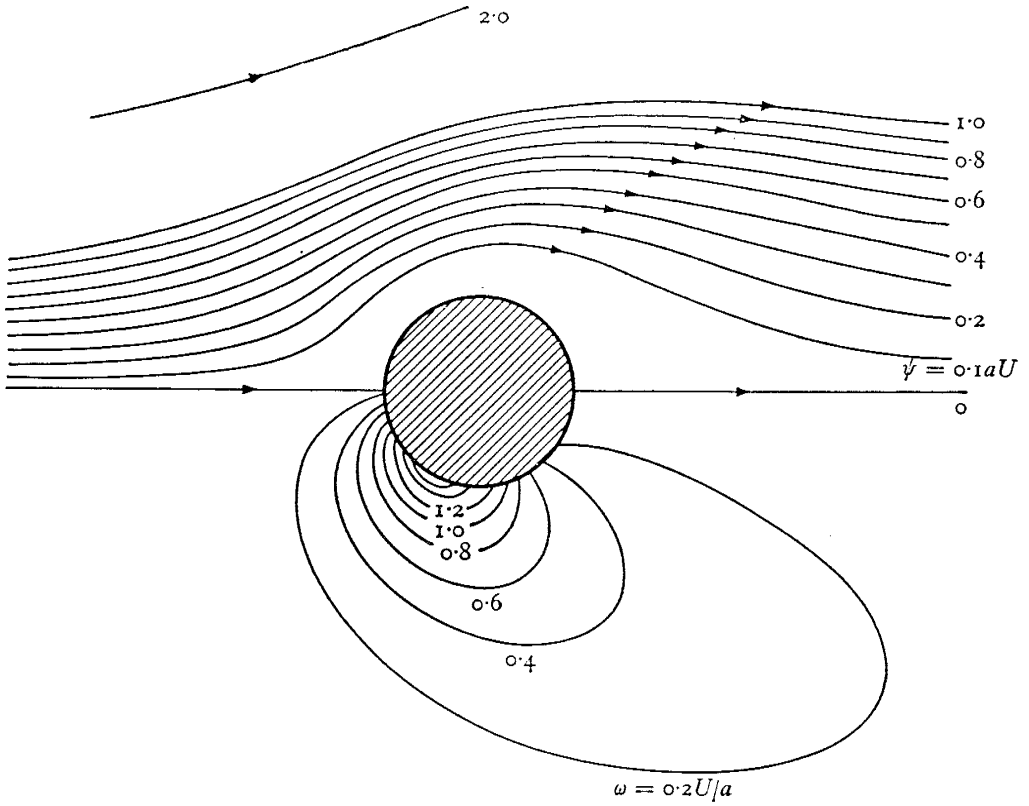

Figure 4.12.2. Streamlines (upper half of figure) and lines of constant vorticity (lower half) in flow past a circular cylinder at $R = 4$, calculated by Keller and Takami (1966).

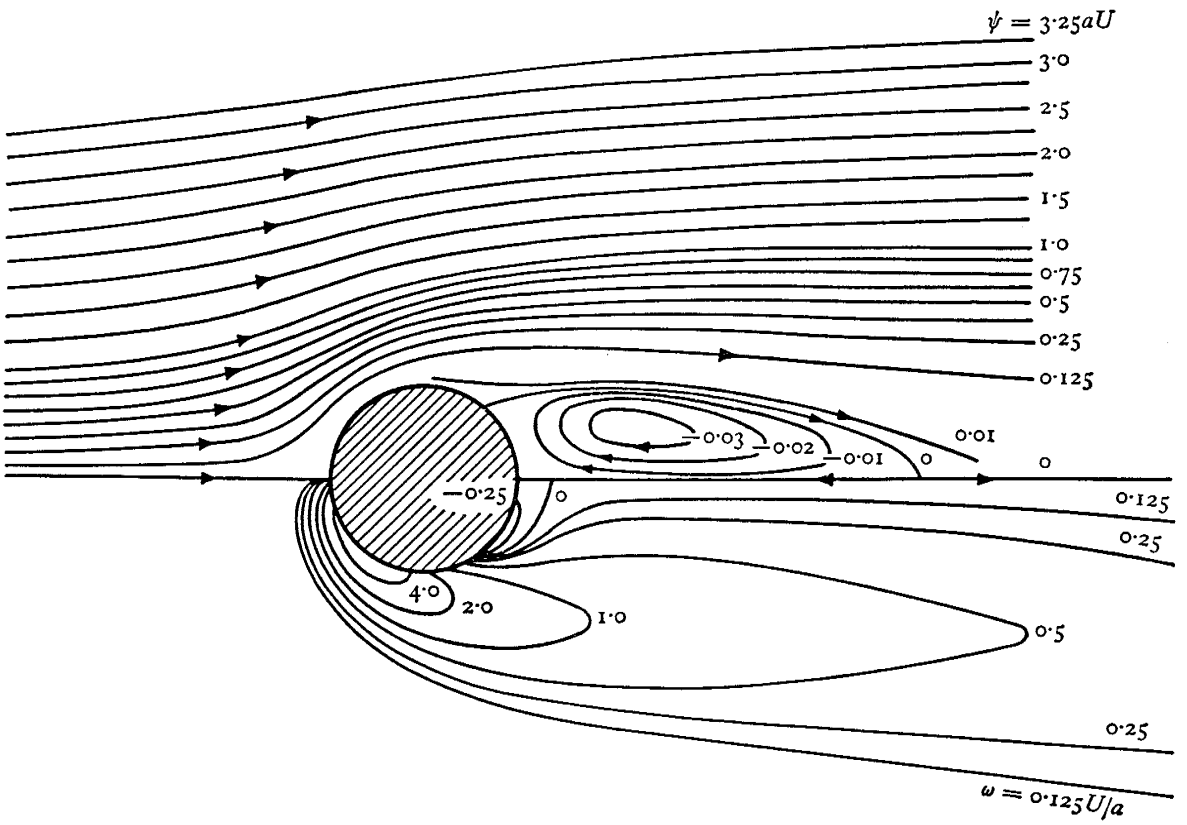

Figure 4.12.3. Streamlines (upper half of figure) and lines of constant vorticity (lower half) in flow past a circular cylinder at $R = 40$, calculated by Apelt (1961).

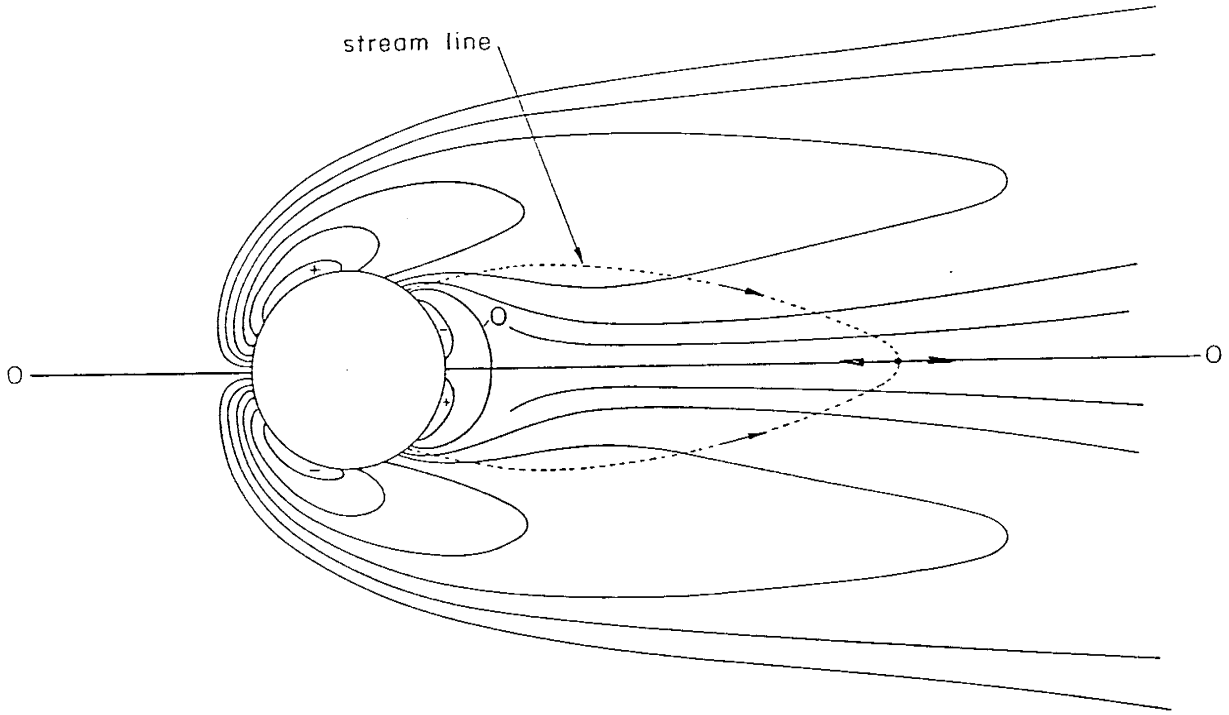

Fig. 4a Lines of constant vorticity, Re = 40. After Apelt, taken from Batchelor.

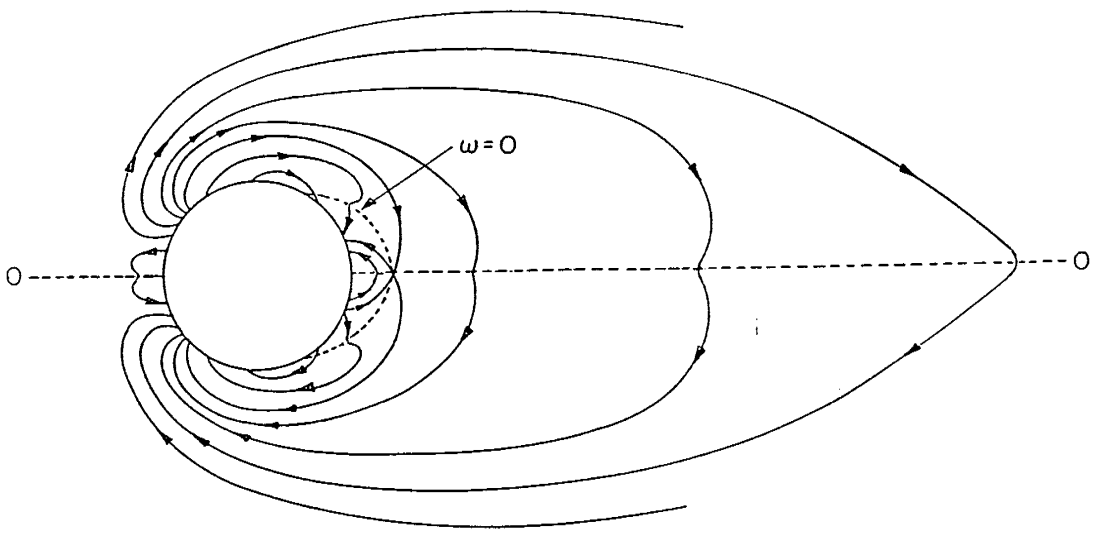

Fig. 4b Lines of vorticity transport, Re = 40. (Sketch only)

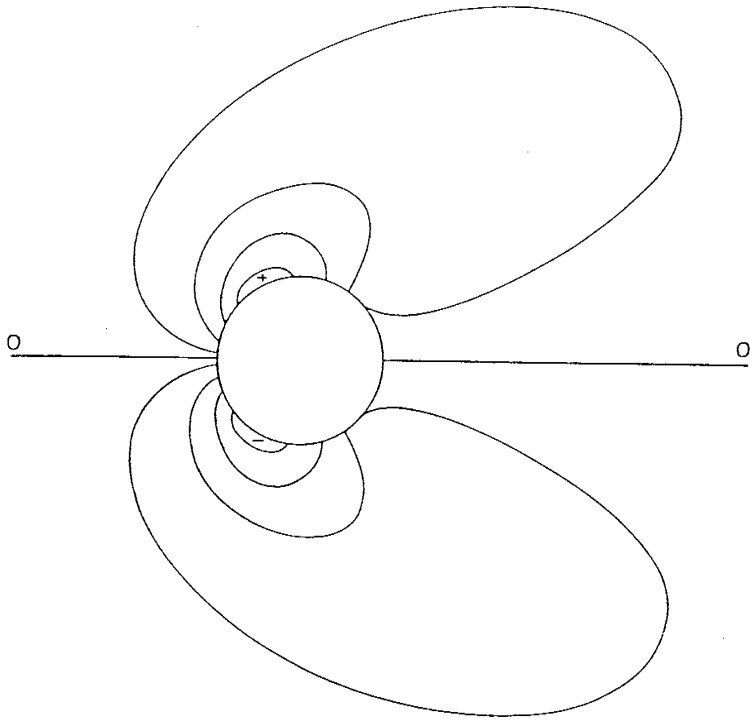

Fig. 3a Lines of constant vorticity, Re = 4. After Keller and Takami, taken from Batchelor.

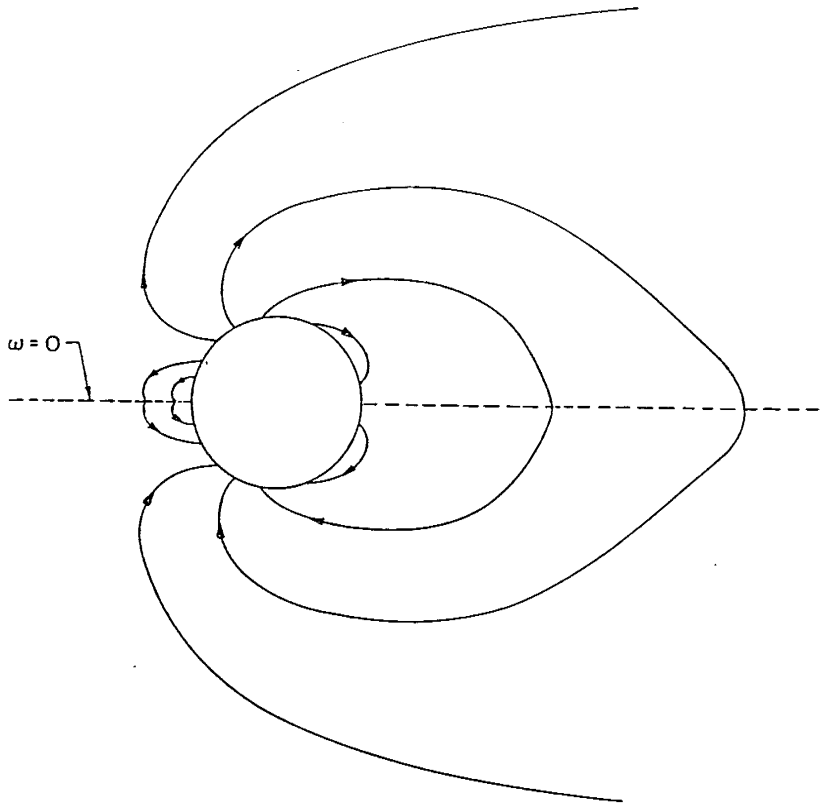

Fig. 3b Lines of vorticity transport, Re = 4. (Sketch only)

4 Boundary layer on a flat plate

The rotational region on an impulsively started body in a Newtonian fluid at const. density depends after a long time Ut/L only on the Reynolds number. For a flat plate, the boundary of the rotational region is sketched approximately:

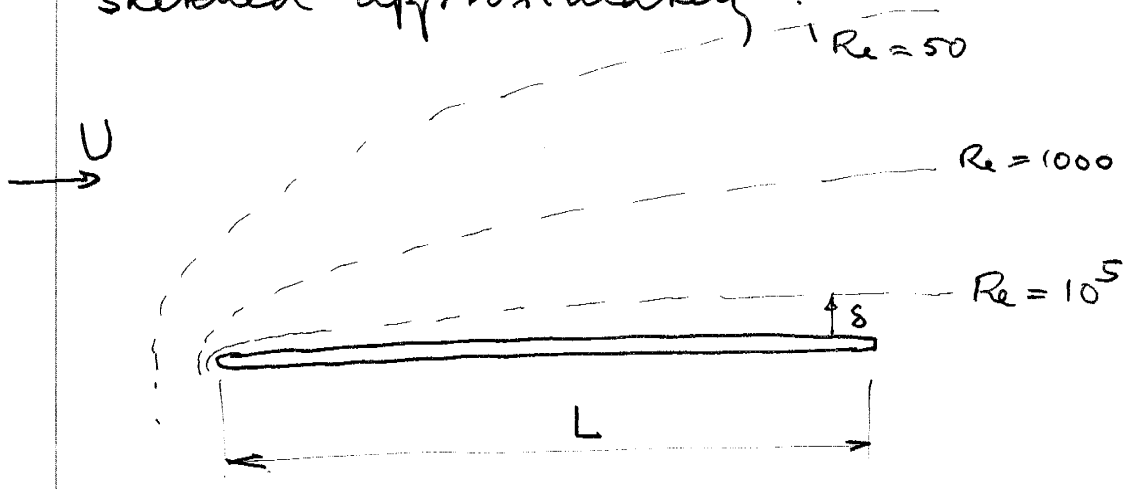

The region will clearly become a thin layer as $Re \to \infty$ because the diffusion distance

$$\delta \sim \sqrt{\nu t}$$

which is reached after a transit time

$$t \sim L/U$$

is only of order

$$\delta \sim \sqrt{\frac{\nu L}{U}}$$

or

$$\frac{\delta}{L} \sim \frac{1}{\sqrt{Re_L}} \qquad \text{Exact} \rightarrow \frac{\delta}{L} \sim \frac{5}{\sqrt{Re}}$$

This result indicates a simplification at large Re:

1. Thin layer of rotational flow
2. Consequently small transverse velocity
3. Consequently small streamline curvature
4. Consequently small transverse pressure gradient

If $\frac{\delta}{x} \sim \frac{1}{\sqrt{Re_x}}$, then

- streamline slope : $\frac{w}{u} = \frac{d\delta}{dx} = \sqrt{\frac{\nu}{U}} \cdot \frac{1}{2\sqrt{x}} \sim \frac{1}{\sqrt{Re_x}} \sim \frac{\delta}{x}$

- $\partial/\partial x \Big/ \frac{\partial}{\partial z}$: $\sim \frac{\delta}{x} \sim \frac{1}{\sqrt{Re_x}}$

- $\frac{\partial p}{\partial z} \sim \rho U^2 \cdot \text{curvature}$: $\sim \rho U^2 \cdot \frac{1}{x} \cdot \frac{1}{\sqrt{Re_x}} \sim \rho U^2 \frac{\delta}{x^2}$

- $\frac{\partial p}{\partial x}$: $\sim \frac{1}{\sqrt{Re_x}} \frac{\partial p}{\partial z} \sim \rho \frac{U^2}{x} \cdot \frac{1}{Re_x}$

In the x-momentum equation

$$u\frac{\partial u}{\partial x} + w\frac{\partial u}{\partial z} = -\frac{1}{\rho}\frac{\partial p}{\partial x} + \nu\frac{\partial^2 u}{\partial x^2} + \nu\frac{\partial^2 u}{\partial z^2}$$

substitute the orders of magnitude

$$\frac{U^2}{x}, \quad \frac{U}{\sqrt{Re_x}} \frac{U}{x}\sqrt{Re_x}, \quad \frac{U^2}{x} \cdot \frac{1}{Re_x}, \quad \frac{\nu U}{x^2}, \quad \frac{\nu U}{x^2} Re_x$$

or $\frac{U^2}{x}\left[1, \quad 1, \quad \frac{1}{Re_x}, \quad \frac{1}{Re_x}, \quad 1\right]$

Consequently, so long as the approximation is not altered by drastic effects, may drop terms of higher order in $(Re_x)^{-1}$. Similarly in the z-momentum equation. Result

$$\left.\begin{aligned} u\frac{\partial u}{\partial x} + w\frac{\partial u}{\partial z} &= \nu\frac{\partial^2 u}{\partial z^2} \\ \frac{\partial u}{\partial x} + \frac{\partial w}{\partial z} &= 0 \end{aligned}\right\} \quad (4.1)$$

in the thin rotational layer near the wall for $Re \to \infty$.

Suspect that u/U = constant along parabolic lines $z \sim \sqrt{x}$. Hence seek similarity solution w.r.t. a variable

$$\eta = \frac{z}{\sqrt{x}}\left(\frac{U}{\nu}\right)^{\frac{1}{2}}, \quad u = U f'(\eta)$$

the dash indicating differentiation w.r.t. η. Note the choice is similar to the similarity variable $z/\sqrt{\nu t}$ in the impulsively started plate. Now use continuity:

$$w = \int -\frac{\partial u}{\partial x}\,dz = -U\int \frac{d\,u/U}{d\eta}\frac{\partial \eta}{\partial x}\,d\eta\,\frac{\partial z}{\partial \eta}$$

$$= \int \frac{\eta}{2x}\,U f''\cdot\sqrt{\frac{\nu x}{U}}\,d\eta$$

$$= \frac{1}{2}\sqrt{\frac{\nu x}{U}}\int \eta f''\,d\eta, \text{ and with } w=0 \text{ at } \eta=0:$$

$$w = \frac{1}{2}\sqrt{\frac{\nu x}{U}}\left(\eta f' - f\right)$$

Similarity may now be tested by substitution into the b.l. equations: The x dependences do indeed all cancel out and

$$\boxed{f''' + \frac{1}{2} f f'' = 0 \quad \text{with } f(0) = f'(0) = 0 \text{ and } f'(\infty) = 1} \quad (4.2)$$

The solution is obtained in series or numerically and looks as shown.

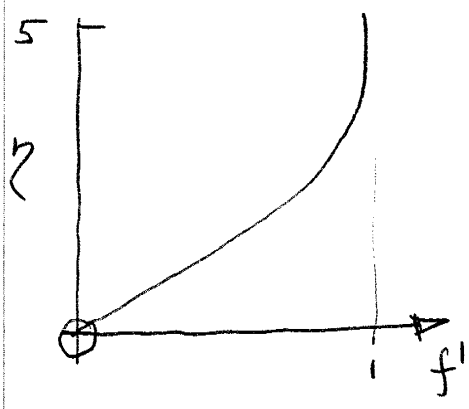

The resulting shear stress at the wall is

$$\tau_0 = \eta \left(\frac{\partial u}{\partial z}\right)_0$$

$$= \rho U^2 \sqrt{\frac{\nu}{Ux}}\, f''(0)$$

$f''(0)$ is a number leading to

$$\boxed{\tau_0 = 0.33 \rho U^2 / \sqrt{Ux/\nu}} \quad (4.3)$$

Boundary layer in accelerated external flow

Consider the case when the speed in the irrotational external flow varies with x.

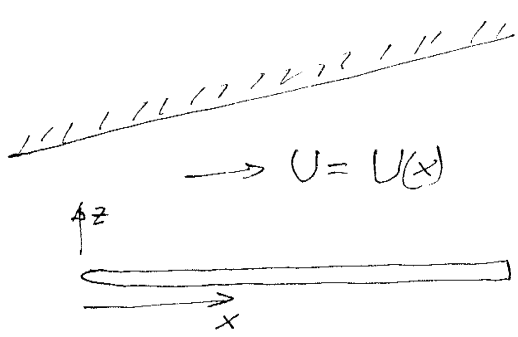

$$U = U(x)$$

If the assumption that $\frac{\partial p}{\partial z} = 0$ in the rotational layer is still valid,

an assumption that needs to be checked a posteriori, then $p = p(x)$, and the boundary layer equations become

$$\left.\begin{aligned} u\frac{\partial u}{\partial x} + w\frac{\partial u}{\partial z} &= -\frac{1}{\rho}\frac{dp}{dx} + \nu\frac{\partial^2 u}{\partial z^2} \\ \frac{\partial u}{\partial x} + \frac{\partial w}{\partial z} &= 0. \end{aligned}\right\} \quad (4.4)$$

In the external flow the momentum equation degenerates to

$$U\frac{dU}{dx} = -\frac{1}{\rho}\frac{dp}{dx} \quad (4.5)$$

so that the pressure gradient term may be replaced by the velocity gradient term.

$$u\frac{\partial u}{\partial x} + w\frac{\partial u}{\partial z} = U\frac{dU}{dx} + \nu\frac{\partial^2 u}{\partial z^2}. \quad (4.6)$$

As in the case of zero pressure gradient, this equation has the property of possessing similar solutions for special forms of the dependence of U on x. One such is

$$U = U_0\left(\frac{x}{L}\right)^m \quad \text{with } U_0, m \text{ const.}$$

The independent similarity variable is then

$$\eta = z\sqrt{\frac{m+1}{2}}\sqrt{\frac{U_0}{\nu L}\left(\frac{x}{L}\right)^{m-1}} = z\sqrt{\frac{m+1}{2}}\sqrt{\frac{U}{\nu x}} \quad (4.7)$$

Note: for $m = 0$ $\quad \eta = \frac{z}{2}\sqrt{\frac{U}{\nu}}$

Substituting these in (4.6) and (C), the x-dependence cancels out and the equation becomes

$$\boxed{\begin{gathered} f''' + \tfrac{1}{2}(m+1) f f'' + m(1-f'^2) = 0 \\ f(0) = f'(0) = 0 \quad ; \quad \underset{\eta \to \infty}{f'(\eta)} = 1 \end{gathered}} \qquad (4.8)$$

an ordinary differential equation for $f' = u/U$. Note that the fact that x-dependence cancelling is possible means that special values of x can cause difficulties. These occur in this instance at $x = 0$ when it is not valid to cancel the x-dependence. Thus, the similarity solution is not valid near $x = 0$!

Numerical solution of (4.8) gives the profiles sketched.

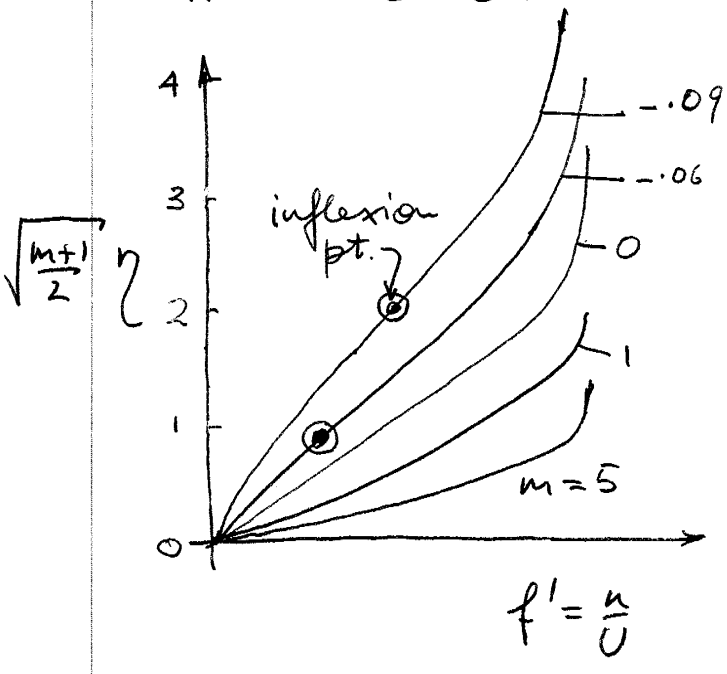

The wall shear stress becomes

$$\tau_0 = \rho \sqrt{\frac{\nu U^3}{x}}\, f''(0)$$

$$\tau_0 \propto x^{\frac{1}{2}(3m-1)}$$

In order to test our assumption that $\frac{\partial p}{\partial z}$ is negligible it is necessary to determine the influence of the boundary layer on the external flow, i.e. the feedback to the external irrotational flow. We therefore seek the equivalent body shape, which, in totally frictionless flow would have the same effect as the presence of the boundary layer. For this purpose we continue the external flow velocity U inwards the wall at a constant value, up to a point $z = \delta^*$. For $z < \delta^*$ we put $u = 0$ and demand that the mass flow rates with the velocity profiles of the dashed and the full curve are the same. This defines the displacement thickness δ^*:

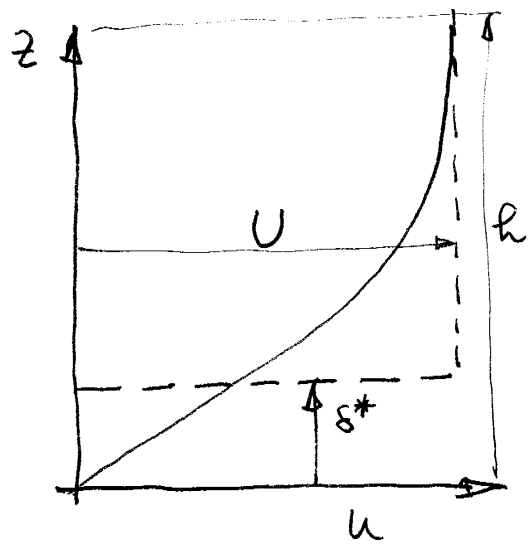

$$\int_0^h u\rho\, dz = \int_{\delta^*}^h \rho_e U\, dz$$

$$= \rho_e U \int_0^h dz - \rho_e U \delta^*$$

$$\boxed{\delta^* = \int_0^h \left(1 - \frac{\rho u}{\rho_e U}\right) dz = \int_0^\infty \left(1 - \frac{\rho u}{\rho_e U}\right) dz} \quad (4.9)$$

If ρ = constant $\quad \delta^* = \int_0^\infty \left(1 - \frac{u}{U}\right) dz$

For the similarity solutions,

$$\delta^* \propto x^{\frac{1}{2}(1-m)}$$

and for $m = 0$ $\quad \boxed{\delta^* = \frac{1.72\, x}{\sqrt{(Ux)/\nu}}}$ (4.10)

For negative m δ^* grows rapidly with x and it may be expected that the assumption $\frac{\partial p}{\partial z} = 0$ will fail at some point, since $\frac{d\delta^*}{dx}$ large implies significant streamline curvature.

5. Separation of the boundary layer. Flow over bodies at high Reynolds number.

Boundary layer theory is not limited to situations that lead to similarity solutions. The boundary layer equations may be solved numerically for more general $U(x)$. For example, one might compute the boundary layer on a circular cylinder in cross flow from the frictionless-flow $U(x)$ distribution. Even (which are of course not strictly applicable) a qualitative discussion using similar solutions shows, however, that this leads to serious difficulties. At the point ①, stagnation point flow, U is linear in x, so $m=1$ and δ^* independent of x. A full velocity profile results. At ②, "dp/dx" is still negative, "m" still positive. Between ② and ③ m falls even to negative values, δ^* increases rapidly, thus affecting the outer flow to such an extent as to modify the pressure distribution drastically. This feed back is

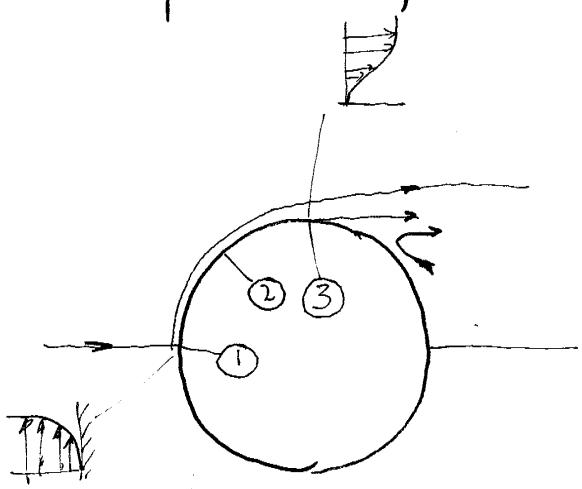

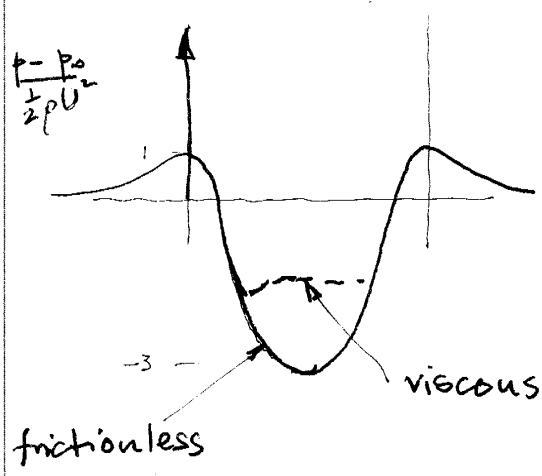

positive, i.e. increase in δ^* causes a less rapid fall or even a rise in pressure, thus causing an even more rapid increase in δ^* and so forth. This leads at the point ③ to a velocity profile for which $\left(\frac{\partial u}{\partial z}\right)_{z=0} = 0$ or $\tau_0 = 0$. To the right of ③ τ_0 becomes negative a region of reverse flow exists. This phenomenon thus causes a streamline to leave the surface at ③, so that a massive transport of rotational boundary layer fluid away from the surface <u>by convection</u> is enabled. Hence, the idea that the distance to which vorticity can be transported away from a body is $\delta \sim 1/\sqrt{Re}$, i.e. that the rotational region decreases monotonically with increasing Re is killed by the separation phenomenon. This is the essential feature about separation: Massive transport of rotational fluid to distances from the body that are comparable to L. Other definitions such as the presence of reverse flow at a surface, i.e. the appearance of a half-saddle point in the streamline pattern at a wall, do not translate unambiguously into three-dimensional flow situations.

Clearly, the appearance of separation invalidates the boundary layer assumptions, since

- $\frac{\partial}{\partial x} \ll \frac{\partial}{\partial z}$ not valid
- thin layer not valid
- $\frac{\partial p}{\partial z} = 0$ not valid.

To illustrate the breakdown of the boundary layer theory, consider a boundary layer on a plane wall in an adverse (positive) pressure gradient. Goldstein (1948) has shown that, for $Re \to \infty$, boundary layer theory gives a solution which is singular at the point where $\tau_0 \to 0$, i.e. at the separation point. The singularity has the following form:

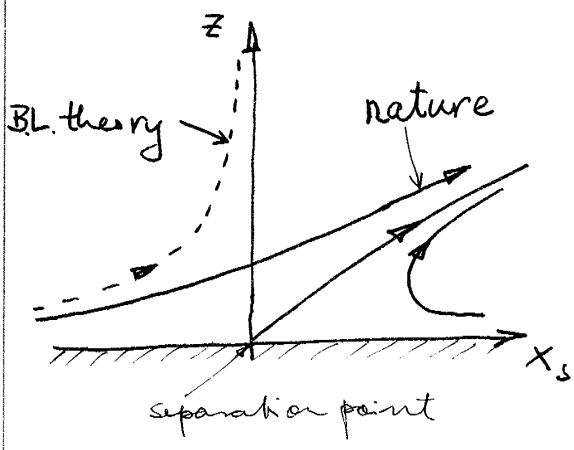

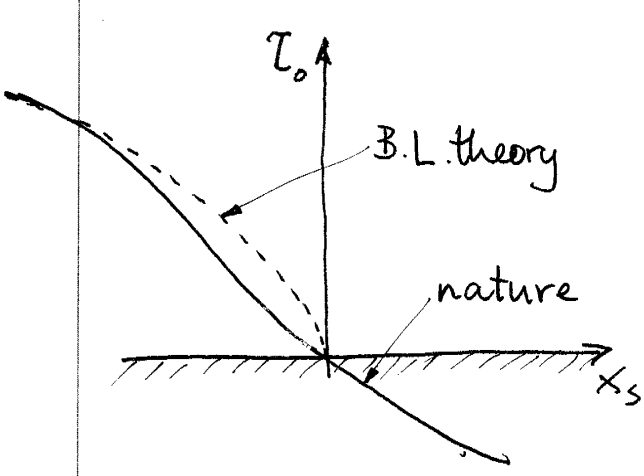

$$\tau_0 \sim (-x_s)^{\frac{1}{2}}$$

$$w \sim (-x_s)^{-\frac{1}{2}}$$

$$\delta^* \sim (-x_s)^{-\frac{1}{2}}$$

Experiments do not exhibit the singularity

i.e. B.L. theory breaks down.

In order to avoid the Goldstein singularity, in the asymptotic sense, $Re \to \infty$, an interaction between the boundary layer and the external flow must be introduced into the theory. This interaction does not exist in first order B.L. theory.

To illustrate higher order theory, consider a model problem. A flat plate b.l. that has developed over a length L encounters a dent in the wall as shown. It is now immediately necessary to distinguish between two limiting cases.

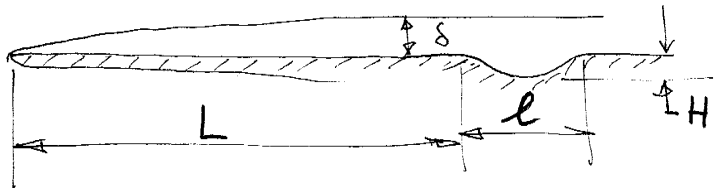

(A) $\frac{\delta}{H} \to \infty$

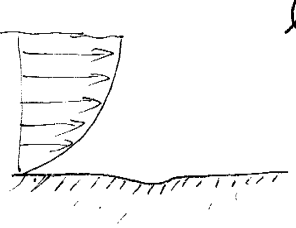

(B) $\frac{\delta}{H} \to 0$

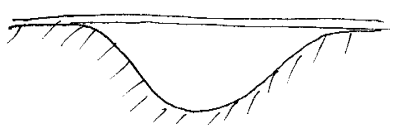

Note that neither of these cases corresponds to separation in the sense of transport of vorticity to distance L from body. However, both require the introduction of interaction

between the layer and the outer flow.

<u>The case (A)</u>

With $Re \to \infty$ and $\delta = 5L/\sqrt{Re_L} \to 0$ the condition

$$\frac{\delta}{H} \longrightarrow \infty$$

is only possible if H is related to Re in such a way that

$$\lim_{Re \to \infty} H = 0$$

For this limiting case the so-called Triple Deck Theory (TDT) applies. We return to case B after an extensive excursion into TDT.

6. Triple Deck Theory

TDT has the following main features. In a "lower deck" ①, a layer thin compared with the arriving b.l. thickness, the velocity profile is strongly modified by the dent.

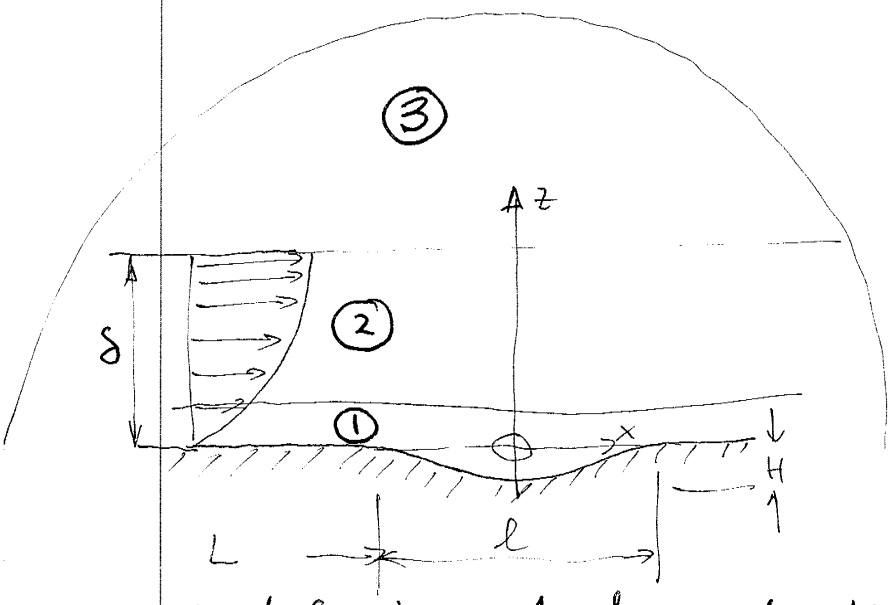

In the rest of the arriving b.l. region, the "main deck", the velocity profile is not changed other than being displaced by the changed displacement thickness due to the <u>change</u> in the lower deck. The upper deck ③ is the region in which the changed displacement effect is felt via frictionless interactions (modified pressure field.) The feed-back of the pressure field change ~~of the b~~ in ③ to the b.l. is then considered and so forth.

It is now necessary to determine the relative size of the 3 regions by making suitable assumptions.

The equations are

$$\left.\begin{aligned}
&\frac{\partial u}{\partial x} + \frac{\partial w}{\partial z} = 0 \\
&u\frac{\partial u}{\partial x} + w\frac{\partial u}{\partial z} = -\frac{1}{\rho}\frac{\partial p}{\partial x} + \nu\left(\frac{\partial^2 u}{\partial z^2} + \cancel{\frac{\partial^2 u}{\partial x^2}}\right) \\
&u\frac{\partial w}{\partial x} + w\frac{\partial w}{\partial z} = -\frac{1}{\rho}\frac{\partial p}{\partial z} + \nu\left(\frac{\partial^2 w}{\partial z^2} + \cancel{\frac{\partial^2 w}{\partial x^2}}\right)
\end{aligned}\right\} \quad (6.1)$$

$O\left(\frac{\delta}{L}\right)$

Since the dent is small, look for a perturbation solution of the Blasius b.l., of the form

$$\left.\begin{aligned}
u &= u_0\left(\frac{x}{L}, \frac{z}{\delta}\right) + \varepsilon\, u_1\left(\frac{x}{\ell}, \frac{z}{\delta}\right) + \cdots \\
w &= w_0\left(\frac{x}{L}, \frac{z}{\delta}\right) + \varepsilon\, w_1\left(\frac{x}{\ell}, \frac{z}{\delta}\right) + \cdots
\end{aligned}\right\} \quad (6.2)$$

where ε is a small parameter to be determined later, and u_0 is the unperturbed Blasius profile that satisfies

$$\left.\begin{aligned}
u_0\frac{\partial u_0}{\partial x} + w_0\frac{\partial u_0}{\partial z} &= \nu\frac{\partial^2 u_0}{\partial z^2} \\
\frac{\partial u_0}{\partial x} + \frac{\partial w_0}{\partial z} &= 0
\end{aligned}\right\} \quad (6.3)$$

Now substitute (6.2) into (6.1b), and use (6.3) to simplify, neglecting higher orders than ε.

$$u_0 \frac{\partial w_0}{\partial x} + w_0 \frac{\partial w_0}{\partial z} + \varepsilon\left(u_0 \frac{\partial w_1}{\partial x} + u_1 \frac{\partial w_0}{\partial x} + w_0 \frac{\partial w_1}{\partial z} + w_1 \frac{\partial w_0}{\partial z}\right)$$

$$= -\frac{1}{\rho}\frac{\partial p}{\partial z} + \nu \frac{\partial^2 w_0}{\partial z^2} + \varepsilon \nu \frac{\partial^2 w_1}{\partial z^2}$$

$$\varepsilon\left\{u_0 \frac{\partial w_1}{\partial x} + u_1 \frac{\partial w_0}{\partial x} + w_0 \frac{\partial w_1}{\partial z} + w_1 \frac{\partial w_0}{\partial z}\right\} = -\frac{1}{\rho}\frac{\partial p}{\partial z} + \varepsilon \nu \frac{\partial^2 u_1}{\partial z^2}$$

$$\varepsilon\left\{\frac{U^2 \delta}{L\ell}, \frac{U^2}{L}\delta, \frac{\delta U^2}{L\ell\delta}, \frac{\delta U}{\ell}\frac{\delta U}{L\delta}\right\} \mp \varepsilon\left\{\frac{p}{\rho \ell \varepsilon}, \nu\right.$$

$$\frac{\partial u_1}{\partial x} \sim \frac{\partial w_1}{\partial z} \sim \frac{\delta U}{\ell \delta}$$

$$\delta \sim \frac{L}{\sqrt{Re}}$$

$$\delta^2 \sim \frac{L^2}{Re}$$

$$\frac{w_0 u_1}{z} \sim \frac{UL}{\ell} \cdot \frac{\delta U}{L\delta}$$

$$\frac{\nu \varepsilon U}{\delta^2} = \frac{\nu \varepsilon U Re}{L^2} = \frac{\varepsilon U^2}{L}$$

$$\cancel{u_0 \frac{\partial u_0}{\partial x}} + \cancel{w_0 \frac{\partial u_0}{\partial z}} + \varepsilon \left\{ u_0 \frac{\partial u_1}{\partial x} + u_1 \frac{\partial u_0}{\partial x} + w_0 \frac{\partial u_1}{\partial z} + w_1 \frac{\partial u_0}{\partial z} \right\}$$

$$= -\frac{1}{\rho}\frac{\partial p}{\partial x} + \cancel{\nu \frac{\partial^2 u_0}{\partial z^2}} + \varepsilon \nu \frac{\partial^2 u_1}{\partial z^2}$$

Hence the leading order perturbation quantities satisfy

$$\frac{\delta U}{\cancel{L}} \cdot \frac{U}{\cancel{\delta}} \cdot \frac{\cancel{\delta}}{\cancel{\delta}} \qquad \frac{\delta U}{\ell} \frac{U}{\delta}$$

$$\varepsilon \left\{ u_0 \frac{\partial u_1}{\partial x} + u_1 \frac{\partial u_0}{\partial x} + w_0 \frac{\partial u_1}{\partial z} + w_1 \frac{\partial u_0}{\partial z} \right\} = -\frac{1}{\rho}\frac{\partial p}{\partial x} + \varepsilon \nu \frac{\partial^2 u_1}{\partial z^2}. \quad (6.4)$$

The orders of magnitude of the normal velocities are likely to be

$$O(w_0) = \frac{\delta U}{L}$$

$$O(w_1) = \frac{\delta U}{\ell}$$

Hence, term by term, the orders in (6.4) are

$$\varepsilon \left\{ \frac{U^2}{\ell}, \frac{U^2}{L}, \frac{U^2}{L}, \frac{U^2}{\ell} \right\}, \frac{p}{\rho \ell}, \frac{\varepsilon \nu U}{\delta^2}$$

Now $\ell \ll L$, so that

$$\boxed{\frac{\nu \varepsilon U}{\delta^2}} \sim \frac{U^2 \varepsilon}{\delta \sqrt{Re}} \sim \frac{\varepsilon U^2}{L} \sim \frac{\varepsilon U^2}{\ell} \cdot \frac{\ell}{L} \ll \boxed{\frac{\varepsilon U^2}{\ell}}$$

Assume also : $\frac{p}{\rho \ell} \ll \frac{\varepsilon U^2}{\ell}$ (to be checked a posteriori)

then, neglecting the appropriate terms,

$$u_0 \frac{\partial u_1}{\partial x} + w_1 \frac{\partial u_0}{\partial z} = 0, \quad \frac{\partial u_1}{\partial x} + \frac{\partial w_1}{\partial z} = 0$$

$$w_1 = u_0 \frac{\partial u_1}{\partial x} \frac{1}{\frac{\partial u_0}{\partial z}}$$

$$-u_0 \frac{\partial w_1}{\partial z} + w_1 \frac{du_0}{dz} = 0$$

$$u_0^2 \frac{\partial}{\partial z} \frac{w_1}{u_0} = -\frac{w_1}{u_0} \frac{du_0}{dz} + \frac{u_0}{u_0} \frac{dw_1}{dz} = 0$$

$$\frac{\partial}{\partial z} \frac{w_1}{u_0} = 0$$

$$\frac{w_1}{u_0} = f(x)$$

$$w_1^2 \frac{\partial}{\partial z}\left(\frac{u_0}{w_1}\right) = w_1^2\left[\frac{1}{w_1}\frac{\partial u_0}{\partial z} - \frac{u_0}{w_1^2}\frac{\partial w_1}{\partial z}\right] = 0$$

Since u_0 and $\partial u_0/\partial z$ do not change significantly over the small length l, they may be chosen at the values they take at the centre of the dent $x = 0$. Introducing dimensionless variables

$$Z = \frac{z}{\delta} \quad , \quad X = \frac{x}{l}$$

which are $O(1)$ in the region of interest, finally get

$$\left.\begin{aligned} u_0(0,Z)\frac{\partial u_1}{\partial X} + w_1 \frac{\partial u_0(0,Z)}{\partial Z} &= 0 \\ \frac{\partial u_1}{\partial X} + \frac{\partial w_1}{\partial Z} &= 0 \end{aligned}\right\} \quad (6.5)$$

These equations have the general solution ~~unless $w_1 = 0$~~

$$\left.\begin{aligned} w_1 &= B(X)\, u_0(0,Z) \\ u_1 &= -\frac{\partial u_0}{\partial Z}\int B\, dX \end{aligned}\right\} \quad (6.6)$$

An important feature of this solution is that it satisfies the boundary condition ($H \ll \delta$)

$$w_1 = 0 \quad \text{on } Z = 0 \quad (6.7)$$

identically, <u>independently of the choice of $B(X)$</u>, since $u_0(0,0) = 0$. Thus, the

function $B(X)$ is free to be chosen. Define

$$A(X) = -\int B\,dX$$

to simplify notation:

$$\boxed{\begin{aligned} w_1 &= -\frac{dA}{dX}\,u_0 \\ u_1 &= A(X)\,\frac{\partial u_0}{\partial Z} \end{aligned}} \qquad (6.8)$$

It is still necessary to determine ε. To obtain this, discuss first the nature of the solution for u_1 and w_1. Put

$$\frac{\partial u_0}{\partial Z}(0,0) = \lambda$$

(Blasius value of τ_0)

Then, on $Z = 0$:

$$u_1 = \lambda A \quad , \quad w_1 = 0$$

the first of these thus gives a slip velocity at $Z = 0$.

on $Z \to \infty$, ~~i.e. applied to Blasius~~

$$u_1 \to 0 \quad , \quad w_1 \to -\frac{dA}{dX}\,U$$

Thus, the solution represents a displacement of the Blasius profile by a distance $\varepsilon A \delta$, since the solution satisfies the Taylor expansion

$$u_0(0, Z + \varepsilon A) = u_0(0,Z) + \varepsilon A \frac{\partial u_0}{\partial Z}(0,Z).$$

Choose δ_ℓ, δ, δ_u as the scales of the lower, main and upper decks. Then consider orders of magnitude in the three regions separately.

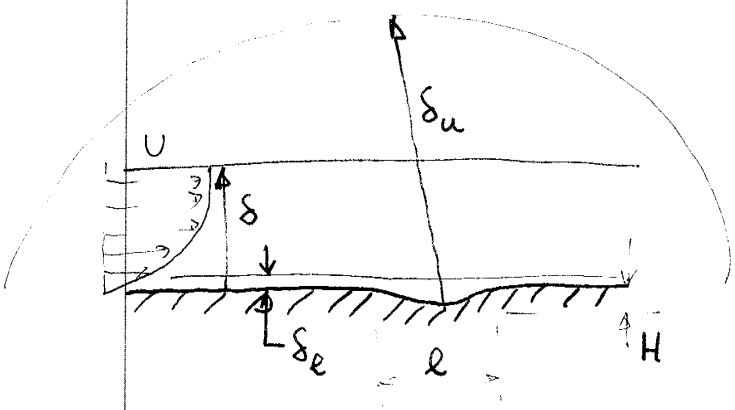

① <u>Lower deck</u>

$$u = O\left(\frac{U}{\delta}\cdot\delta_\ell\right)$$

- Assume that the perturbation velocity εu_1 is not greater than $U(\delta_\ell/\delta)$ in this region. This restricts H

- Assume normal perturbation velocity

$$\varepsilon w_1 \sim O\left(\frac{U\delta_\ell}{\delta}\cdot\frac{H}{\ell}\right) \qquad (6.9)$$

- Thus, continuity gives

$$\varepsilon u_1 \sim O\left(\frac{\ell}{\delta_\ell}\cdot\frac{U\delta_\ell}{\delta}\frac{H}{\ell}\right) = O\left(\frac{UH}{\delta}\right) \qquad (6.10)$$

- From momentum eqn: $u\frac{\partial u}{\partial x} \sim \nu\frac{\partial^2 u}{\partial z^2}$

$$\frac{U\delta_\ell}{\delta}\cdot\frac{\varepsilon u_1}{\ell} \sim \frac{\nu\varepsilon u_1}{\delta_\ell^2}$$

$$\delta_\ell^3 = O\left(\frac{\nu}{U}\ell\delta\right)$$

$$\frac{\delta_e^3}{\delta^3} = O\left(\frac{\nu \ell}{U \delta^2}\right) = O\left(\frac{\ell}{\delta\sqrt{Re}}\right) = O\left(\frac{\frac{\nu \ell}{U \delta \frac{L}{\sqrt{Re}}}}{}\right) = O\left(\frac{\ell}{\delta\sqrt{Re}}\right)$$

$$\frac{\delta_e}{\delta} = O\left(\frac{\ell}{\delta\sqrt{Re}}\right)^{\frac{1}{3}} \qquad (6.11)$$

— pressure perturbation ξp_x

$$\frac{\partial p}{\partial x} \sim \rho u \frac{\partial u}{\partial x}$$

$$p \simeq O\left(\rho \frac{U \delta_e}{\delta} \cdot \frac{UH}{\delta} \cdot \frac{1}{\ell}\right)$$

$$p \simeq O\left(\rho \frac{U^2 H \delta_e}{\delta^2}\right) \qquad (6.12)$$

the normal momentum equation gives p independent of z if $\delta_e \ll \ell$.

② <u>Main deck</u>

$$\varepsilon u_1 = O\left(\frac{UH}{\delta}\right) \quad \text{i.e.} \quad \varepsilon \sim \frac{H}{\delta} \qquad (6.13)$$

— continuity →

$$\varepsilon w_1 = O\left(\frac{\delta}{\ell} \cdot \frac{UH}{\delta}\right) = O\left(\frac{UH}{\ell}\right) \qquad (6.14)$$

— momentum →

$$\frac{u\, \partial u/\partial x}{\frac{1}{\rho}\frac{\partial p}{\partial x}} = O\left(U \cdot \frac{UH}{\delta} \cdot \frac{1}{\ell} \cdot \frac{1}{\frac{\rho U^2}{\rho} \frac{H \delta_e}{\delta^2} \cdot \frac{1}{\ell}}\right)$$

$$= O\left(\frac{\delta}{\delta_e}\right)$$

i.e., since $\delta_e \ll \delta$, the pressure gradient is negligible in the main deck. The pressure perturbation is also independent of z if

$$\delta^3 \ll \delta_e \ell^2$$

from the z momentum equation.

③ <u>Upper deck</u>

Normal velocity perturbation arises from

value in ② $\rightarrow$ $\varepsilon w_1 = O\left(\frac{UH}{\ell}\right)$ ——— (6.15)

continuity $\rightarrow$ $\varepsilon u_1 = O\left(\frac{UH}{\delta_u}\right)$ ——— (6.16)

in the upper deck, the displacement effect of the maindeck is eliminated by the pressure perturbation

$$u\frac{\partial \varepsilon w_1}{\partial x} \sim -\frac{1}{\rho}\frac{\partial p}{\partial z} \Rightarrow p \sim O\left(\frac{\rho U^2 H \delta_u}{\ell^2}\right)$$

$$u\frac{\partial \varepsilon u_1}{\partial x} \sim -\frac{1}{\rho}\frac{\partial p}{\partial x} \Rightarrow p \sim O\left(\frac{\rho U^2 H}{\delta_u}\right)$$

For these two to be consistent, need

$$\ell = O(\delta_u) \quad ; \quad \text{hence } p = O\left(\frac{\rho U^2 H}{\ell}\right) \text{ ——— (6.17)}$$

Now assume that the pressure perturbation in the upper deck is the same as that in the lower deck since it is

$$\ell = \frac{\delta^2}{\delta_\ell}$$

$$\delta_\ell^3 = O\,\frac{\delta^4}{\delta_\ell \sqrt{Re}}$$

$$\frac{\delta_\ell}{\delta} \sim \frac{1}{Re^{1/8}}$$

independent of z in the main deck. Thus (6.12 = 6.17)

$$\frac{\rho U^2 H \delta_\ell}{\delta^2} = O\left(\frac{\rho U^2 H}{\ell}\right)$$

or $$\ell \delta_\ell = O(\delta^2) \qquad (6.18)$$

Combine with (6.11):

$$\delta_\ell^3 = O\left(\frac{\ell \delta^2}{\sqrt{Re}}\right)$$

to get $\ell = O(\delta Re^{\frac{1}{8}})$ and $\delta_\ell = O(\delta Re^{-\frac{1}{8}})$

so that $\ell \gg \delta \gg \delta_\ell$.

Also, $\frac{\ell}{L} = O\left(\frac{\delta Re^{\frac{1}{8}}}{\delta Re^{\frac{1}{2}}}\right) = O(Re)^{-3/4}$ (6.19)

so that $\ell \ll L$

The relations in (6.19) define the triple deck scaling: This leads to $\varepsilon = Re^{-\frac{1}{8}}$.

Note:

Re	ε
10^8	0.1
10^6	0.178
10^4	0.316
10^2	0.56

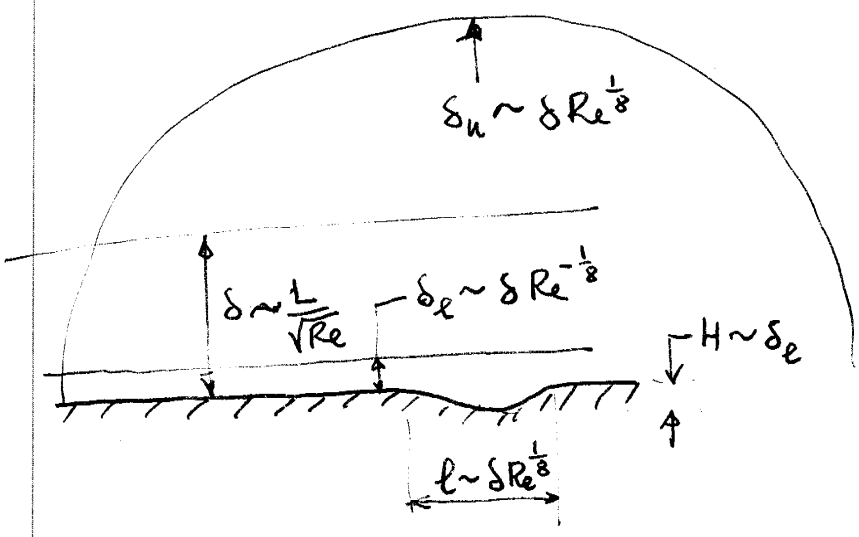

The mechanism of triple-deck interaction can best be illustrated by a schematic diagram

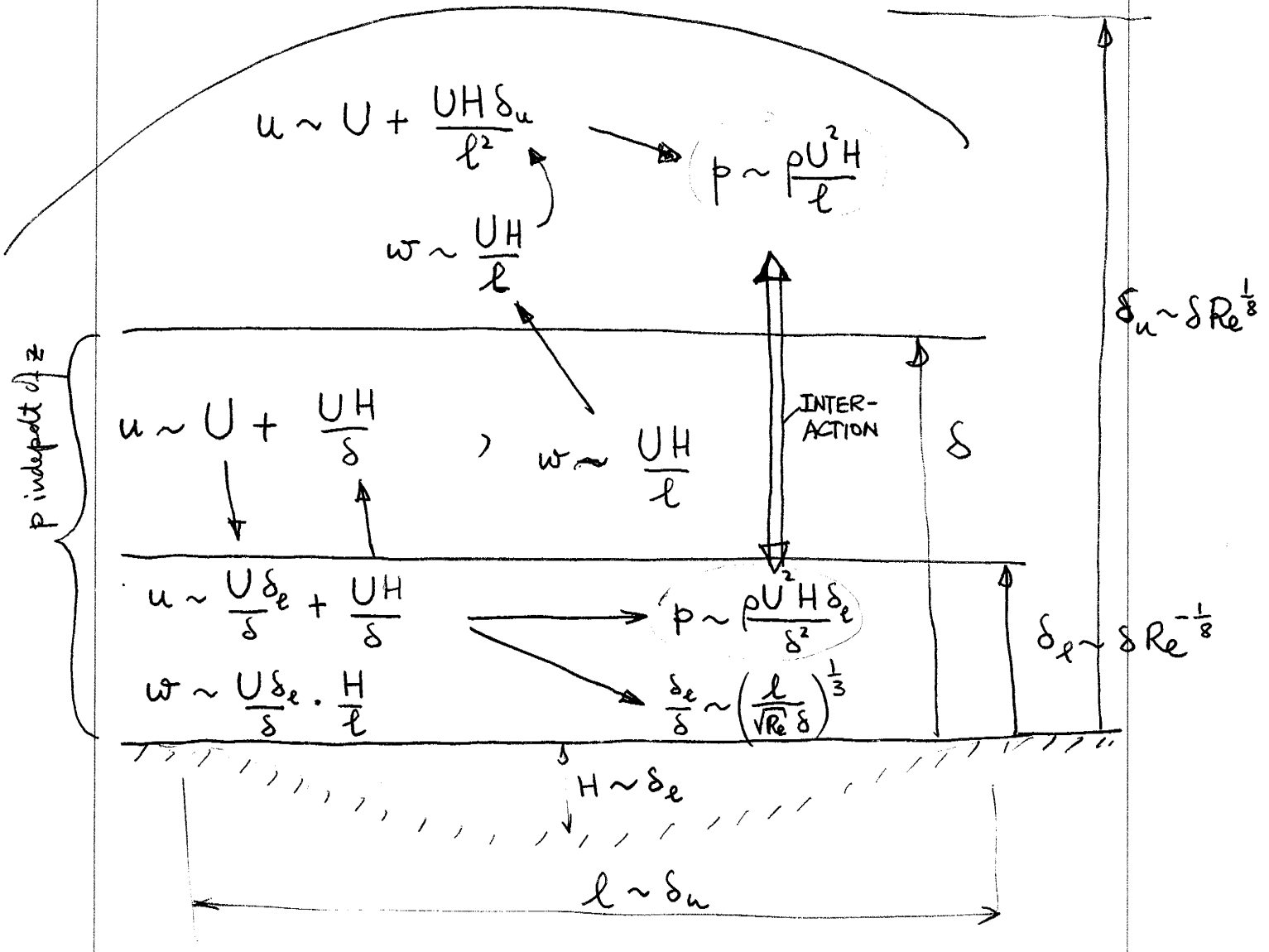

In an actual problem the solution is obtained iteratively e.g. as follows:

a) Assume displacement $A(x)$ [const. across main deck]

b) Solve b.l. eqns. in lower deck (6.8) $\Rightarrow$ $p(x)$, $u(x,z)$, $v(x,z)$ to satisfy no slip cn.

c) Thin airfoil theory in upper deck with $p(x)$ gives new $A(x)$

d) back to b) till convergence.

A further explanation of the features is obtained by presenting the features of a separated flow solution in a sketch

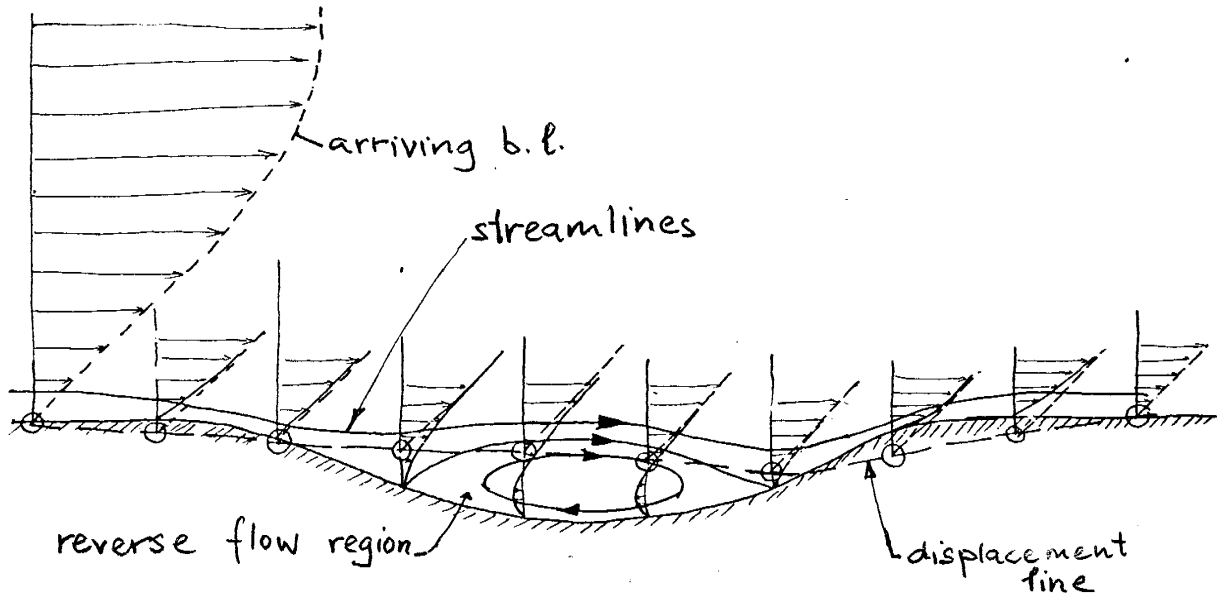

<u>Lower Deck</u>: significant modification of velocity profile

<u>Main Deck</u>: origin of linear profile moved by displacement due to lower deck.

<u>Upper Deck</u>: Pressure perturbation compatible with displacement via thin airfoil theory

This application of triple deck theory is only able to cope with separated regions whose extent is small compared with the boundary layer thickness, i.e. l and H must be tied to the Reynolds number such that they go to zero when $Re \to \infty$. The diagrams on the next page show examples of two calculations.

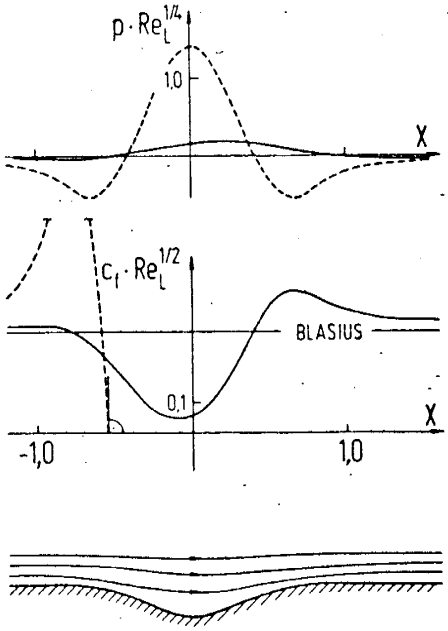

These diagrams represent two calculations of dent shapes as shown. In the top one the boundary layer calculation is shown as a dashed line. This shows the Goldstein Singularity in the skin friction plot.

$$\frac{H}{\ell \varepsilon^2} = 0.5 \ , \quad \frac{L}{\ell}\varepsilon^3 = 0.5$$

---- b.l. without interaction

—— triple deck

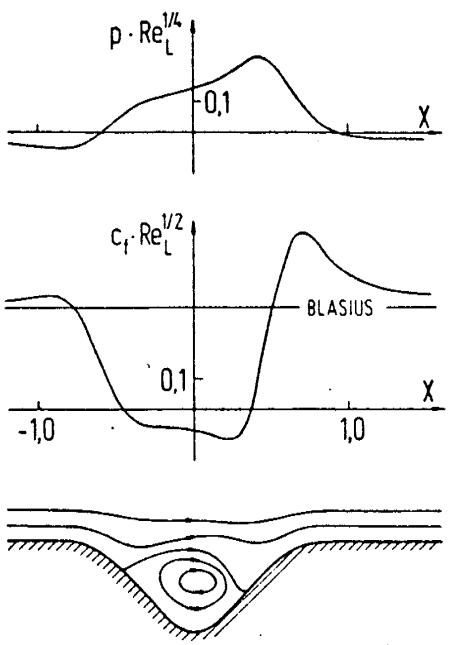

$$\frac{H}{\ell \varepsilon^2} = 1.5 \ , \quad \frac{L}{\ell}\varepsilon^3 = 0.5$$

7. Separation, case (B) $H/\delta \to \infty$

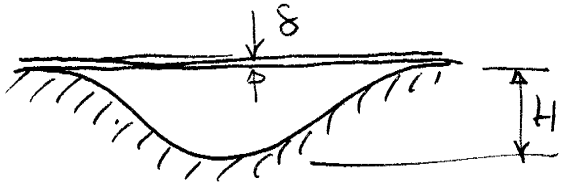

This case is closer to what one might regard as "genuine" separation as distinct from a reverse flow region within the boundary layer treated as case (A). Here, streamlines that were originally close to the wall move many boundary layer thicknesses away from it.

Recall that, in case (A), the Goldstein singularity was avoided by coupling H and ℓ to Re in such a way that the resulting pressure perturbation disappears as $Re \to \infty$:

$$p \sim \rho U^2 \frac{H}{\ell} \sim \rho U^2 Re^{-\frac{1}{4}}$$

In case (B) this is not possible since $H \gg \delta$. A new strategy is required. The zeroth order solution for $Re \to \infty$ must now be a frictionless solution. The attached potential flow (i.e. the irrotational flow) solution is not suitable for this purpose, since it always leads to the Goldstein Singularity. It appears more attractive to choose as the zeroth order solution a frictionless but rotational flow with a "free" streamline, i.e. a solution of

the Euler equations,

$$\rho \frac{D\underline{u}}{Dt} = -\text{grad}\, p \qquad \text{——— } 7.1$$

in place of the Navier-Stokes equations. For a given geometry and given far-field boundary conditions, the Euler equations possess infinitely many solutions. For example, take the flow over a dent in the case when an inner region with uniform vorticity ω_0 is separated from an irrotational outer flow by a streamline from x_0 to x_1, locations of halfsaddle points in the streamline pattern. Even with these restrictions, ~~at~~ x_0 and ω_0 are free to be chosen to give an infinite set of possibilities. (Note: no diffusion of vorticity). The question therefore arises as to which Euler solution is the <u>correct</u> starting point for an asymptotic theory.

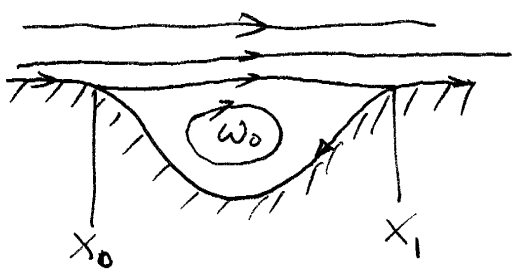

We seek that Euler solution which is reached when we apply the limiting process $Re \to \infty$ to the solution of the Navier-Stokes

equations for the given boundary conditions. (We assume the Navier-Stokes solution to be unique). It is interesting to observe that this leads to a constant vorticity in the region of closed streamlines, since the vanishingly small diffusivity at $Re \to \infty$ has available to it an infinite amount of time to distribute ω uniformly in the separated region, while this is not possible outside. A steady state is therefore only reached when the vorticity has become uniform in the separated region. This is the basis of the Prandtl-Batchelor model of separation in two dimensional steady flow.

However, since the solution of the Navier-Stokes equation is not known, we are no further ahead.

Instead, demand that the starting Euler solution has the property that, at the separation point, no Goldstein singularity exists:

at separation, $\frac{\partial p}{\partial x} = 0$ at $Re = \infty$.

To argue for this choice, suppose a separating streamline were to leave the

wall at a finite angle as shown. If the flow is inviscid and irrotational (potential flow) the speed along the separatrix is

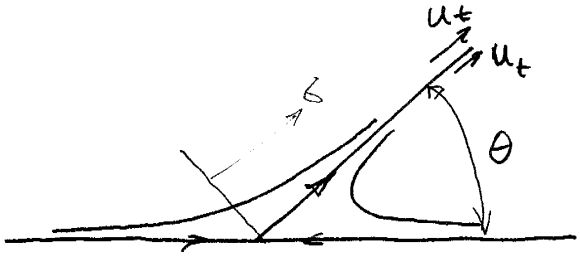

$$u_t = \frac{\pi A}{\theta} \sigma^{(\pi-\theta)/\theta}$$

on the downstream side. We want to match the pressures across the separatrix. Hence, the velocity must also be matched (starting from same stagnation point). Thus, at any point on the separatrix the tangential velocity u_t is the same on opposite sides. Clearly this is only possible if $\theta = \pi/2$ in potential flow. Such a configuration would, however, lead to very large adverse pressure gradient upstream of the stagnation point, so that, if a thin boundary layer ($Re = \infty$) were to exist under such an inviscid flow, it would separate upstream of the stagnation pt, giving a contradiction.

A possible alternative is to consider the downstream flow to be at spatially uniform vorticity ω_0, i.e. rotational.

In such a case the flow in a corner leads to

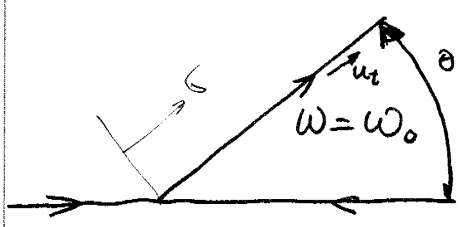

$$u_t \sim \frac{1}{2}\omega_0 \sigma \tan\theta \qquad (7.1)$$

at small σ. If the pressure is to be matched along the separatrix with the upstream irrotational, then we see that this is again not possible since the upstream value of

$$u_t = \frac{\pi A}{\pi - \theta}\sigma^{\frac{\theta}{\pi-\theta}} \qquad (7.2)$$

Even if the total pressure is different in the two regions, this does not allow pressure matching across the separatrix, unless $\theta = 0$. In this special case, the pressure gradient along the separatrix is zero at the separation point and the value of the total pressure in the rot$^{\underline{l}}$ region downstream of the separatrix is equal to the static pressure upstream.

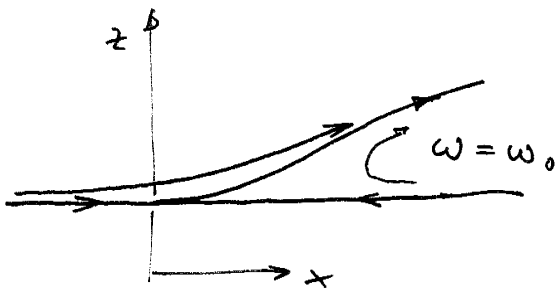

If the equation of the separatrix is

$$z = s(x)$$

the equation for the streamfunction in the rotational region,

$$\nabla^2 \psi = \omega_0$$

or, approximately, (thin region)

$$\frac{\partial^2 \psi}{\partial z^2} = \omega_0$$

has the solution

$$\psi = \frac{1}{2}\omega_0 z\left(s(x) - z\right)$$

with the boundary conditions $\psi = 0$ on $z = 0$ and on $z = s(x)$. The tangential velocity is therefore

$$u_t \sim \frac{\partial \psi}{\partial z} \text{ on } z = 0$$

$$u_t = \frac{1}{2}\omega_0 \, s(x) . \qquad (7.3)$$

Comparing this with 7.1, putting $s(x) = \delta \tan\theta$, we observe that the approximate result agrees with the local solution for $\theta = 0$.

A frictionless solution with a rotational region separated from an irrotational region by a separatrix that leaves the wall tangentially is therefore a possible starting point for an asymptotic approach to separation in the case B.

In the case of flow over a body at high Reynolds number, the vorticity originates in a thin attached boundary layer and extends into the flow as a <u>shear layer</u> springing from the separation point. We may therefore have to include a vortex sheet between the rotational flow and the potential flow. This would exhibit a velocity profile as shown, with a discontinuity of tangential velocity across the separation line,

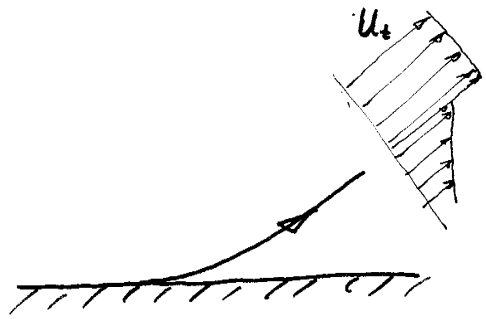

and a vorticity profile with an infinite spike at the separation streamline as shown

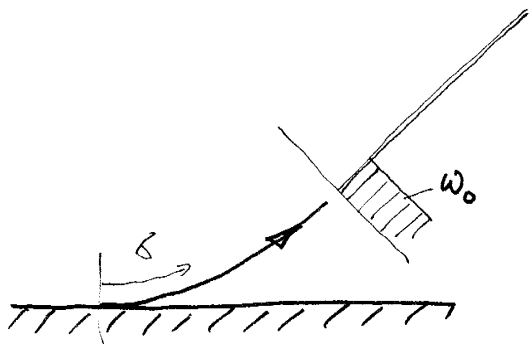

This flow configuration is possible if the total pressure

$$p + \frac{1}{2}\rho u^2$$

is smaller in the rotational part of the flow than in the irrotational upstream part. We need again to match the pressure along the vortex sheet.

The tangential velocities on opposite sides of the sheet are now different, however.

On the irrotational side we have

$$u_{ti}^2 = \frac{2(p_{oi} - p_i)}{\rho}$$

along the sheet and on the rotational side

$$u_{tr}^2 = \frac{2(p_{or} - p_r)}{\rho} .$$

With $p_i = p_r$, differentiation with respect to σ gives

$$\boxed{\frac{du_{ti}^2}{d\sigma}} = -\frac{2}{\rho}\frac{dp_i}{d\sigma} = -\frac{2}{\rho}\frac{dp_r}{d\sigma} = \boxed{\frac{du_{tr}^2}{d\sigma}},$$

since $\frac{dp_{oi}}{d\sigma} = \frac{dp_{or}}{d\sigma} = 0$, the total pressure being uniform over each of the two regions. Consequently the quantity

$$\frac{du_t^2}{d\sigma}$$

<u>is continuous across the vortex sheet.</u>

Consider again the various possibilities for separation from a smooth surface:

a) <u>Finite θ</u>

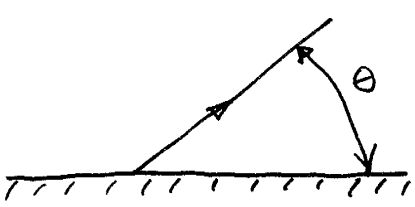

Since p is continuous across the sheet and, at the stagnation point, $p = p_o$ on both sides, the total pressure is also continuous

across the sheet at the stagnation point. Since the sheet is a streamline, p_0 must be continuous across the sheet everywhere. Hence the tangential velocity is also continuous across the sheet and there is no vortex sheet, i.e. contradicting the assumption of a sheet. Finite θ is therefore out, and the sheet must leave the wall tangentially.

b) <u>Tangential departure, $u_{tr} = 0$</u>.

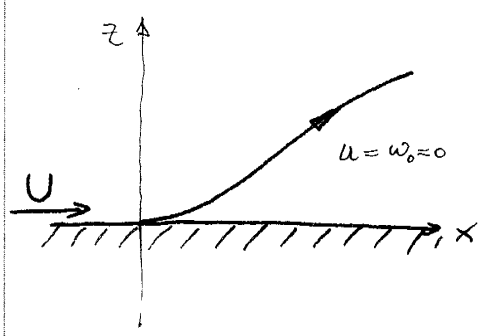

We now have a tangential velocity $U \neq 0$ at the upstream side of the separation point $x = 0_-$, and a stagnation point on the downstream side $x = 0_+$. Since the pressures are equal at $x = 0_\pm$, there must be a total pressure loss of $\frac{1}{2}\rho U^2$ from 0_- to 0_+, and therefore across the sheet everywhere. The downstream flow can thus not be expected to be irrotational potential flow. <u>One possibility</u> is, however, that the downstream flow is at rest relative to the body. This implies that the uniform total pressure is equal to the static pressure $p_{0r} = p_r$

Hence the pressure in the downstream region is uniform and $dp/ds = 0$, giving the separating vortex sheet as a <u>constant pressure streamline</u>. An example of this possibility is the well-known Kirchhoff (1869) solution of flow over a circular cylinder.

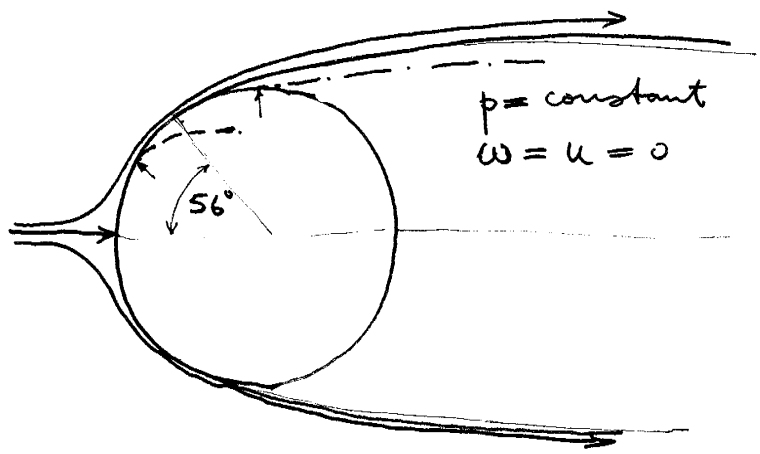

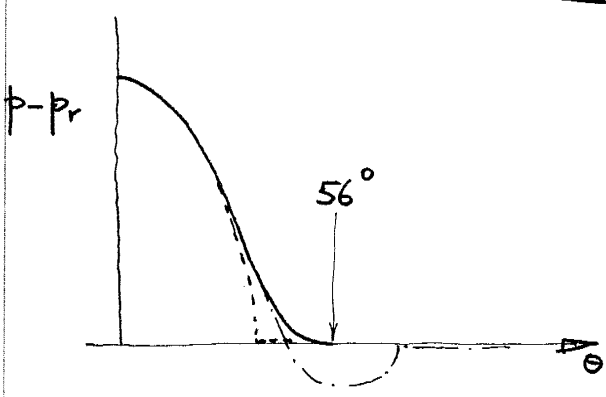

It is interesting to observe that here too it is possible to choose the separation point freely, and still obtain a valid solution of the Euler equation. If separation occurs at $\theta > 56°$, the pressure distribution on the body upstream of separation is as shown by the chain dotted curve. If it occurs at $\theta < 56°$ the separation streamline goes into the body (unphysical). If $\theta = 56°$ at separation, the pressure merges smoothly into the free streamline pressure, giving "<u>smooth separation</u>". In the case of smooth

separation, the pressure gradient is zero at separation and the curvature of the sheet remains finite at $\sigma \to 0$. In general, the curvature of the sheet behaves as $\sigma^{-\frac{1}{2}}$ as $\sigma \to 0$ and the pressure gradient upstream

$$\lim_{\sigma \to 0_-} \frac{dp}{d\sigma} \sim |\sigma|^{-\frac{1}{2}}$$

also, except for the special case of smooth separation.

c) <u>Tangential departure $u_{tr} \neq 0$.</u>

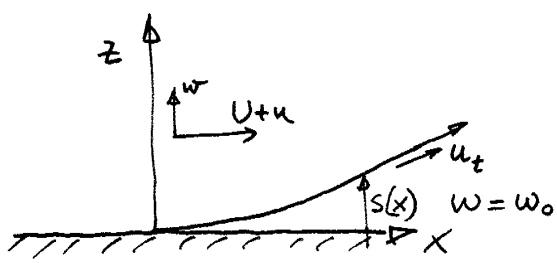

If the downstream flow is not at rest it will be rotational and the downstream tangential velocity is given by

$$u_t = \frac{1}{2} w_0 \, s(x)$$

The flow <u>upstream of the separation line</u> may be approximated near the separation point by a linear approximation with the sheet represented by a w-distribution at the x-axis. Let the disturbance velocities be u and w, with $u = w = 0$ at $x = 0$.

Since $\frac{d}{d\sigma}\left(u_t^2\right)$ is continuous across

the sheet and $\frac{d}{ds} \doteq \frac{d}{dx}$ near $x = 0$,

$$\frac{d}{dx}\left(U^2 + 2uU + \cancel{u^2} + \cancel{w^2}\right) \doteq 2U\frac{du}{dx} = \frac{d}{dx}\left(u_t^2\right) \qquad (7.4)$$

Since $u = u_t = 0$ at $x = 0$, this gives

$$u = u_t^2/2U. \qquad (7.5)$$

But

$$u_t = \tfrac{1}{2}\omega_0 s(x),$$

so

$$\left.\begin{aligned} u &= \omega_0^2 s^2(x)/(8U) \\ &\text{for } z = 0,\ x > 0 \end{aligned}\right\} \qquad (7.6)$$

Also, since the wall and the sheet are a streamline,

$$\left.\begin{aligned} w &= U s'(x), \quad z = 0,\ x > 0 \\ w &= 0, \quad z = 0,\ x < 0 \end{aligned}\right\}. \qquad (7.7)$$

The flow upstream of the sheet is an irrotational flow, for which $(u - iw)$ must be an analytic function of $\zeta = x + iz$. This, together with the boundary conditions 7.6, 7.7 was used by J.H.B. Smith (1977) to get a solution for $s(x)$ giving regular behaviour for u and v:

$$\boxed{s(x) = L\left\{\tfrac{2}{3}c_0\left(\tfrac{x}{L}\right)^{3/2} + \tfrac{2}{5}c_1\left(\tfrac{x}{L}\right)^{5/2} + \dots\right\}} \qquad (7.8)$$

This has the features of the free-streamline solutions (Kirchhoff), that the rotational downstream flow is compatible with an analytic irrotational upstream flow.

The pressure distribution upstream of separation is then

$$p - p_s = \rho U^2 \left\{ -\left(\frac{-x}{L}\right)^{\frac{1}{2}} c_0 + c_1 \left(\frac{-x}{L}\right)^{3/2} + \dots \right\}, \; x<0 \quad (7.9)$$

and

$$\frac{dp}{dx} = \frac{\rho U^2}{L} \left\{ \frac{c_0}{2} \left(\frac{-x}{L}\right)^{-\frac{1}{2}} - \frac{3}{2} c_1 \left(\frac{-x}{L}\right)^{\frac{1}{2}} + \dots \right\}, \; x<0 \quad (7.10)$$

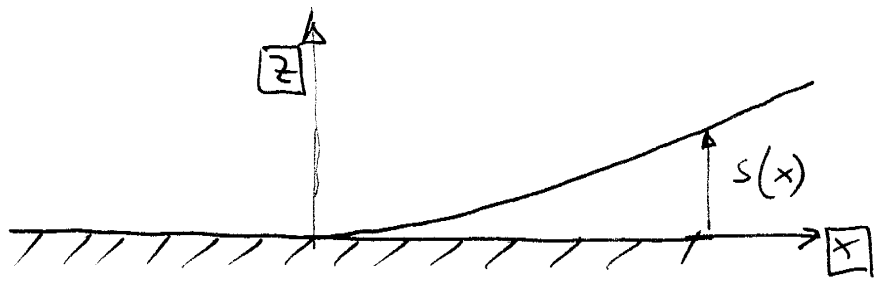

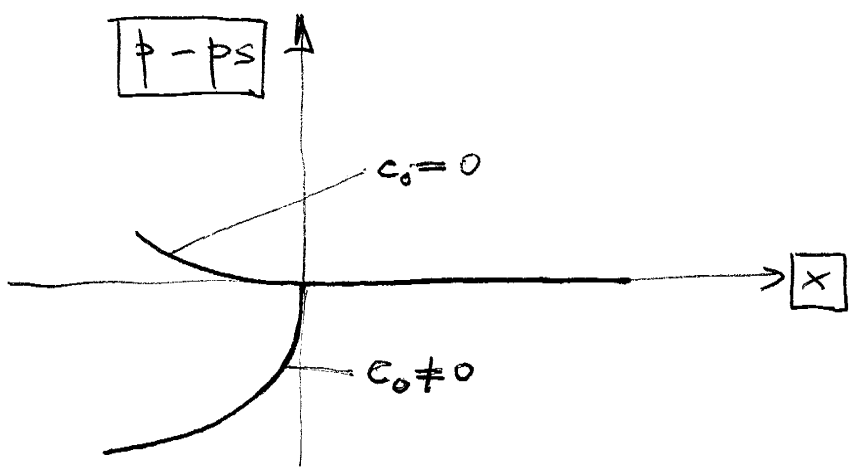

Thus, $\frac{dp}{dx} = 0$ only when $c_0 = 0$, just as in the Kirchhoff solution. $c_0 = 0$ also corresponds to zero curvature of the sheet at $x = 0$.

We see, therefore, that only the smooth separation case of these solutions is suitable as the zeroth order solution for separation at $Re = \infty$. This is, because the other cases, with $c_0 \neq 0$, give infinite adverse pressure gradient upstream of separation, leading to separation upstream of separation, i.e. a contradiction.

If equation (7.10) with $c_0 = 0$ is the asymptotic form for $Re = \infty$, then it may, of course, be possible that $c_0 \to 0$ as $Re \to \infty$ and (7.10) is valid even when $Re \neq \infty$. In this broader view of (7.8) – (7.10), the coefficients $c_0, c_1 \ldots$ are functions of the Reynolds number such that, e.g.

$$\lim_{Re \to \infty} c_0(Re) = 0. \qquad (7.11)$$

This idea was used by V.V. Sychev (1972) to study the behaviour of separation in case (B).

An important feature of the Sychev theory is that this step again links the pressure disturbance to the Reynolds number in such a way as to remove it at $Re = \infty$.

This feature allows the triple deck scaling ideas to be used here too: In the immediate vicinity of the separation point

$$\frac{L}{\rho U^2}\frac{dp}{dx} = \frac{c_0}{2}\left(-\frac{x}{L}\right)^{-\frac{1}{2}}.$$

Let $c_0(Re) = O(\varepsilon)$, ε to be determined by interaction of pressure disturbance in lower deck with pressure disturbance in upper deck.

<u>Lower deck</u>, $\boxed{\frac{p}{\rho U^2} \sim \varepsilon\left(-\frac{x}{L}\right)^{1/2}}$

x momentum: $u\frac{\partial u}{\partial x} \sim \frac{1}{\rho}\frac{\partial p}{\partial x} \sim \frac{U^2}{L}\varepsilon\left(-\frac{x}{L}\right)^{-\frac{1}{2}}$

$$\therefore \quad \frac{u}{U} \sim \varepsilon^{\frac{1}{2}}\left(-\frac{x}{L}\right)^{+1/4} \qquad (7.12)$$

the shear rate U/δ gives $\frac{\partial u}{\partial z}$ with $\delta \sim L/\sqrt{Re}$

$$\therefore \quad \frac{z}{L} \sim O\left(\varepsilon^{1/2}\left(-\frac{x}{L}\right)^{\frac{1}{4}} Re^{-1/2}\right) \qquad (7.13)$$

Also $\frac{1}{\rho}\frac{\partial p}{\partial x} \sim \nu\frac{\partial^2 u}{\partial z^2}$

$$\rightarrow \left(-\frac{x}{L}\right) \sim O(\varepsilon^6) \qquad (7.14)$$

<u>Main deck</u>

Velocity profile modified only by lower deck u:

$$u \sim U\left(1 + \varepsilon^{\frac{1}{2}}\left(-\frac{x}{L}\right)^{+\frac{1}{4}}\right) \qquad (7.15)$$

Continuity $\frac{\partial u}{\partial x} + \frac{\partial w}{\partial z} = 0 \Rightarrow w \sim \frac{z}{x} u \sim \frac{\delta}{L} u \cdot \frac{L}{x}$

$$\Rightarrow \quad w \sim U Re^{-\frac{1}{2}} \varepsilon^{\frac{1}{2}} \left(-\frac{x}{L}\right)^{-3/4} \qquad (7.16)$$

<u>Upper deck</u> w as in middle deck:

$$w \sim U Re^{-\frac{1}{2}} \varepsilon^{\frac{1}{2}} \left(-\frac{x}{L}\right)^{-3/4} \qquad (7.17)$$

Hence $p \sim \rho w U \sim \rho U^2 Re^{-\frac{1}{2}} \varepsilon^{\frac{1}{2}} \left(-\frac{x}{L}\right)^{-3/4}$ (7.18)

Now we match the pressure perturbation (7.18) with that in the lower deck

$$\rho U^2 Re^{-\frac{1}{2}} \varepsilon^{\frac{1}{2}} \left(-\frac{x}{L}\right)^{-3/4} \sim \varepsilon \left(-\frac{x}{L}\right)^{\frac{1}{2}} \rho U^2$$

$$\varepsilon^{\frac{1}{2}} \sim Re^{-\frac{1}{2}} \left(-\frac{x}{L}\right)^{-5/4}. \qquad (7.19)$$

With $\left(-\frac{x}{L}\right) \sim \varepsilon^6$ from lower deck, (7.19) gives

$$\varepsilon^{\frac{1}{2}} \sim Re^{-\frac{1}{2}} \cdot \varepsilon^{-15/2}$$

$$\left.\begin{array}{l} \boxed{\varepsilon \sim Re^{-\frac{1}{16}}} \\ \boxed{-\frac{x}{L} \sim Re^{-3/8}} \end{array}\right\} \qquad (7.20)$$

Detailed solution of the problem in the lower deck and matching leads to

$$\boxed{s = \kappa x^2 + Re^{-\frac{1}{16}} \left\{ \frac{2}{3} \alpha_0 \lambda^{9/8} \right\} \left(\frac{x}{L}\right)^{\frac{3}{2}} + \frac{2}{5} C_1 \left(\frac{x}{L}\right)^{\frac{5}{2}} + \ldots} \qquad (7.21)$$

where κ is the body curvature at the separation point, α_0 is a numerical constant determined by F.T. Smith (1977) as 0.44, λ is the skin friction coefficient (divided by $(Re^{-\frac{1}{2}})$) of the arriving boundary layer, and the term in $(x/L)^{5/2}$ is the leading inviscid term. If the arriving boundary layer is a Blasius layer, $\lambda = 0.33$ and

$$c_0 = \alpha_0 \lambda^{9/8} \, Re^{-\frac{1}{16}}$$

$$= 0.44 \times (0.33)^{9/8} \, Re^{-\frac{1}{16}}$$

$$\boxed{c_0 = 0.126 \, Re^{-\frac{1}{16}}} \qquad (7.22)$$

If $\kappa = 0$, the first term disappears and

$$\frac{S}{L} = 0.084 \, Re^{-\frac{1}{16}} \left(\frac{x}{L}\right)^{3/2} + \frac{2}{5} c_1 \left(\frac{x}{L}\right)^{\frac{5}{2}} + \dots$$

$$\frac{\rho w U}{\rho U^2} = \frac{p - p_s}{\rho U^2} = -0.126 \, Re^{-\frac{1}{16}} \left(\frac{-x}{L}\right)^{\frac{1}{2}} + c_1 \left(\frac{-x}{L}\right)^{\frac{3}{2}} + \dots$$

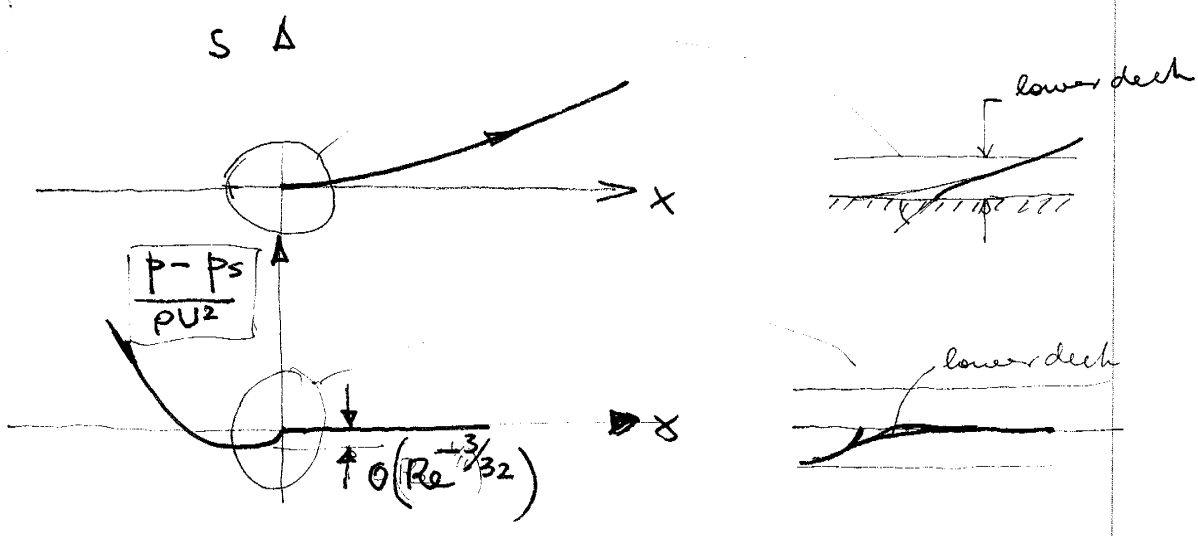

To estimate the position of the separation point, the procedure is as follows:

1. Solve the inviscid free streamline problem to determine U at inviscid sep$^{\underline{n}}$
2. Integrate the boundary layer equations from the stagnation point on the body to the separation point to find λ.
3. Solve for change in the free streamline solution at the given Reynolds number.

Clearly, the separation point moves upstream as $Re \to \infty$ and the displacement of the separation point downstream from the inviscid separation point is $O(Re^{-\frac{1}{16}})$.

The configuration of the zeroth order inviscid (free streamline) solution for the Sychev theory may be sketched approximately for other geometries.

<u>Dent</u>

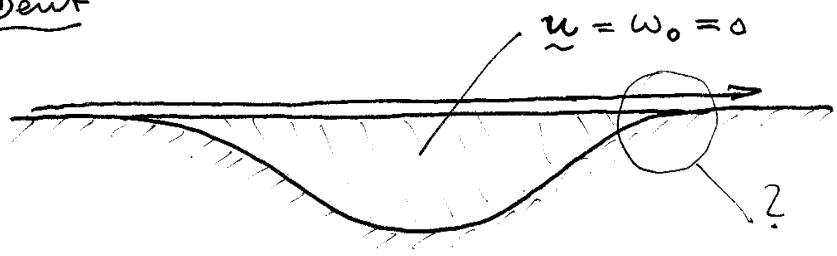

bump

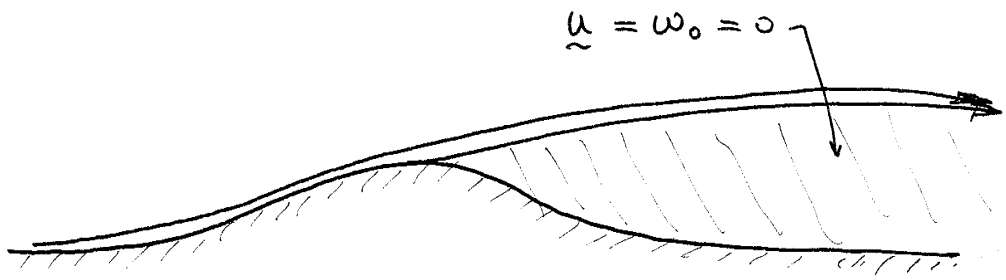

reattachment ?

combination

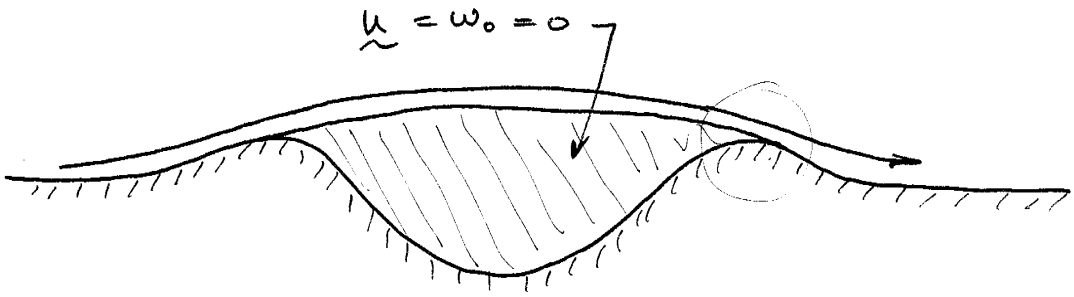

body

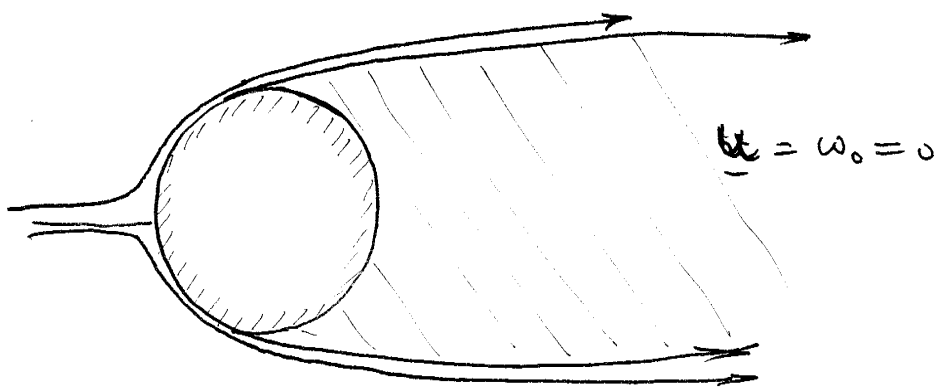

In each of these cases, the question arises about the closing of the separated flow region. Even if we disregard the phenomenon we observed in the photographs of Taneda, showing oscillations at the

closing saddle point of the separated region at $Re = 40$ i.e. the tendency toward unsteadiness, this problem is of substantial difficulty. If the flow is forced to remain steady, the "triple deck" treatment of the reattachment, which is possible, becomes a multiple deck treatment. Because in reality the flow always becomes unsteady at large Reynolds numbers, this treatment will be omitted here.

It is necessary to point out, however, that flow over bodies with corners is also amenable to the free streamline theory. J.H.B. Smith (1982) has analysed separation at a corner of angle δ, with the vortex sheet leaving the downstream side at an angle θ as shown. Many possibilities exist depending on the values of δ and θ. Some of the possible configurations are sketched here. In each case the enclosed regions may have finite vorticity.

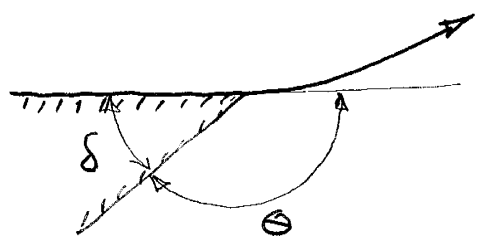

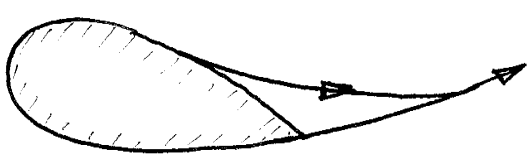

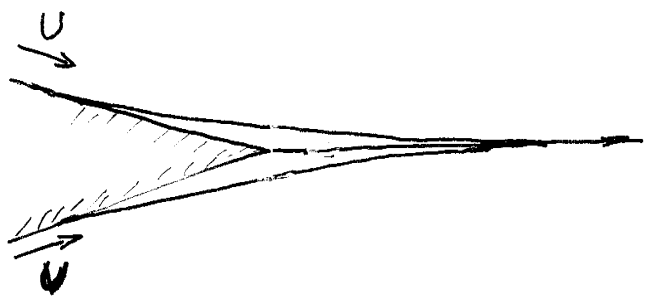

Symmetrical

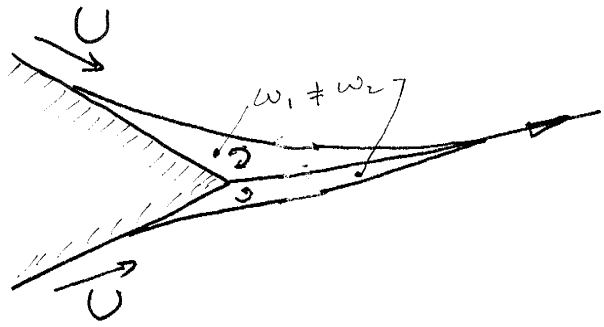

Small incidence

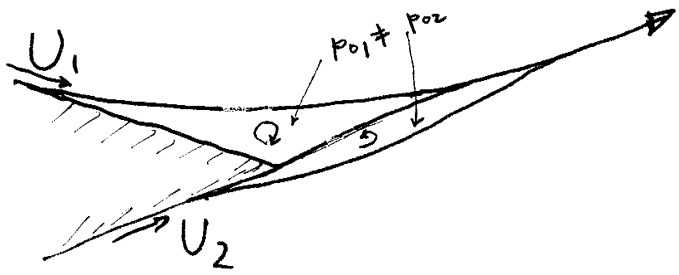

larger incidence
$U_1 \neq U_2$, $U_2 < U_1$

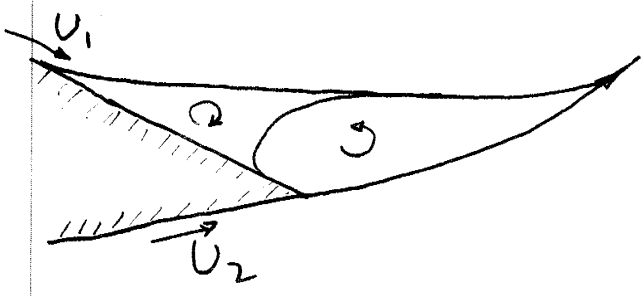

still larger incidence

Clearly these are of importance to aeronautics, many other possibilities exist and much work still needs to be done to understand this zoo and its behaviour at $Re \to \infty$ instead of at $Re = \infty$

References

Goldstein, S. Quarterly Journal of Mech. + App. Mech. 1 (1948) p. 43.

Stewartson, K. J. Fluid Mech. 44 (1970) p. 347

Smith, J.H.B. RAE-TR-77058 (1977)

Sychev, V.V. Fluid Dynamics 7 (1972) p. 407 (Izvestia Akad. Nauk (1972) p. 42)

Batchelor, G.K. J. Fluid Mech. 1 (1955) p 177

Kirchhoff, G. J. f. reine und angew. Math. 70 (1869) p. 289

Smith, F.T. J. Fluid Mech 92 (1979) p 171, + more recent papers

Smith, J.H.B. in "Vortex Motion", Hornung, Müller, ed. Vieweg 1982, p. 157.

Fornberg J. Fluid Mech (1980) also more recent papers

Henrici H. Z.F.W. 6 (1982) p 266.

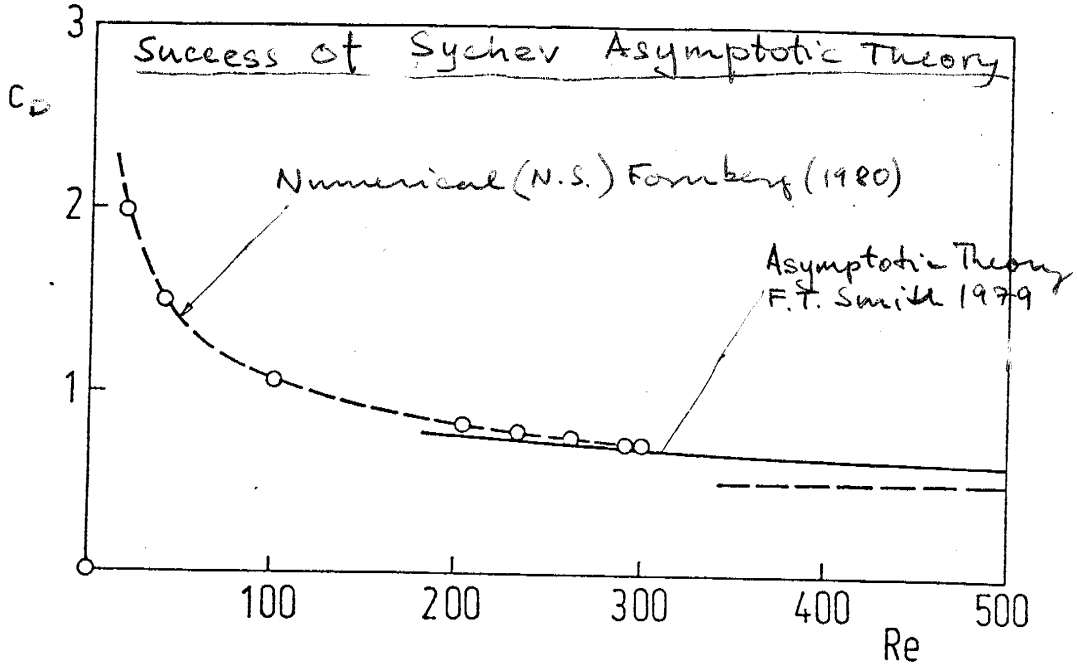

8. Instability, Turbulence

The asymptotic treatment assumes that the boundary layers and shear layers of the flow remain steady in the limiting process as $Re \to \infty$. This is physically not the case. Since, in a physical situation, the boundary conditions of a flow are never exactly steady, we have to live with unsteady disturbances. The two photos on the next page show the natural convection boundary layer on a heated plate in interferograms. Small disturbances are introduced in the form of a vibrating ribbon. Short wavelength disturbances are damped (left), longer wavelengths are amplified (right). The latter illustrates the instability of the laminar boundary layer, which, under suitable conditions may lead to turbulence.

Shear layers are even more unstable, so that a case (B) separation would always have an unsteady reattachment point, thus violating the assumptions made in the asymptotic treatment.

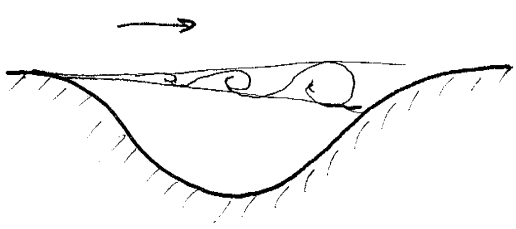

Sketch of linear stability theory for b.l.'s

The Orr-Sommerfeld theory assumes the arriving boundary layer flow to be independent of x (parallel streamlines) corresponding to $Re = \infty$. At the same time it takes Re to be finite. This is an inconsistency which makes it an approximate theory which does, however, give useful results. The steps in the theory are as follows

① Assume two-dimensional unsteady disturbances such that

$$u = U(z) + u'(x,z,t)$$
$$w = w'(x,z,t)$$
$$p = P(x,z) + p'(x,z,t)$$

primed variables small compared w. unprimed

② Substitute these in N.S. + C.

③ Assume that U, P satisfy steady N.S.+C.

Result of these three steps:

$$\left.\begin{aligned} &\frac{\partial u'}{\partial t} + U\frac{\partial u'}{\partial x} + w'\frac{\partial U}{\partial z} + \frac{1}{\rho}\frac{\partial p'}{\partial x} = \nu \operatorname{div}\operatorname{grad} u' \\ &\frac{\partial w'}{\partial t} + U\frac{\partial w'}{\partial x} + \frac{1}{\rho}\frac{\partial p'}{\partial z} = \nu \operatorname{div}\operatorname{grad} w' \\ &\frac{\partial u'}{\partial x} + \frac{\partial w'}{\partial z} = 0 \quad , \quad \begin{array}{l}\text{wall } u' = w' = p' = 0 \\ \text{far field } u' = w' = p' = 0\end{array} \end{aligned}\right\} \quad (8.1)$$

(4) Assume stream function of the form

$$\psi = \psi(x,z,t) = \phi(z)\, e^{i(\alpha x - \beta t)} \qquad (8.2)$$

for the disturbances, $\frac{\partial \psi}{\partial z} = u'$, $\frac{\partial \psi}{\partial x} = -w'$

This is a harmonic wave whose phase velocity is

$$c = c_r + i c_i = \frac{\beta}{\alpha}$$

If $c_i > 0$ the wave is amplified,
$c_i = 0$ neutrally stable
$c_i < 0$ damped

(5) Substitute (8.2) in (8.1) to get

$$(U-c)(\phi'' - \alpha^2\phi) - U''\phi = -\frac{i}{\alpha Re_\delta}(\phi'''' - 2\alpha^2\phi'' + \alpha^4\phi) \qquad 8.3$$

the Orr-Sommerfeld equation, with

$$\phi(0) = \phi'(0) = \phi(\infty) = \phi'(\infty) = 0$$

$$Re_\delta = \frac{U_\infty \delta}{\nu}$$

Solution method:

a) $U(z)$ is assumed known
b) Re, α are fixed
c) Solution yields an eigenvalue $c(\alpha, Re)$
If $c_i > 0 \rightarrow$ unstable.
Repeat with new α till $c_i = 0$
Repeat with new Re etc.

The resulting stability boundaries are

sketched in Re, α space

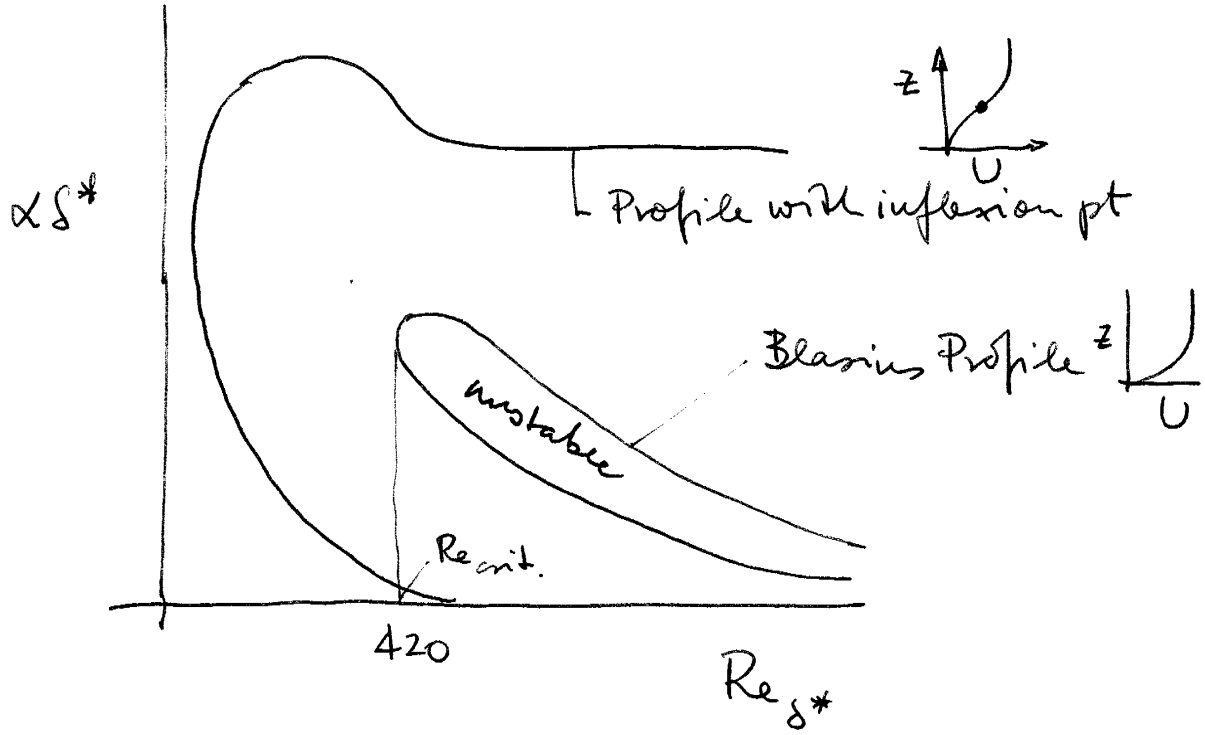

In the case $Re \to \infty$, the Orr Sommerfeld equation degenerates to

$$(U-c)(\phi''-\alpha^2\phi)-U''\phi=0, \qquad (8.4)$$

which indicates that, at an inflexion point of U $(U''=0)$, $U=c$ or $c_i=0$, neutral stability. This means that inflexional profile boundary layers are unstable for low enough wave numbers at all wave numbers.

Other factors affecting stability (except Re, α, $U(z)$)

- curvature of the wall
- temperature gradient
- three-dimensional disturbances

Transition to turbulence

As soon as a laminar boundary layer becomes unstable, larger disturbances appear only short distances downstream of the instability, in the wake of which a "turbulent spot" grows linearly with downstream distance as it propagates downstream. In the turbulent spot the disturbance amplitudes are large, they no longer may be treated by linear theory. Longitudinal vortical structures remain after the passage of a turbulent spot (see photos) for some time. The more frequently turbulent spots appear, the more probable it is that they grow together to fill the entire boundary layer. This becomes impossible to avoid once the stability boundary Reynolds no. (eg. $Re_{\delta^*} = 420$ for Blasius) is exceeded by a sufficient amount. The formation of turbulent spots is then so frequent that the whole b.l. exhibits non-linearly large and unpredictably occurring disturbances: turbulent boundary layer.

An important property of turbulent boundary layers may be seen from the

photos: The b.l. edge at a fixed time exhibits large spatial variation, the edge of the turbulent region exhibits large incursions of regular flow. The turbulent vortical structures exhibit a strong preferred direction. They appear to lean downstream at an angle of ~ 45°.

The complex four-dimensional phenomenon of turbulent boundary layers has not been modelled successfully mathematically.

Turbulent boundary layer

The next best thing to do is to treat the turbulent boundary layer as a phenomenon that possesses temporal averages for all dynamical variables, and to derive new equations which relate these averages to each other by making averages of the unsteady equations. Because the equations of motion are nonlinear, this leads to quantities that are functions of averages over products of the unsteady components of the flow. These lead, for example to the Reynolds stress terms, which behave in a manner that may not be determined from the equations without

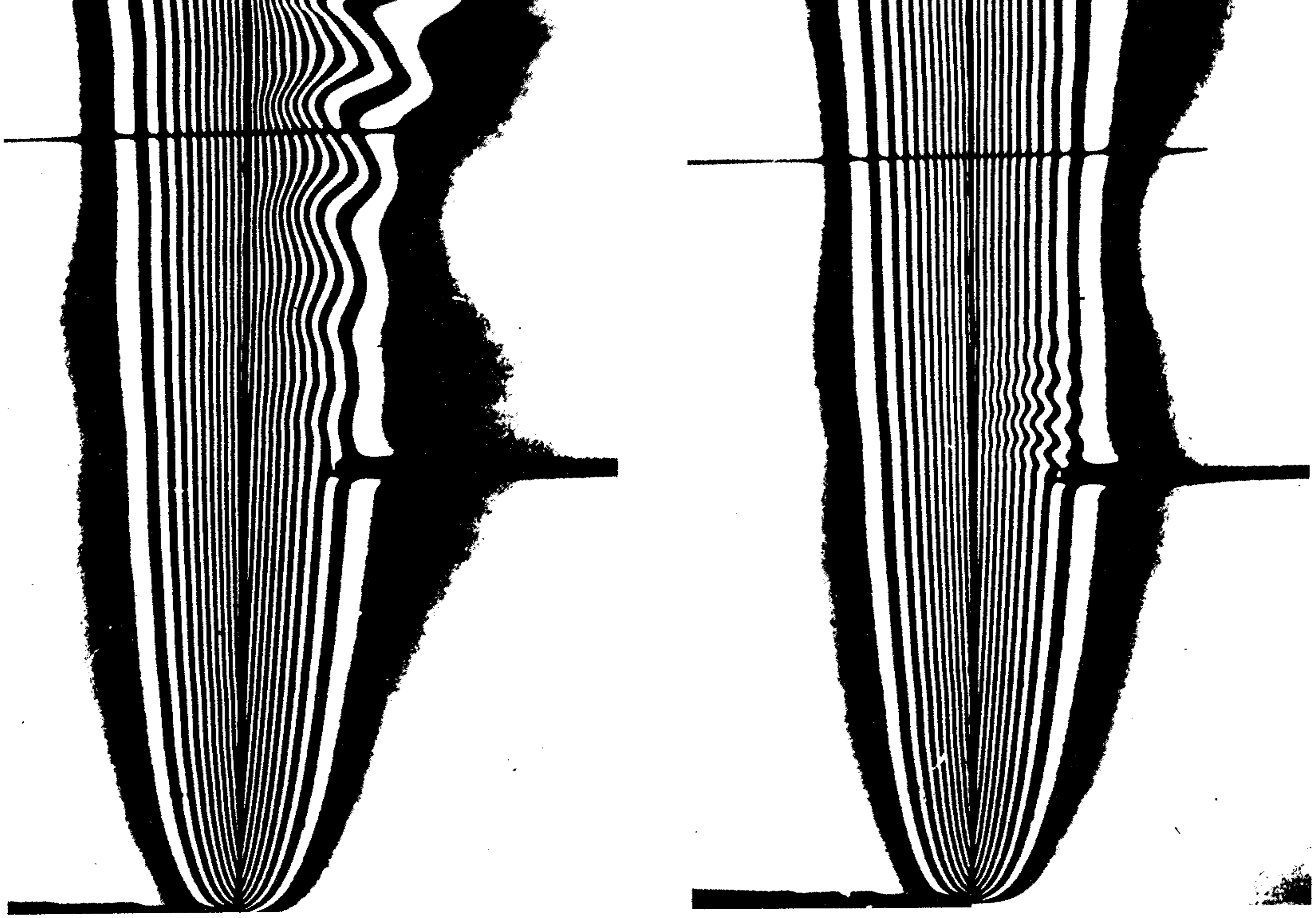

214. Instability in convection from a vertical plate. A ribbon is oscillated in the laminar free-convection boundary layer on an electrically heated foil in nitrogen at 16 atmospheres. Interferograms magnified six-fold in width show disturbances damped on the left at 11.5 Hz but amplified on the right at 3 Hz, in accord with linear stability theory. Polymeropoulos & Gebhart 1967

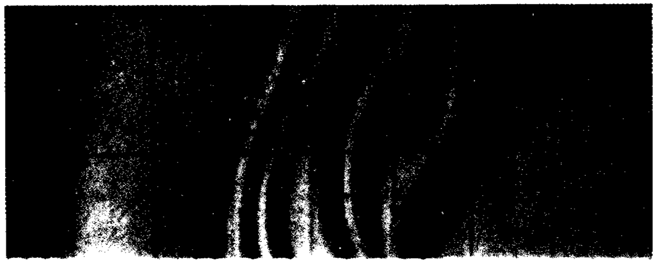

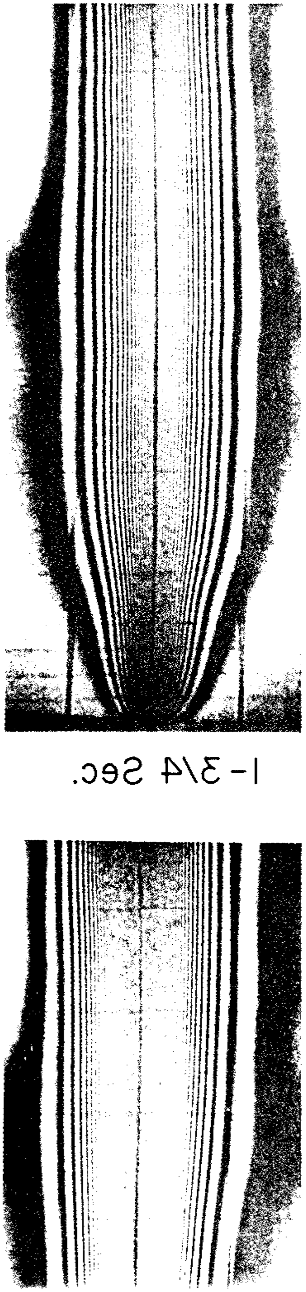

159. Sublayer of a turbulent boundary layer. A suspension of aluminum particles in a stream of water shows the streaks in the sublayer of a turbulent boundary layer on a flat wall. A mirror is used to show a simultaneous side view. *Cantwell, Coles & Dimotakis 1978*

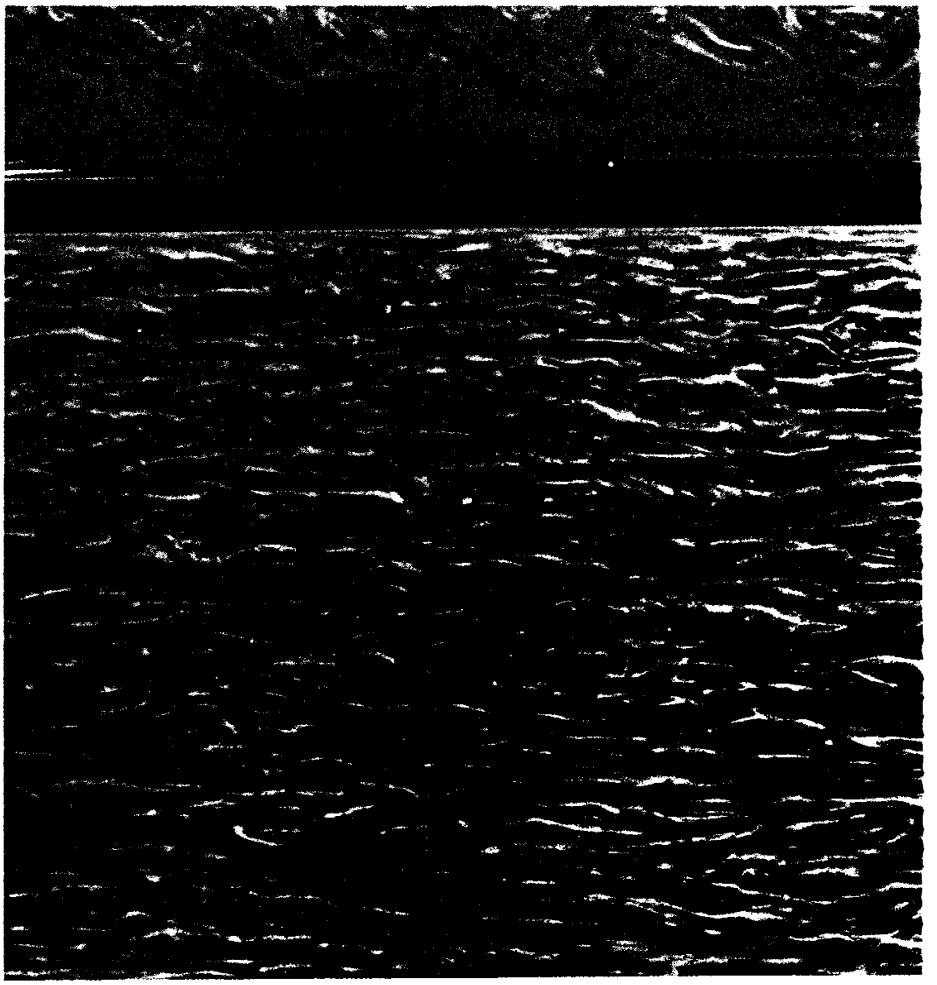

160. Detail of the sublayer. A close-up view of smoke in the turbulent boundary layer on a wind-tunnel floor shows "pockets" and streaks in the viscous sublayer. *Falco 1980*

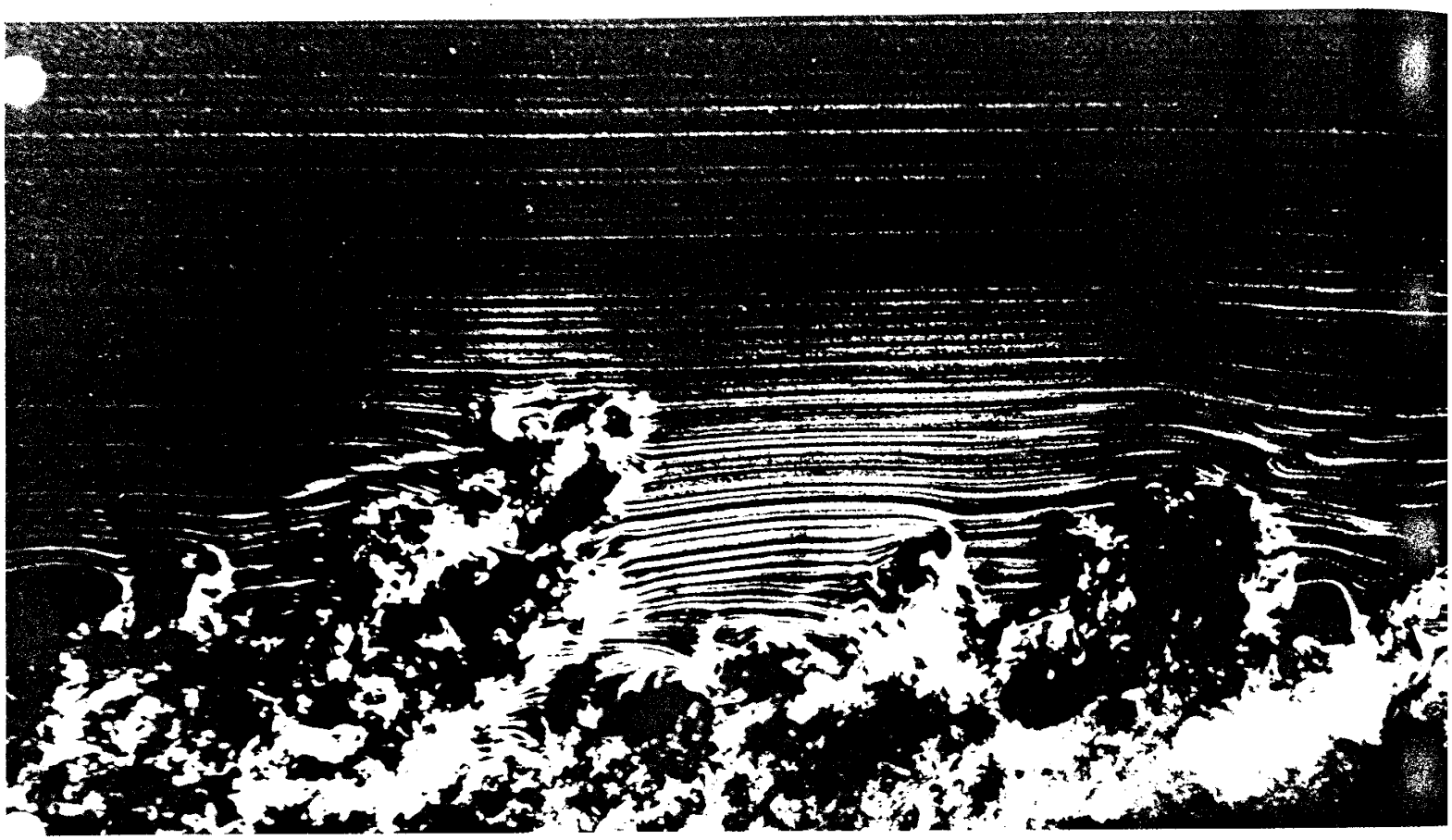

157. Side view of a turbulent boundary layer. Here a turbulent boundary layer develops naturally on a flat plate 3.3 m long suspended in a wind tunnel. Streaklines from a smoke wire near the sharp leading edge are illuminated by a vertical slice of light. The Reynolds number is 3500 based on the momentum thickness. The intermittent nature of the outer part of the layer is evident. *Photograph by Thomas Corke, Y. Guezennec, and Hassan Nagib.*

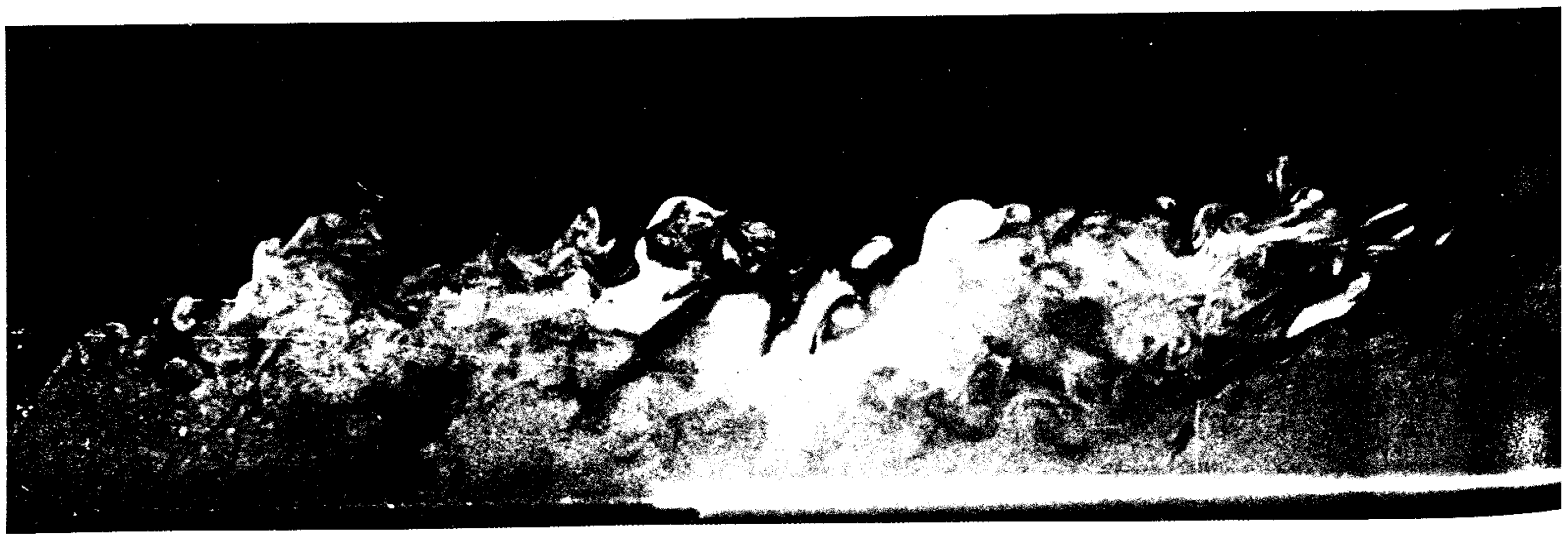

158. Turbulent boundary layer on a wall. A fog of tiny oil droplets is introduced into the laminar boundary layer on the test-section floor of a wind tunnel, and the layer then tripped to become turbulent. A vertical sheet of light shows the flow pattern 5.8 m downstream, where the Reynolds number based on momentum thickness is about 4000. *Falco 1977*

$R=100{,}000$

$R=200{,}000$

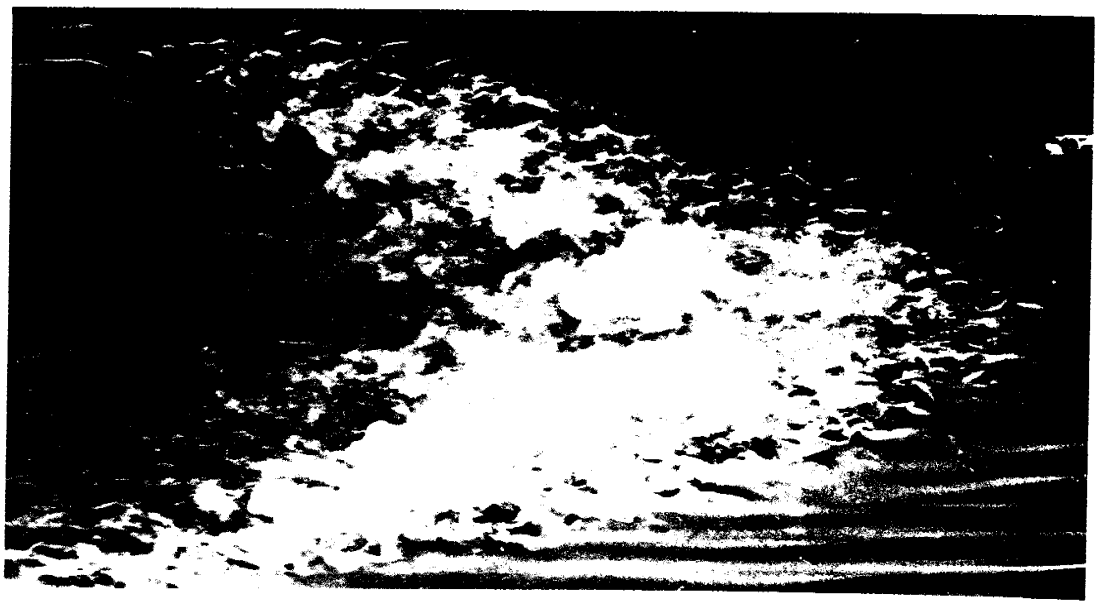

$R=400{,}000$

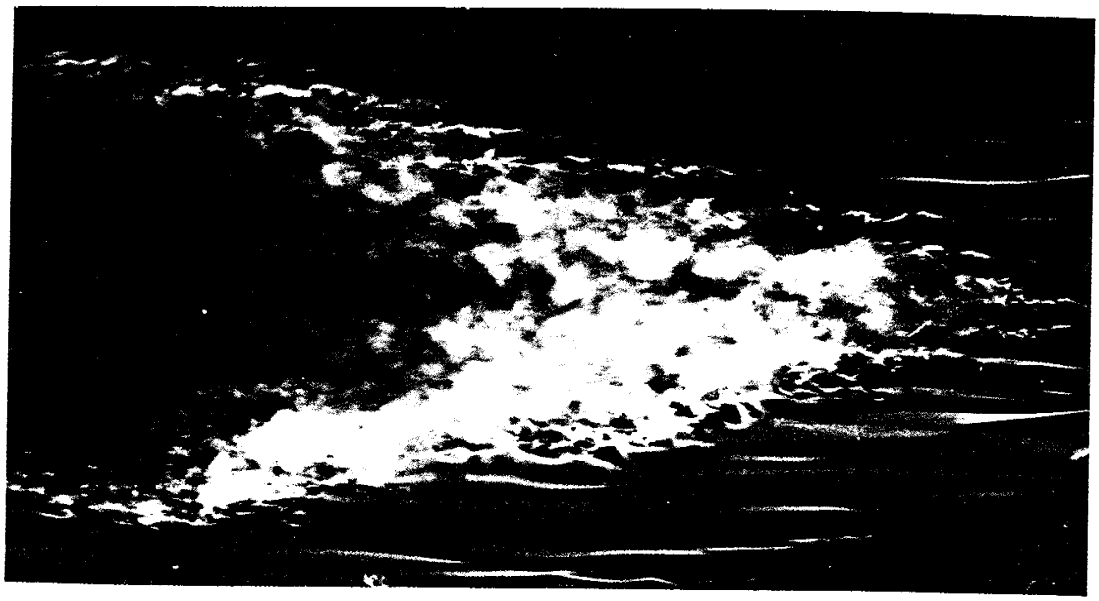

111. Turbulent spot at different Reynolds numbers. The outline of the spot becomes more regular, and the angle of its leading edge steeper, as the Reynolds number increases. Visualization is by smoke in air with flood lighting. *Photograph by R. E. Falco*

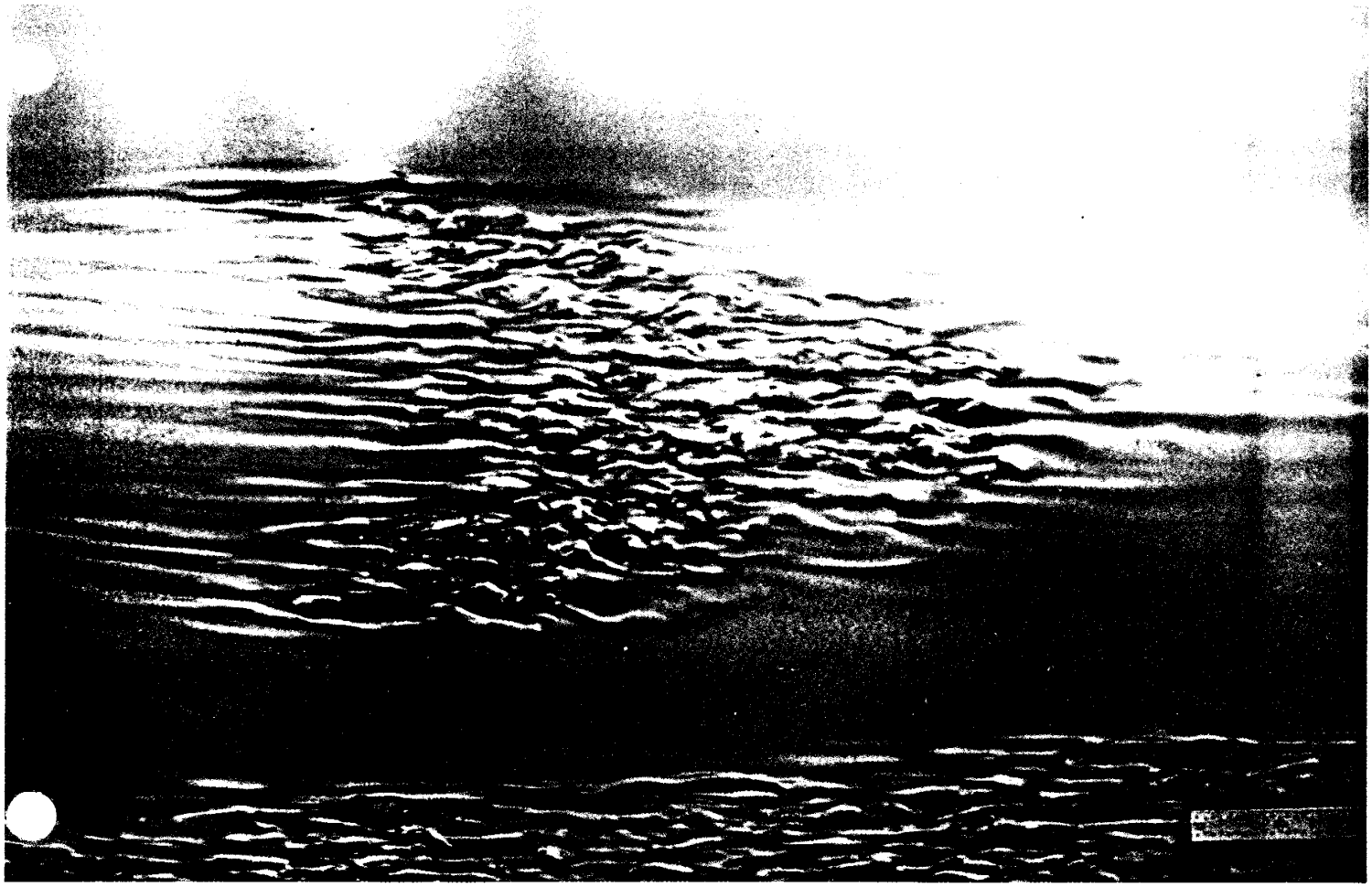

109. Emmons turbulent spot. On a flat plate, transition from a laminar to a turbulent boundary layer proceeds intermittently through the spontaneous random appearance of spots of turbulence. Each spot grows approximately linearly with distance while moving downstream at a fraction of the free-stream speed, and maintaining the characteristic arrowhead shape that is shown here by a suspension of aluminum flakes in water. Transverse contamination is seen spreading from the bottom of the channel. At the center of the spot the Reynolds number is 200,000 based on distance from the leading edge. *Cantwell, Coles & Dimotakis 1978*

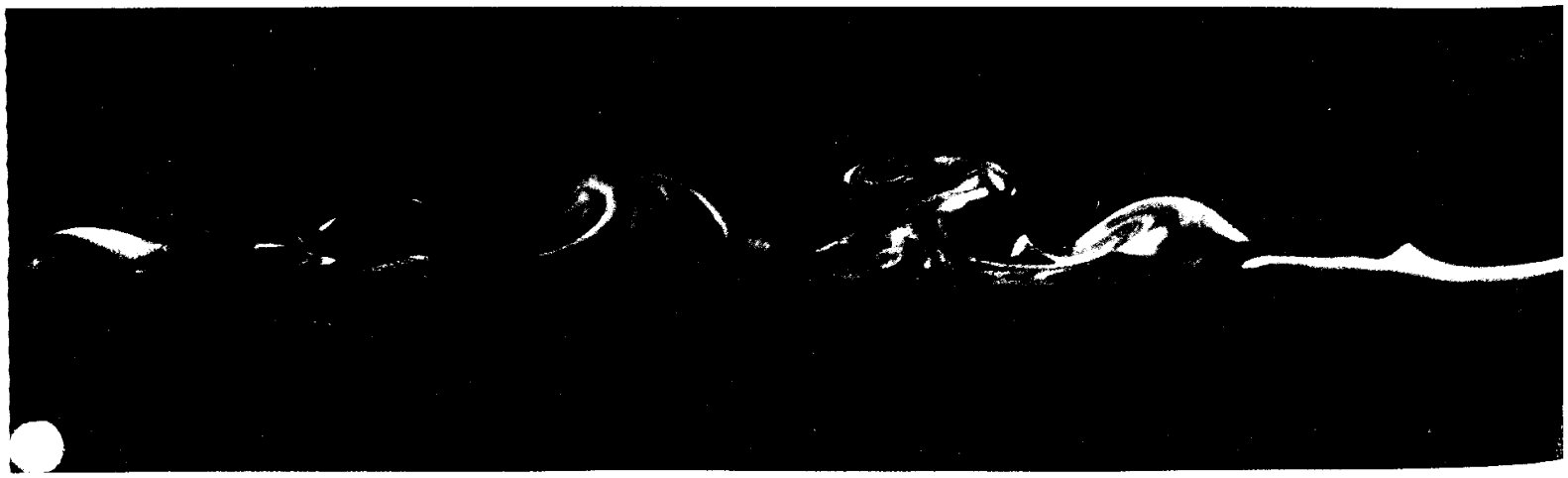

110. Cross section of a turbulent spot. A turbulent spot at an early stage of development is seen in a cross section normal to the stream. Smoke in a wind tunnel is illuminated by a sheet of laser light. *Perry, Lim & Teh 1981*

solving the unsteady problem. In certain benign situations a phenomenological approach together with dimensional analysis leads to a useful model for the mean flow in turbulent boundary layers.

<u>Law of the Wall and Defect Law</u>

In the turbulent b.l. the mean velocity u depends on the following variables:

$$u = u\left(\rho, \eta, \tau_w, \delta, z, \frac{dp}{dx}, \text{roughness, etc}\right) \quad (8.5)$$

Assume a smooth wall and neglect the influence of the ceiling. In the immediate vicinity of the wall ($z \ll \delta$) also neglect the effect of δ. Then, for a flat plate at zero incidence ($\frac{dp}{dx} = 0$)

$$u = u\left(\rho, \eta, \tau_w, z\right) \quad (8.6)$$

Applying dimensional analysis,

$$\boxed{\frac{u}{u_\tau} = f\left(\frac{z u_\tau}{\nu}\right)}, \quad u_\tau = \frac{\tau_w}{\rho}. \quad (8.7)$$

This is called the Law of the Wall.

In the immediate vicinity of the wall, any vortical motion (with axis // wall) must have a scale no larger than the distance from the wall.

Right at the wall, the stress must therefore be purely viscous,

$$\tau = \tau_w = \eta\left(\frac{\partial u}{\partial z}\right)_w$$

Asymptotically, for $z \to 0$, the law of the wall must therefore become

$$\lim_{\frac{z u_\tau}{\nu} \to 0} \frac{u}{u_\tau} = \frac{z u_\tau}{\nu} \qquad (8.8)$$

Right at the wall, the law of the wall is therefore independent of the pressure gradient! Ludwieg and Tillmann (1949) have shown experimentally that this independence of the law of the wall from the pressure gradient applies also at larger distances from the wall. If may be determined by experiment, it has "universal" character in the sense that a large class of turbulent boundary layers obey it.

In the outer part of the boundary layer where the scale of the vertical flow can be of the same order as the thickness δ, it makes more sense to discuss the velocity defect $U-u$ relative to the free stream velocity U. Since the viscous stress is relatively unimportant compared to the Reynolds stresses,

in this region, it is appealing to assume that η is not important. Hence write

$$U-u = \text{fn. of } \left(\tau_w, \rho, \delta, z, \frac{dp}{dx}\right)$$

or

$$\boxed{\frac{U-u}{u_\tau} = g_1\left(\frac{z}{\delta}, \frac{\delta}{\tau_w}\frac{dp}{dx}\right)} \qquad (8.9)$$

This is called the Defect Law. When $\frac{\delta}{\tau_w}\frac{dp}{dx}$ = constant (e.g. for flat plate = 0, for pipe flow = −2) it follows that

$$\frac{U-u}{u_\tau} = g\left(\frac{z}{\delta}\right). \qquad (8.10)$$

This behaviour is also substantiated by an extensive body of experimental data.

The features of $f(zu_\tau/\nu)$ and of $g(z/\delta)$ may be illustrated in diagrams.

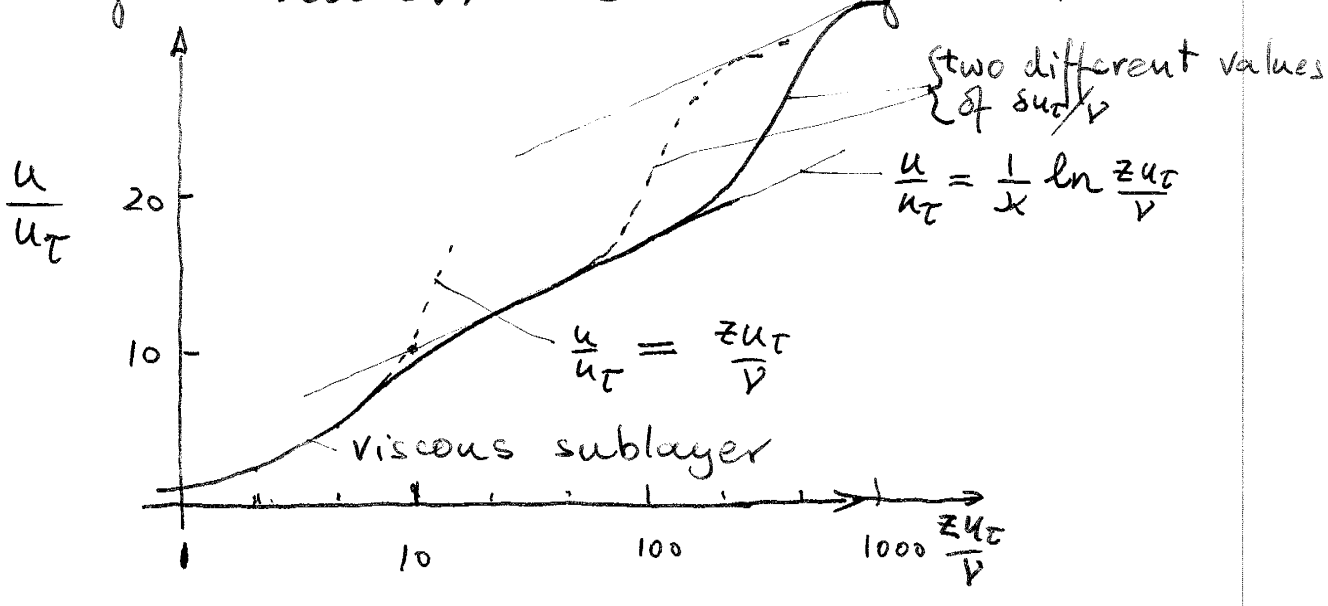

The behaviour close to the wall is linear, there is a logarithmic region and a departure from the logarithmic behaviour which is of the same form for a given constant value of $\frac{\delta}{\tau_w}\frac{dp}{dx}$ but shifted (in these coordinates) depending on $\delta u_\tau/\nu$.

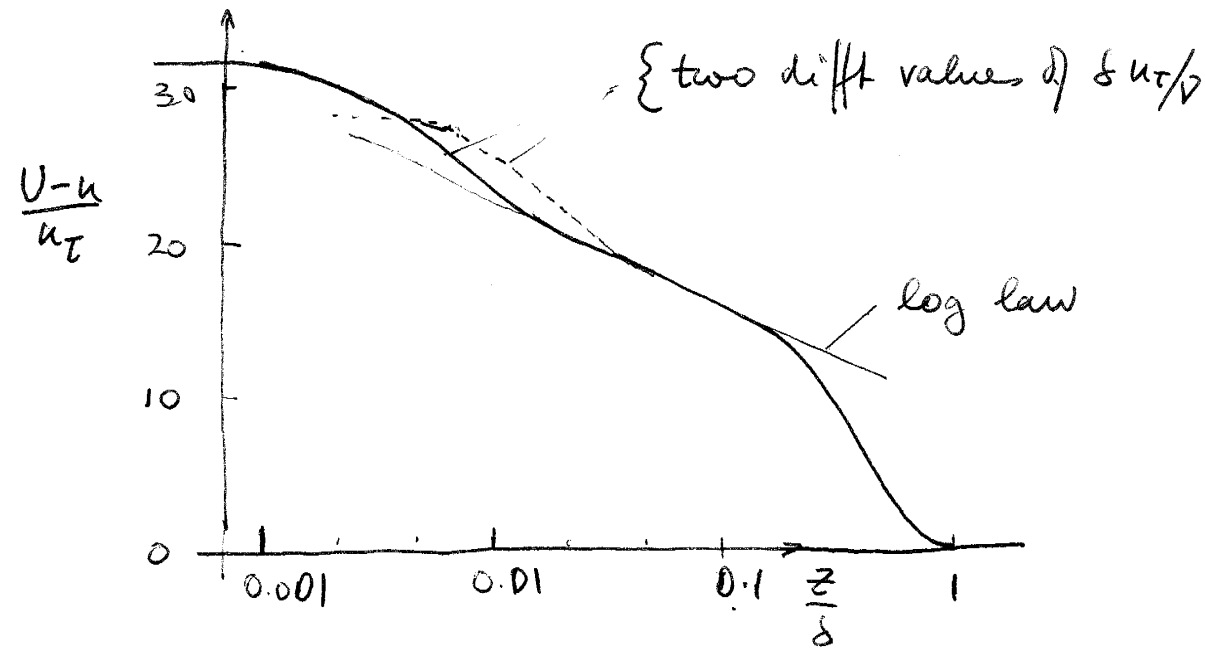

If the same data are plotted in "defect coordinates", they collapse at the outer edge of the b.l. and in the logarithmic region and disperse in the "viscous sublayer". The fact that the deviation of the velocity profile from the logarithmic law of the wall is of a form which depends only on $\frac{\delta}{\tau_w}\frac{dp}{dx}$ (if constant) was recognized by Coles (1956), who also found experi-

mentally that for all boundary layers with constant $\frac{\delta}{\tau_w}\frac{dp}{dx}$, the departure from the logarithmic law may be written in the separation of variables form:

$$\boxed{\frac{u}{u_\tau} = \frac{1}{\kappa}\ln\left(\frac{z u_\tau}{\nu}\right) + \Pi\left(\frac{\delta}{\tau_w}\frac{dp}{dx}\right) W\left(\frac{z}{\delta}\right)} \quad (8.11)$$

where the function W "wake function" is closely approximated by $W \doteq \frac{1}{2}\left(1-\cos\frac{\pi z}{\delta}\right)$, and the function Π is determined by experiment to increase strongly with increase of its argument. At $\frac{\delta}{\tau_w}\frac{dp}{dx} = -2$, as in pipe flow, it is nearly zero.

The law of the wall and wake function describe the behaviour of the <u>mean</u> flow field of a <u>class of t.b.l.'s</u> fairly well and are based on a phenomenological ~~[illegible]~~ set of arguments and on experiment. The description they give <u>does not apply</u> to situations where $\delta/\tau_w \frac{dp}{dx}$ varies with x or where rapid or spatially abrupt changes occur in the boundary conditions.

9 Effect of turbulence on separation

Averageing and diffusion

If there were no thermal molecular motion in a gas, it would not have a viscosity. In a continuum model the thermal motion is averaged. This causes the viscosity to emerge as a material property.

This may be illuminated by considering a simple shear flow with constant du/dz. Let the thermal motion be characterized by its characteristic velocity $\sqrt{RT} \sim a$ and the mean free path λ. Thus, the kinematic shear stress τ/ρ depends on du/dz, a, λ. Applying dimensional analysis to this gives

$$\frac{\tau}{a\lambda\rho\frac{du}{dz}} = f\left(\frac{du}{dz}\frac{\lambda}{a}\right). \qquad (9.1)$$

Now consider the symmetry of f with respect to flow reversal. For stable fluids, τ must oppose the deformation rate, i.e. f must be an even function. If f is regular near the origin of its argument f must therefore become

constant K, say, as its argument goes to zero.

$$\therefore \quad \tau = K\rho\lambda a \frac{du}{dz}\left(1 + O\left(\frac{du}{dz}\frac{\lambda}{a}\right)^2\right), \qquad (9.2)$$

$$\text{or} \quad \frac{\eta}{\rho} = \nu = K\lambda a. \qquad (9.3)$$

The kinetic theory of gases yields the numerical constant K to be $O(1)$. Thus the property of diffusivity is brought about by averaging over the molecular motion to form a continuum model.

In a similar way the averaging over the turbulent unsteady motion leads to the Reynolds stresses which may be thought of as turbulent momentum diffusion. The characteristic length must here be considered as the distance over which a vortical structure of the turbulence maintains its identity. In a turbulent boundary layer this is likely to be of the order of the distance from the wall. The characteristic velocity scale is likely to be u_τ. Thus we expect a turbulent diffusivity

$$\nu_T \sim z u_\tau \qquad (9.4)$$

in a turbulent boundary layer. This is in fact a fairly good approximation in a turbulent wall shear.

The ratio of the turbulent to the molecular diffusivity is thus

$$\frac{\nu_T}{\nu} \sim \frac{z u_\tau}{\nu} \sim Re \sqrt{C_f} .$$

This suggests that as the Reynolds number increases, an increasing dominance of the turbulent diffusivity may be expected. An indication of this behavior is given by the C_f - Re diagram

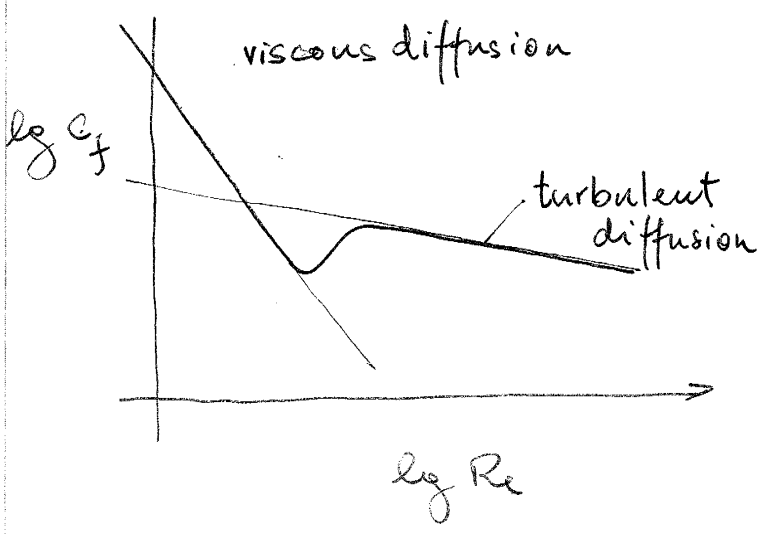

<u>Implications for separation.</u>

The question arises as to how the separation point would be moved if the diffusive transport is increased. Recall that in the Sychev theory the free streamline solution

gives the zeroth order location of separation and that it moves downstream, as diffusion is introduced, by an order $L\left(\frac{\nu}{LU}\right)^{\frac{1}{16}}$. Thus, expect the effect of turbulence to be a downstream shift of the separation point. This is exemplified by the behaviour of laminar and turbulent separation on a circular cylinder. In many ways the turbulent separation exhibits the <u>qualitative</u> features of a lower Reynolds number laminar separation:

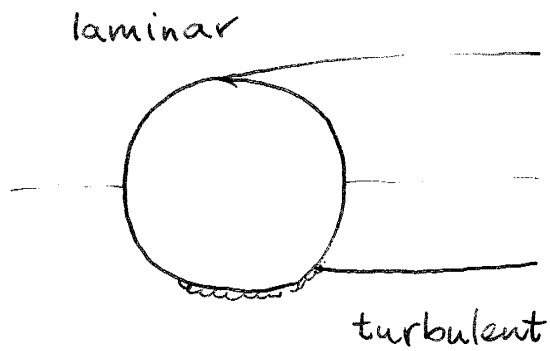

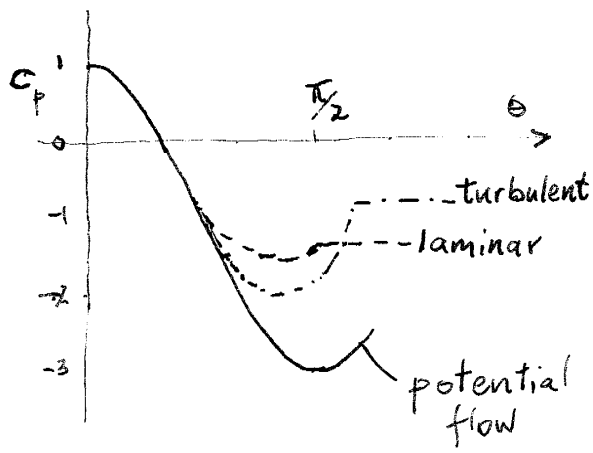

- separation pt further downstream,
- increased pressure rise to separation.

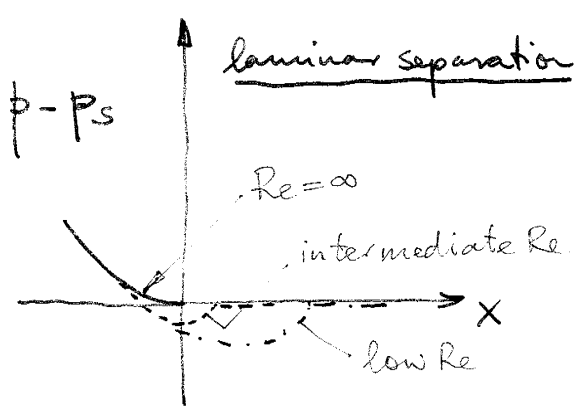

Compare this with the predictions of the Sychev theory shown at left for three Reynolds numbers.

To show the danger of using schematic sketches as C_p-θ above,

a plot of actually measured pressures is given here.

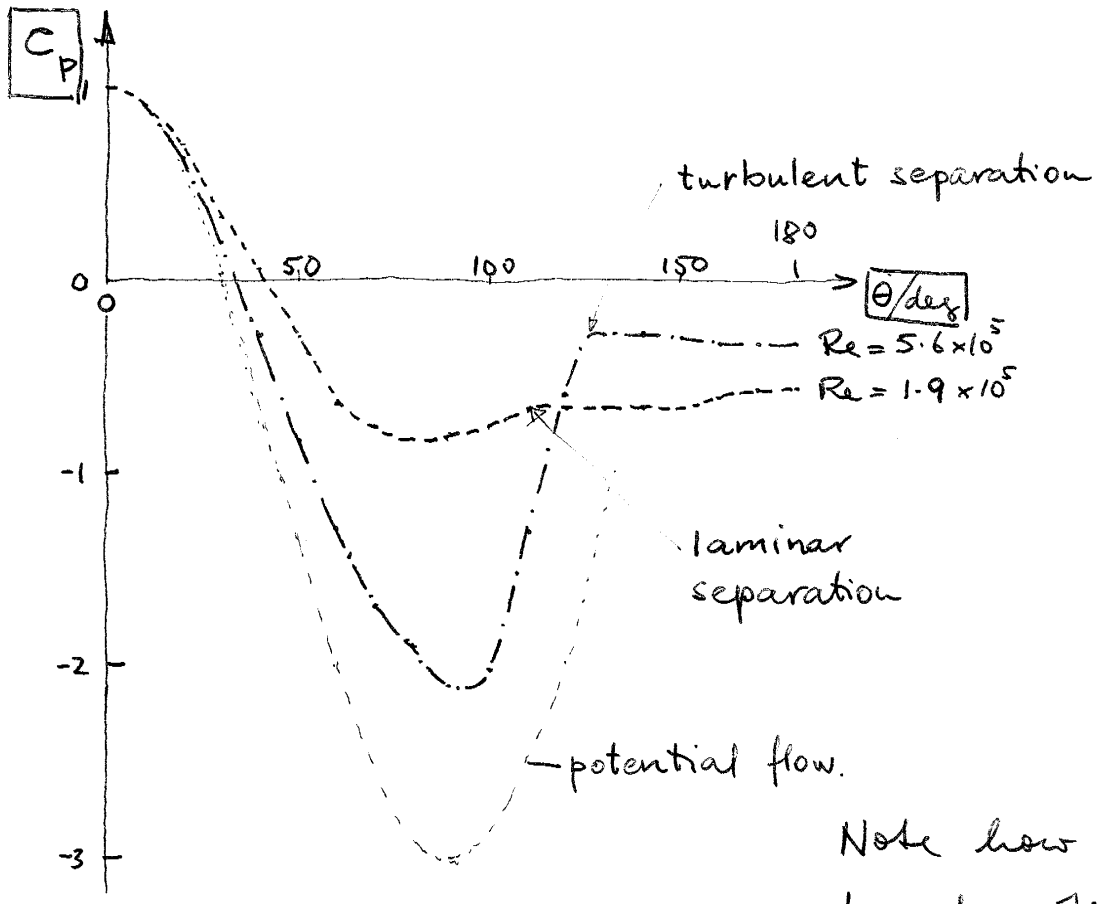

Note how the trend with Reynolds number goes opposite to the Sychev theory, but if Re were formed with the appropriate turbulent diffusivity, it would fit in with the Sychev theory.

The important conclusion is that a significantly stronger pressure gradient and a larger pressure rise can be withstood to separation by a turbulent boundary layer than by a laminar boundary layer.

An important practical point is that this conclusion applies if separation takes

place at a smooth surface without edges. At a sharp convex corner, the zeroth order solution always gives separation. Also, lowering the Reynolds number from $Re = \infty$ will not cause this separation point to move away from the edge, because this would cause an infinite pressure gradient to appear at the edge. ~~Separation therefore always occurs~~ A sharp corner is therefore always ($Re \geq 40$) a separation point, and the Reynolds number dependence of separation location is restricted to ~~smooth~~ continuous slope surfaces.

10. Location of separation in practical situations

To complete the discussion of two-dimensional steady-flow separation, we look at the practical implications of the discussion so far. If the flow has (nominally) steady and two-dimensional boundary conditions, even a turbulent flow separation will have a temporal mean which is two-dimensional and steady. This steady 2-d flow has streamlines which are such that in a separated region, they are closed. At sufficiently high Reynolds number, separation is controlled essentially by the pressure gradient at the wall, and by the condition of the boundary layer. We may therefore take a guess at the location of separation by using continuity and Bernoulli to guess the pressure distribution

$$p + \frac{1}{2}\rho u^2 = \text{const}$$

$$u A = \text{const} \qquad [\rho \text{ const.}$$

with A = streamtube area. A sketch of the streamline pattern gives a guess at $A(x)$. Continuity then gives a guess at $u(x)$ and Bernoulli a consequent guess at $p(x)$.

We do this in several examples now.

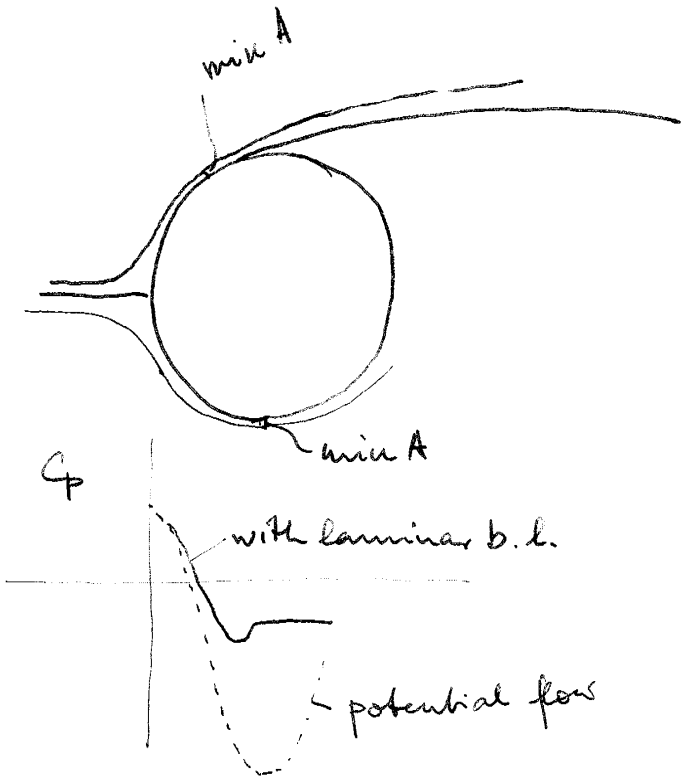

On bodies with smooth surfaces, the stream tube exhibits a narrowest cross-sectional area beyond which an adverse pressure gradient exists which may lead to separation. This causes the location of A_{min} to change so that the pressure gradient is also changed, and the guess may have to be iterated on.

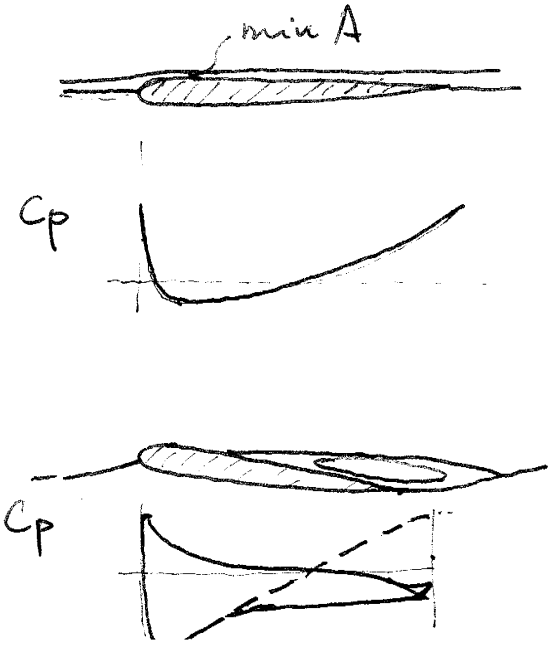

Small adverse gradients do not cause the boundary layer to separate, larger pressure gradients do. E.g. suction side of airfoil.

The separated shear layer of a laminar flow separation may become unstable, go turbulent and reattach as a turbulent boundary layer, producing a short separation "bubble". This may even happen in situations where the pressure gradient is still adverse, the turbulent b.l. being able to remain attached in a larger adverse pressure gradient than the laminar one. Usually, such separation bubbles exhibit three-dimensional structure.

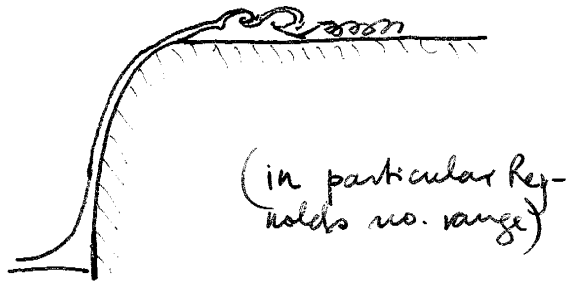

Sharp corners would exhibit infinite pressure gradient at the area minimum in irrotational flow. Sharp edges always lead to separation in incompressible flows unless Re is very small. The condition of the boundary layer (laminar or turbulent) does not influence this.

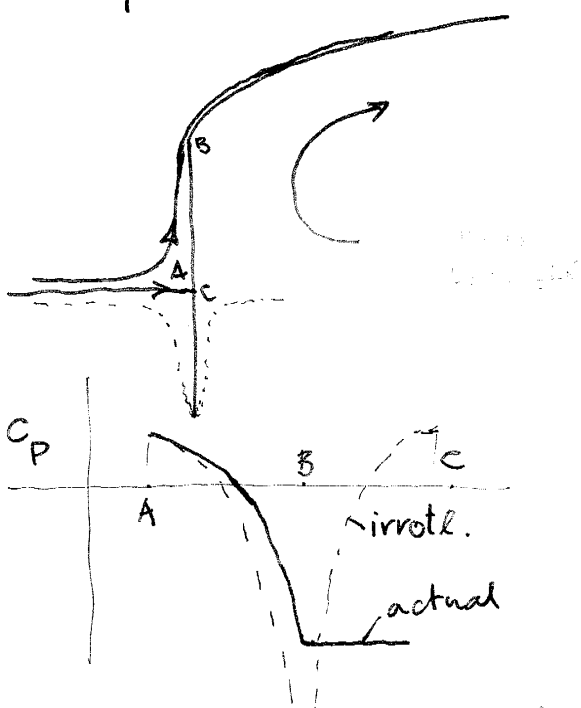

<u>Body with forward splitter plate</u>. The pressure field upstream of the body causes the pressure to increase along the splitter plate. At some point this is sufficient to separate the b.l. causing a bubble to appear in the junction and the pressure distribution to change as shown.

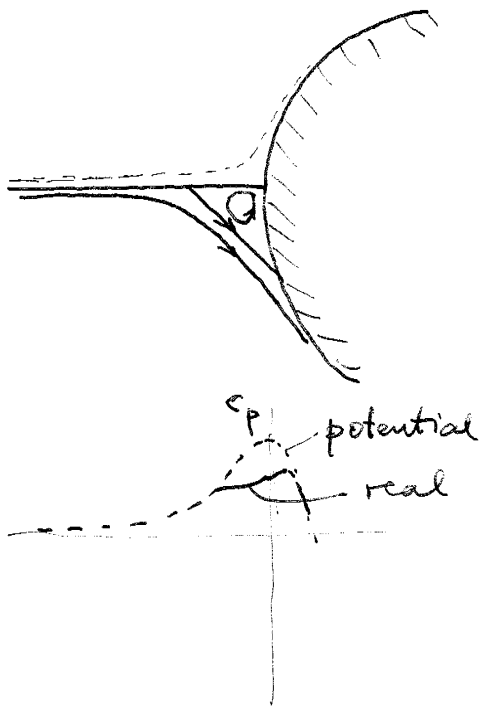

Internal flows may be treated by the same principles, however, they often exhibit bistability: As soon as separation occurs on one side, the pressure gradient is reduced sufficiently to cause the b.l. to remain attached on the other side. In internal flows a situation where Reynolds number dependent and Re independent flows occur

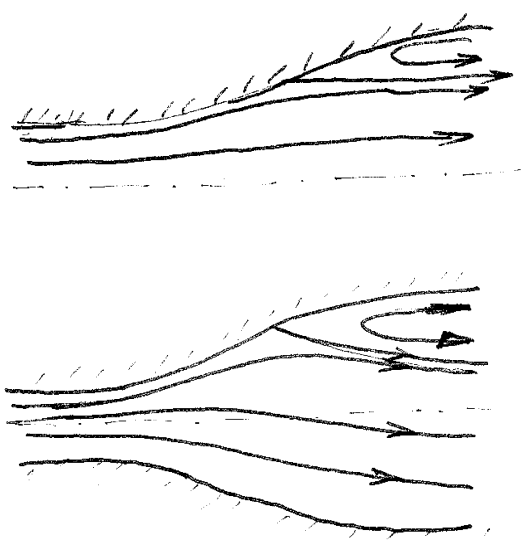

together is common: Upstream of an area reduction, the situation is like that on a splitter plate. At the convex corner, the separation is Re-independent.

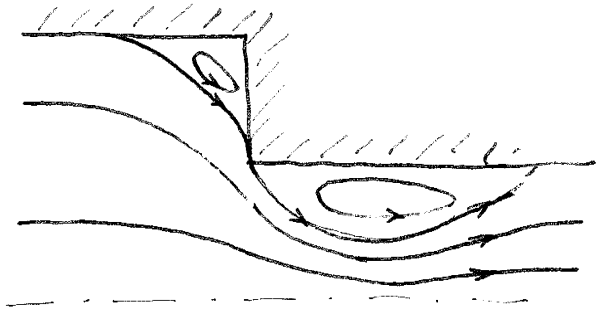

Before moving to three-dimensional steady separation it is important to point out a topological feature of 2-d steady separation: In 2-d steady separated flows, the separation streamline is also the reattaching streamline. Separated regions are regions of <u>closed</u> streamlines

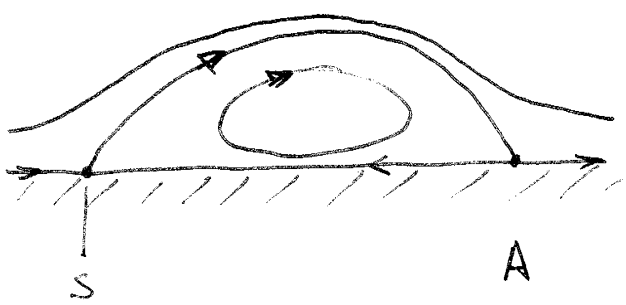

$t=1.0$ s

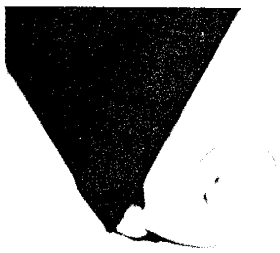

3.0 s

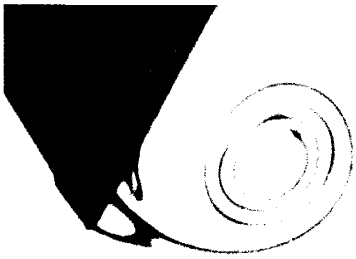

$t=5.0$ s

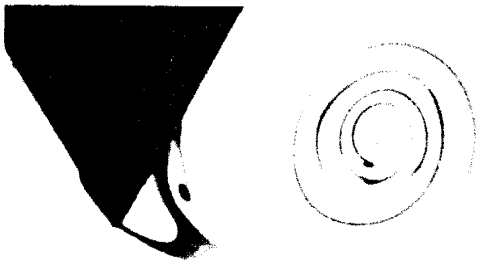

7.0 s

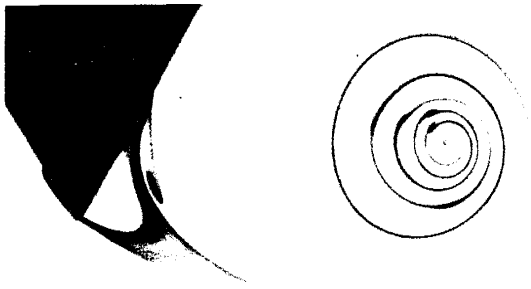

$t=9.0$ s

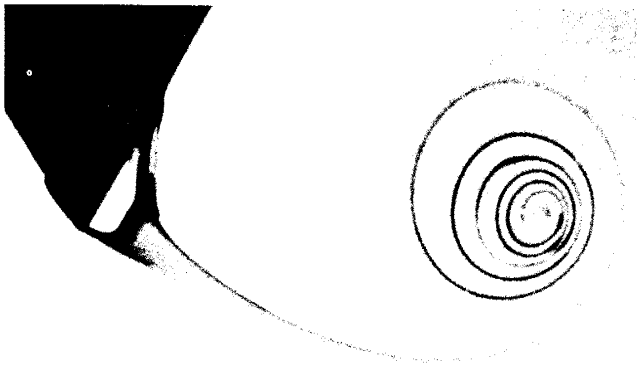

11.0 s

$t=13.0$ s

80. Starting vortex on a wedge. A piston drives water with almost constant speed normal to the axis of a wedge of 30° semi-vertex angle. Neutrally buoyant dye is injected into the water from small holes in the wedge surface. The characteristic Reynolds number is of order 1000. The piston stops at 12.5 s, producing a stopping vortex in the last photograph. *Pullin & Perry 1980*

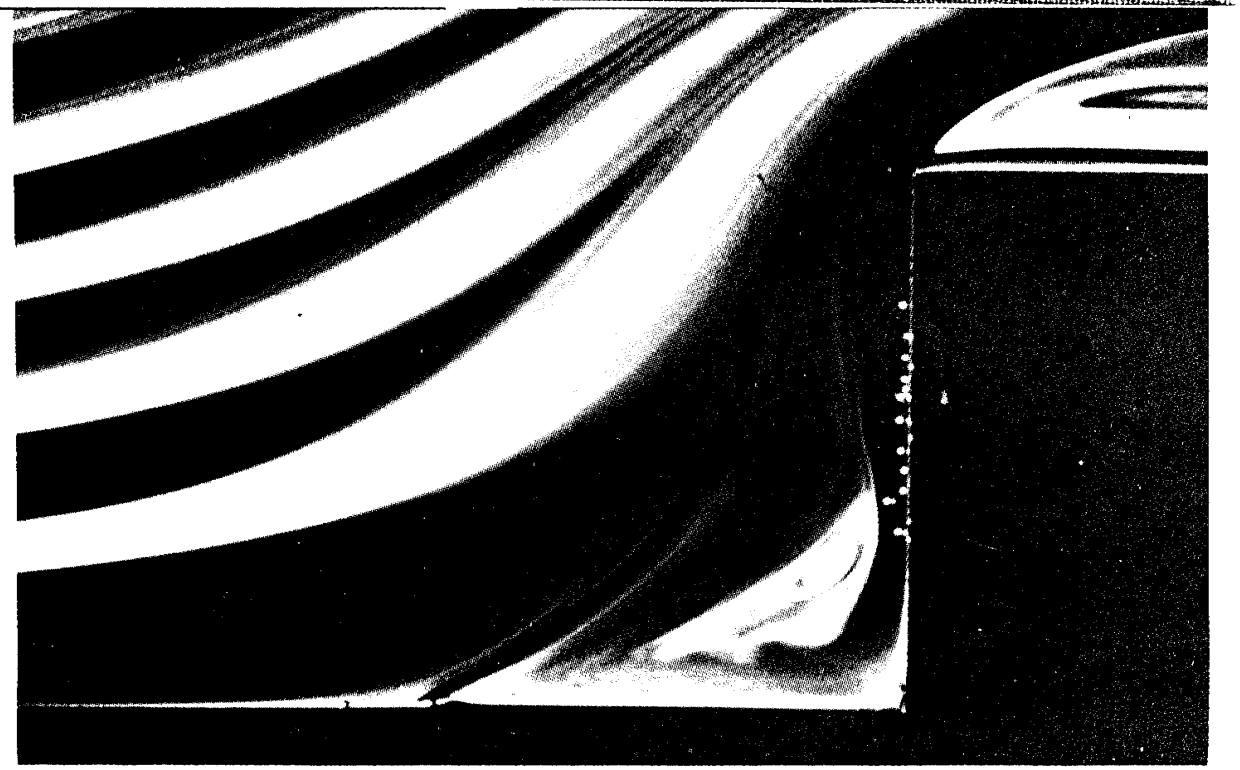

69. Laminar flow up a step. The obstacle spans a 1-mm gap between glass plates, as in the Hele-Shaw photographs of figures 1-5, but water gives a Reynolds number of 1000. The separation pattern is closer to that of figure 11 than of figure 5 or 39. Streamlines are shown by colored fluid. *ONERA photograph, Werlé 1960*b

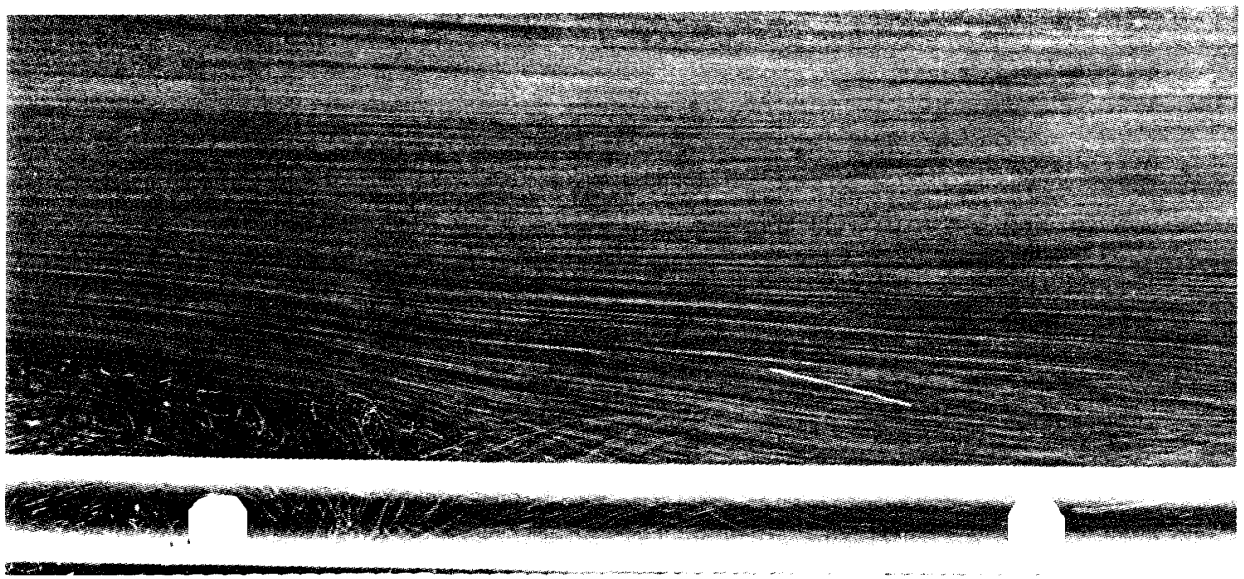

70. Axisymmetric flow down a step. At a Reynolds number of 10,000 based on body length, the boundary layer is laminar as it

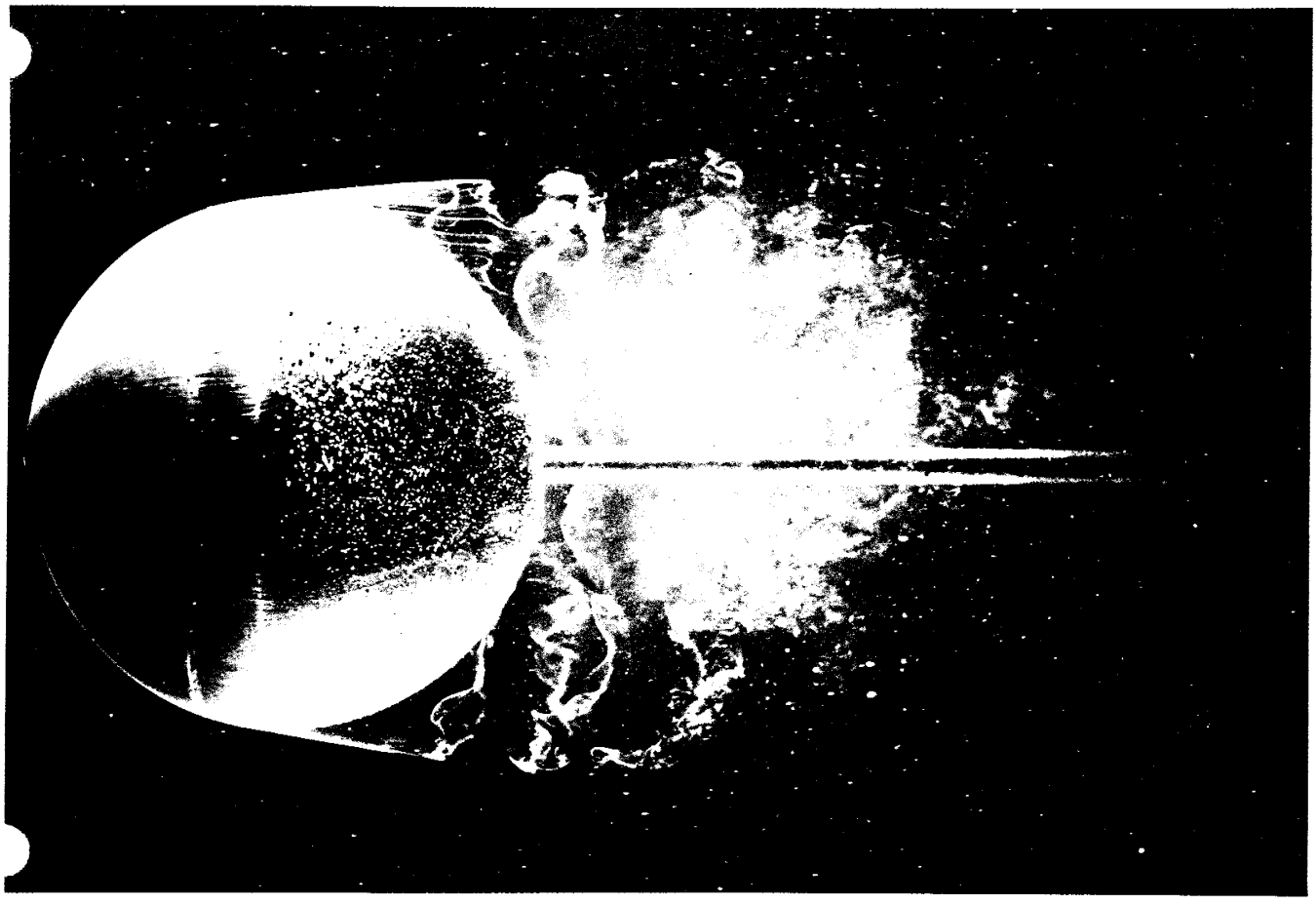

55. Instantaneous flow past a sphere at R=15,000. Dye in water shows a laminar boundary layer separating ahead of the equator and remaining laminar for almost one radius. It then becomes unstable and quickly turns turbulent. *ONERA photograph, Werlé 1980*

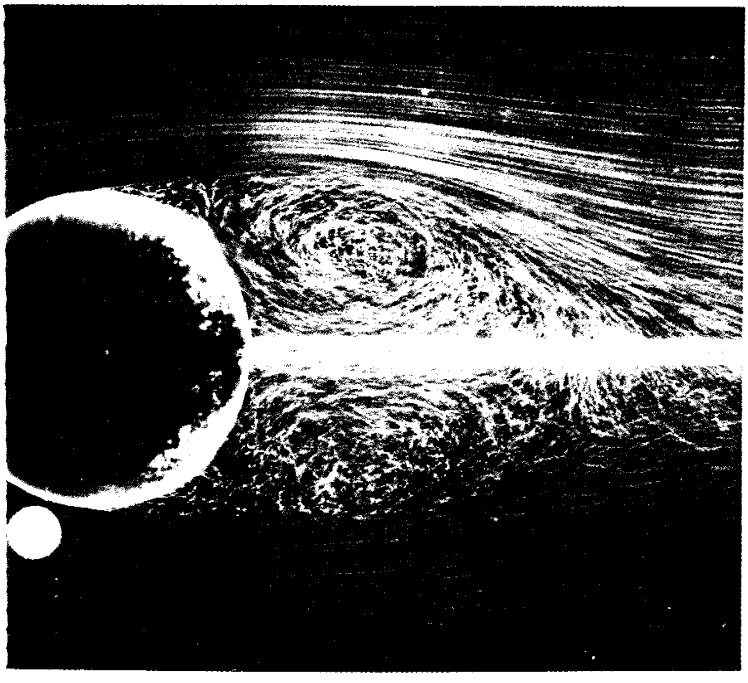

56. Mean flow past a sphere at R=15,000. A time exposure of air bubbles in water shows an averaged streamline pattern in the meridian plane for the flow that was photographed instantaneously above. *ONERA photograph by Henri Werlé*

11. Threedimensionality

It is convenient to subdivide the dimensionality of steady flows into four distinct levels. To do this, introduce the concept of a "streamsurface". Consider a curve that is fixed in the reference frame embedded in a steady flow field. The streamlines that pierce this curve form a surface which we call a streamsurface. A streamsurface is therefore defined by the generating curve and by the flow field. $\underset{\sim}{u}(\underset{\sim}{x})$

<u>Level 1</u> Flows for which cartesian coordinates (x_1, x_2, x_3) may be chosen in such a way that $\underset{\sim}{u}$ always lies in the $(x_1 x_3)$ plane or in a plane parallel to it. This means that a streamsurface generated by a curve contained in the $(x_1 x_3)$ plane is plane, and that derivatives w.r.t. x_2 are everywhere zero. (<u>Plane Flow</u>)

<u>Level 2</u> Flows for which orthogonal coordinates (x_1, x_2, x_3) may be chosen in such a way that $\underset{\sim}{u}$ is alloays contained in a plane that is normal to x_2. This means that a streamsurface generated by the

x_3 axis is plane and that derivatives w.r.t x_2 are zero everywhere. (<u>Axisymmetric flow</u>: x, θ, r; $\frac{\partial}{\partial \theta} \equiv 0$, $\underset{\sim}{u}$ in the (rx) plane.)

<u>Level 3</u> Flows for which orthogonal coordinates (x_1, x_2, x_3) may be chosen in such a way that derivatives w.r.t x_2 are everywhere zero. This means that $\underset{\sim}{u}$ ~~may~~ does not have to lie in the $(x_1 x_3)$ plane. This level will now be illustrated with examples.

a) <u>Infinitely long yawed cylindrical body</u>

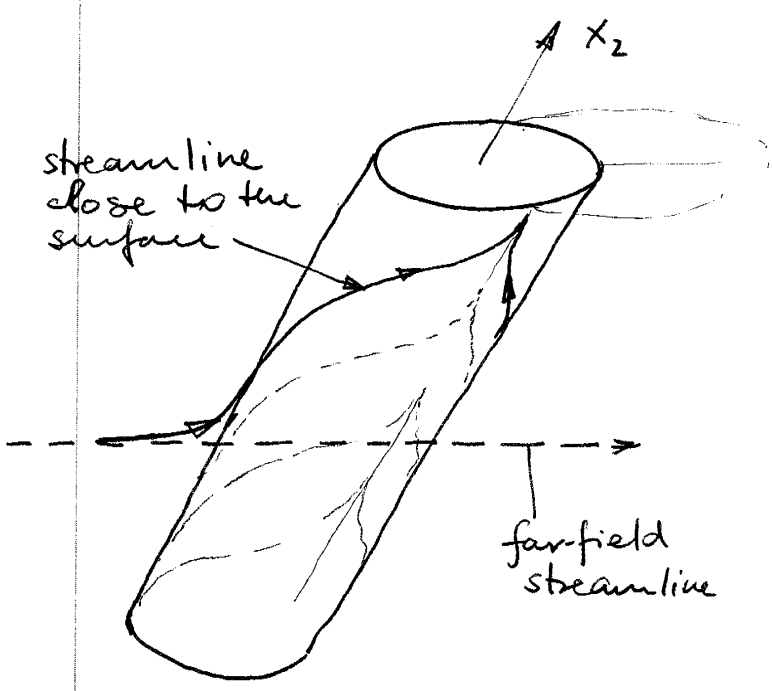

$\frac{\partial}{\partial x_2} \equiv 0$, but stream surfaces are not plane. Streamlines close to the surface and far-field streamlines do not remain in the plane they occupy far upstream. This means that the boundary layer in such a flow has a completely different character. The velocity direction changes with distance from the wall, not only within the wall-normal

plane, but also within the wall-parallel plane.

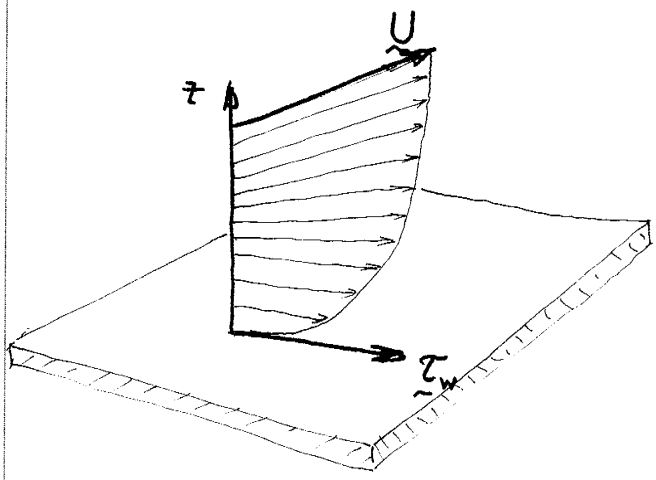

The velocity profile is "twisted". An attempt to sketch this state of affairs is made here. Near the wall, the velocity points in a direction // to $\underset{\sim}{\tau}_w$. At the b.l. edge it is parallel to $\underset{\sim}{U}$. $\underset{\sim}{U}$ and $\underset{\sim}{\tau}_w$ are not parallel.

b) <u>Axisymmetric flow with body rotation</u>

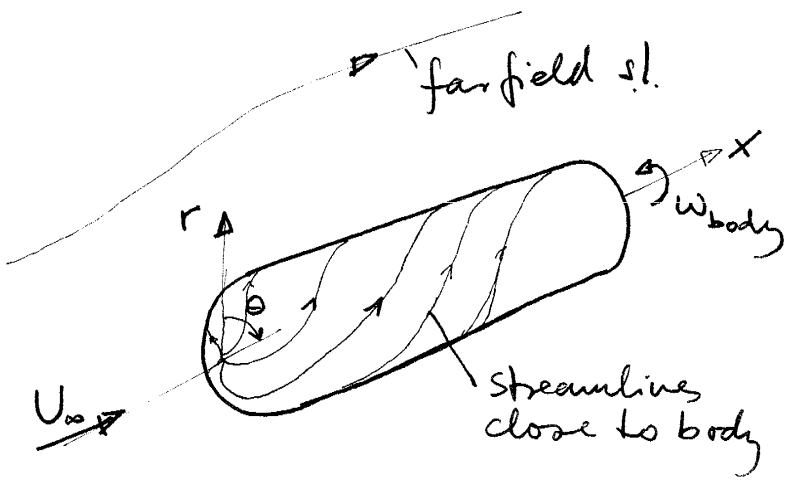

$\frac{\partial}{\partial\theta} \equiv 0$, but stream surfaces generated by the r-axis are not plane.

<u>Level 4</u> Flows, for which no orthogonal coordinates exist such that derivatives w.r.t. x_2 are everywhere zero.

Flows which belong to levels ① and ② are called <u>two-dimensional</u>. Those of level ③ are called <u>quasi two-dimensional</u>

Those in level (4) are called genuinely <u>three-dimensional</u>.

Each level contains the lower levels as special cases. The photographs show examples in flow visualizations.

Streamlines and streamsurfaces.

A two-dimensional steady flowfield can be uniquely described by streamlines. This is true for plane or axisymmetric flow. The streamline-field is the same in all of the planes $x_2 = \text{const}(=\theta)$

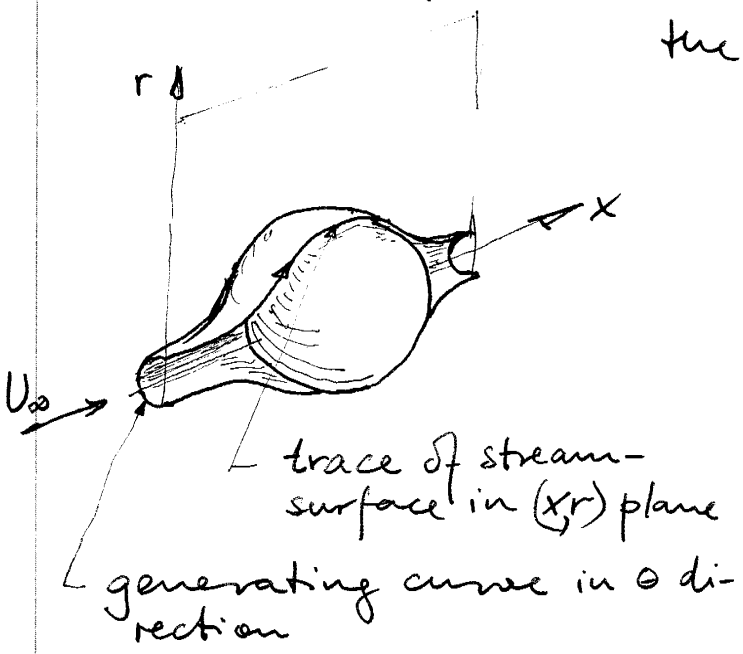

A streamline may be thought of as the trace in the (x,r)-plane of a streamsurface generated by a curve r = const. x = const. Since $\frac{\partial}{\partial\theta} \equiv 0$ and the θ-component of $\underset{\sim}{u} = 0$, this trace defines the streamsurface; i.e. the <u>streamline</u> field in an (x,r) plane defines the flow field unambiguously.

Separated Flows

In steady two-dimensional flows a separated flow region is distinguished by the feature that the streamlines within the separated region are closed curves, unlike those of the rest of the flow. The streamline that separates the two regions from each other is both a closed streamline and one that runs from upstream ∞ to downstream ∞. It consists of a separating streamline and the wall.

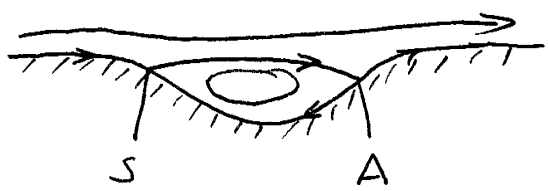

At S, the "wall" parts of the streamline unite to form the separating streamline, and at the pt. A the separating streamline bifurcates to form ~~into~~ the wall streamlines. Two-dimensional flows (streamline fields) always exhibit two bifurcation points, or half-saddle points at the wall, points where the separating streamline bifurcates. At A it bifurcates "positively" in the local streamline direction, at S it bifurcates "negatively". A separation point is therefore a <u>negative streamline bifurcation</u>.

The velocity is, of course, $= 0$ at the wall. A streamline is the integral curve of the direction field of $\underset{\sim}{u}(\underset{\sim}{x})$. The "wall streamline" can be defined only because, though the magnitude of $\underset{\sim}{u}$ is zero, its direction is defined everywhere except at bifurcation points. A particle at the wall never reaches the point S. It therefore never leaves the wall. The velocity along the separation streamline is also equal to zero at S and A.

12 Separation in three-dimensional steady flow

In plane flow a separation point is a negative streamline bifurcation. A stagnation point, like a reattachment point, is a positive streamline bifurcation. Streamline bifurcation points at a wall correspond to points at which the wall shear stress is zero. A streamline is able to separate one region of the flow from another.

We now wish to extend these concepts systematically to three-dimensional space. In the quasi two dimensional flow of an infinite yawed cylinder,

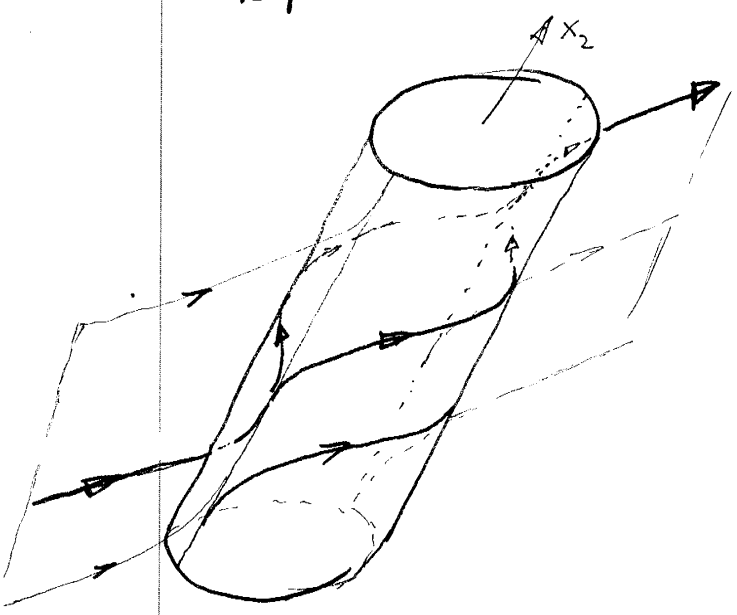

the stagnation point of two-dimensional flow is extended to a stagnation line, at which the stagnation stream-surface bifurcates positively. At the rear stagnation line a negative stream surface bifurcation forms the departing stagnation stream surface.

The property of this flow that $\frac{\partial}{\partial x_2} \equiv 0$, implies that the projection of this flow onto a plane

normal to x_2 is topologically the same as a corresponding two-dimensional flow. The only important difference between the two is that the wall shear stress does not have any zeros any more. In the two-dimensional flow, the bifurcation points had $\tau_w = 0$.

At stream surface bifurcations the wall streamlines (integral curves of direction field of $\underset{\sim}{\tau}_w$) converge onto the bifurcation line, if it is a negative bifurcation (separation) and diverge from it if it is a positive bifurcation. The arrow heads on the stream surfaces thus give the sign of the bifurcation.

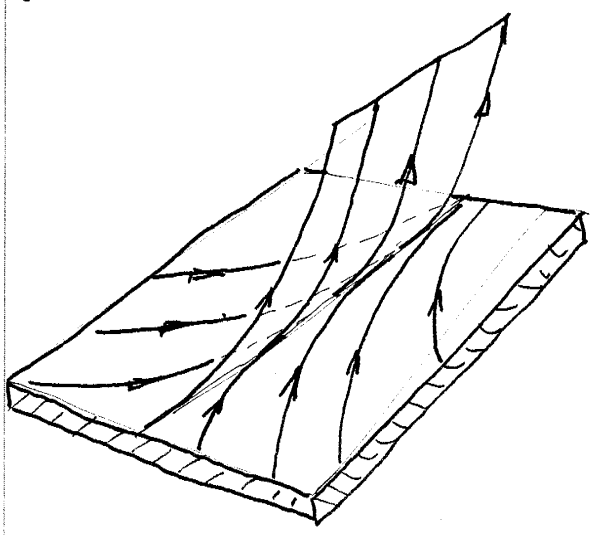

negative stream s. bifurcation

Of course, separation also occurs in quasi two-dimensional flows. If it does, it is accompanied by stream surface bifurcations. For example in the flow over a yawed cylinder, the separation may manifest itself as shown in two stream surface bifurcations S_2 and S_3 as shown:

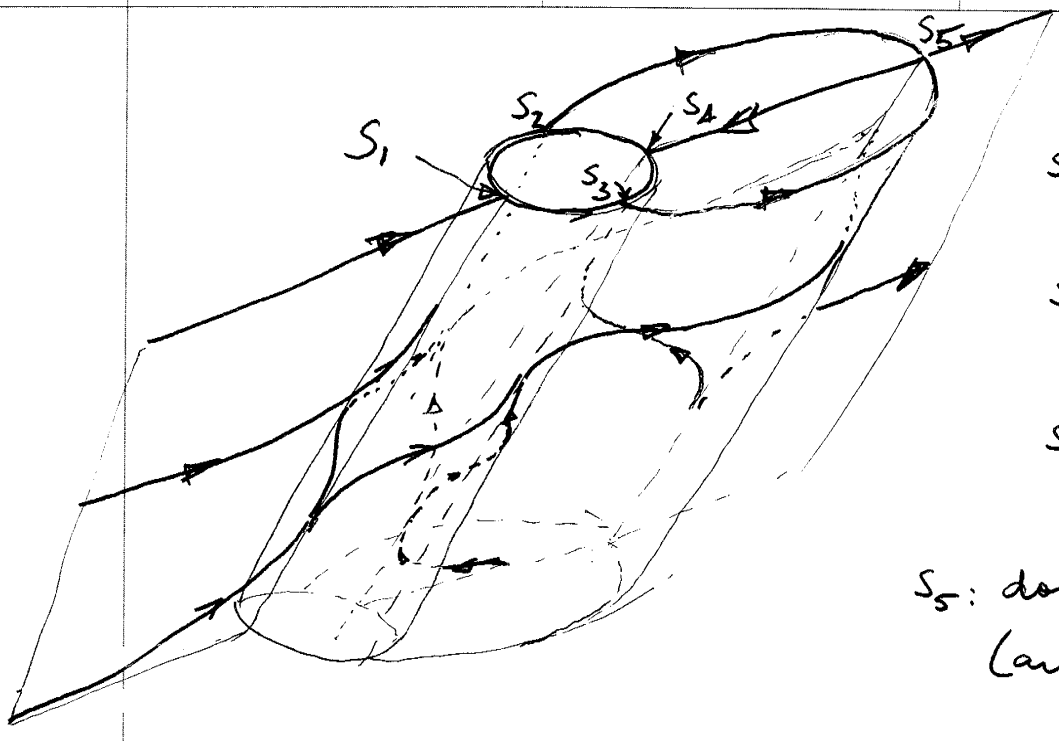

S_1 : positive bifurcation (attachment line)

S_2, S_3 : negative b. (separation lines)

S_4: positive b. (attachment line)

S_5: double b. (away from the wall)

Again, the wall shear stress field does not exhibit any zeros. For zeros to occur in τ_w we have to consider genuine three-dimensional flows of level 4. In order to understand such flows it is necessary to study the features of the flow in the vicinity of points where $\tau_w = 0$.

<u>Critical points in the wall streamline field</u>

A genuinely three-dimensional flow might exhibit a wall streamline pattern as shown in View A which contains two saddle points and two vortical nodes of ~~reattachment~~ separation (also called "stable foci". Each of these four points ~~correspond~~ is ~~to~~ a "critical point", in the

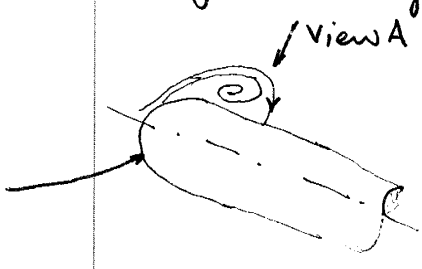

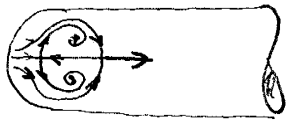

View A

sense that the direction of the wall streamlines at such points is indeterminate, $\tau_w = 0$.

We wish to write the velocity field in the vicinity of such critical points as a series expansion in powers of the space dimensions. This assumes that the flow field is regular. In general, such an expansion is of the form

$$u_i = A_i^1 + A_{ij}^2 x_j + A_{ijk}^3 x_j x_k + A_{ijkl}^4 x_j x_k x_l + \ldots \qquad (12.1)$$

where the A^n are the coefficients of the nth term and are tensor quantities of nth degree. For example, $x_j x_k$ is $x^2, y^2, z^2, xy, xz, yz$, etc.

At the wall, $u_i = 0$ because of the no-slip condition. It follows that $A_i^1 = 0$. Also,

$$\lim_{z \to 0} \left(\frac{\underset{\sim}{u}}{z} \right) = \text{const.} \qquad (12.2)$$

at any point on the wall ($z = 0$). It therefore makes sense to expand

$$\frac{\underset{\sim}{u}}{z} = B_i^1 + B_{ij}^2 x_j + \ldots \qquad (12.3)$$

instead of (12.1). Furthermore, at a critical point $\underset{\sim}{\tau}_w = 0$, so that $B_i^1 = 0$ for critical

points. We therefore write the expansion in the vicinity of a critical point $(x, y, z) = (0, 0, 0)$ as

$$\frac{\underset{\sim}{u}}{z} = \underset{\approx}{F}\,\underset{\sim}{x} + \ldots, \qquad (12.4)$$

or in matrix notation

$$\begin{bmatrix} \frac{u}{z} \\ \frac{v}{z} \\ \frac{w}{z} \end{bmatrix} = \begin{bmatrix} a_1 & b_1 & c_1 \\ a_2 & b_2 & c_2 \\ a_3 & b_3 & c_3 \end{bmatrix} \begin{bmatrix} x \\ y \\ z \end{bmatrix} + \ldots \qquad (12.5)$$

we now determine the elements of $\underset{\approx}{F}$ by substituting into the equations of motion. For constant density, the continuity equation demands that

$$c_3 = -(a_1 + b_1)/2. \qquad (12.6)$$

The nonlinear terms in the Navier-Stokes equation are of second order in the ~~space~~ coordinates, the leading order is

$$-\frac{1}{\rho}\,\mathrm{grad}\,p + \nu\,\mathrm{div}\,\mathrm{grad}\,\underset{\sim}{u} = 0$$

which leads to

$$c_1 = \frac{1}{\rho}\,p_x/2\nu \quad , \quad c_2 = \frac{1}{\rho}\,p_y/2\nu$$

It is convenient to introduce $P = \frac{p}{\rho}$, so that

$$c_1 = P_x/2\nu \quad , \quad c_2 = P_y/2\nu. \qquad (12.7)$$

Also the vorticity components are

$\underset{\sim}{\omega} = (\xi, \eta, \zeta)$ say and

$$\eta = \frac{\partial u}{\partial z} - \frac{\partial w}{\partial x}$$

$$= a_1 x + b_1 y + 2c_1 z - a_3 z$$

so that $\eta_x = a_1$ ——— (12.8)

Similarly,
$$\left.\begin{aligned} \eta_y &= b_1 \\ \xi_x &= -a_2 \\ \xi_y &= -b_2 \end{aligned}\right\} \quad \text{——— (12.9)}$$

Hence

$$\left.\begin{aligned} a_1 &= \eta_x & b_1 &= \eta_y & c_1 &= P_x/2\nu \\ a_2 &= -\xi_x & b_2 &= -\xi_y & c_2 &= P_y/2\nu \\ a_3 &= 0 & b_3 &= 0 & c_3 &= (\xi_y - \eta_x)/2 \end{aligned}\right\} \quad (12.10)$$

At a critical point the wall streamline direction is undefined. Thus

$$\left(\frac{dy}{dx}\right)_{WSL} = \left(\frac{v}{u}\right)_{z\to 0} = \left(\frac{v/z}{u/z}\right)_{z=0} = \frac{a_2 x + b_2 y}{a_1 x + b_1 y} = \frac{N}{D}.$$

The direction $\arctan\left[(dy/dx)_{WSL}\right]$ of the WSL has a well defined value unless $N = D = 0$, such as the critical points under study.

In the plane of the wall,

$$\begin{bmatrix} u/z \\ v/z \end{bmatrix} = \begin{bmatrix} a_1 & b_1 \\ a_2 & b_2 \end{bmatrix} \begin{bmatrix} x \\ y \end{bmatrix} \quad \text{——— (12.11)}$$

Write $\quad tr = a_1 + b_2$ ——— (12.12)

i.e. the trace of the matrix of coefficients, and

$$det = a_1 b_2 - a_2 b_1 \qquad (12.13)$$

the determinant of the matrix. The matrix then has two eigenvalues

$$\lambda_{1,2} = \frac{1}{2}\left[tr \pm \left((tr)^2 - 4det\right)^{\frac{1}{2}}\right] \qquad (12.14)$$

The values of λ_1 and λ_2 may be used to classify the type of critical point encountered. When $tr^2 - 4det > 0$ both eigenvalues are real and the critical point is a saddle (if $det < 0$) or a node (if $det > 0$). If $tr^2 < 4det$, the eigenvalues are complex and the critical point is a vortical node (focus) which is "stable" if $tr < 0$ and "unstable" if $tr > 0$. The sign of tr determines the direction of the arrows in the nodes, ($det > 0$). On the positive det axis the vortical node degenerates to a centre (closed streamlines. On the curve $tr^2 = 4det$ the node degenerates to a star node

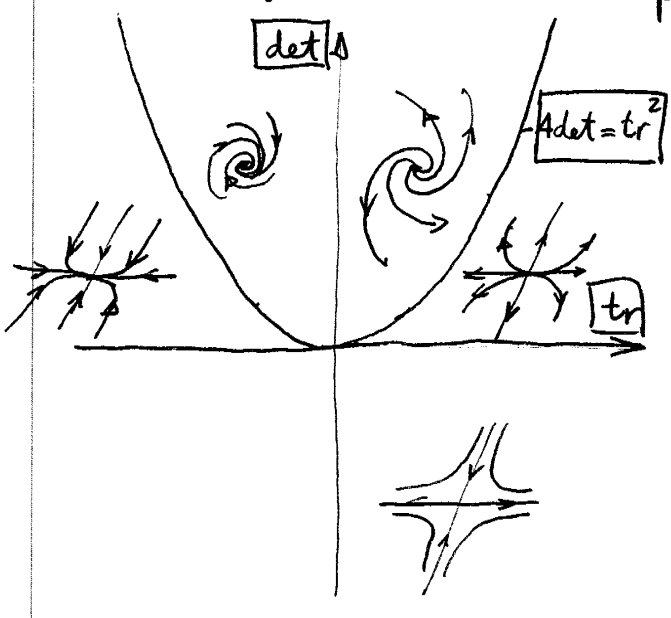

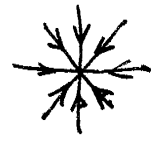

Note

$$P_{xx} = \frac{1}{\rho}\frac{\partial^2 p}{\partial x^2} = \nu \frac{\partial}{\partial x}\left(\frac{\partial^2 u}{\partial x^2} + \frac{\partial^2 u}{\partial y^2} + \frac{\partial^2 u}{\partial z^2}\right)$$

$$= \nu$$

P_x, η_x, η_y, ξ_x, ξ_y are ~~$O(x^2)$~~ const. to leading order

For regular behavior of N.S. solution has to be true.

Implies that, near a wall critical point,

$$P_{xx} = P_{yy} = P_{xy} = P_{yx} = 0 \quad \text{~~to leading order~~}$$

$$\eta_{xx} = \eta_{yy} = \eta_{yx} = \eta_{xy} = 0$$

$$\xi_{xx} = \xi_{yy} = \xi_{yx} = \xi_{xy} = 0$$

tangential pressure gradient extremum

extremum of tangential vorticity gradient ~~gradient~~

i.e. of tangential gradient of wall shear str

At a critical point of the wall streamline field (WSL-field), consider again the local expansion of the three-dimensional velocity field

$$\begin{bmatrix} \frac{u}{z} \\ \frac{v}{z} \\ \frac{w}{z} \end{bmatrix} = \begin{bmatrix} \eta_x & \eta_y & P_x/2\nu \\ -\xi_x & -\xi_y & P_y/2\nu \\ 0 & 0 & (\xi_y-\eta_x)/2 \end{bmatrix} \begin{bmatrix} x \\ y \\ z \end{bmatrix} + \ldots = \underset{\approx}{F}\,\underset{\sim}{x} + \ldots \quad (12.15)$$

If the eigenvalues of the matrix $\underset{\approx}{F}$ are all real there will be three special planes, intersecting at the critical point, which are distinguished by the fact that they contain streamlines (are stream surfaces). These planes are also the planes defined by pairs of eigenvectors. The wall is always one of these planes.

To simplify matters, choose the elements of $\underset{\approx}{F}$ in such a way as to make the flow symmetrical about the yz-plane. This requires that the component of the pressure gradient normal to the symmetry plane is zero

$$P_x = 0 \;;$$

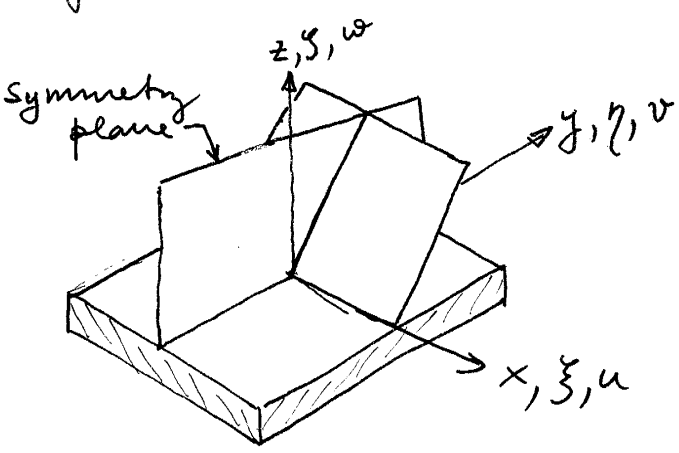

On the tr axis the node or saddle degenerates to a stagnation line:

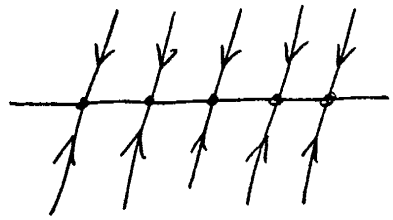

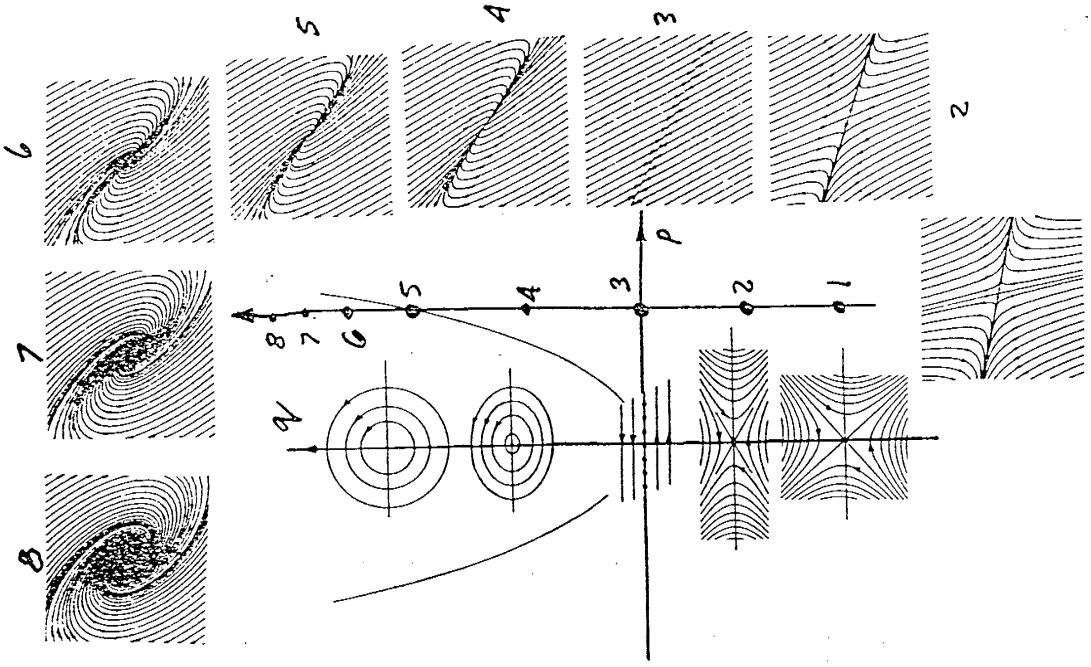

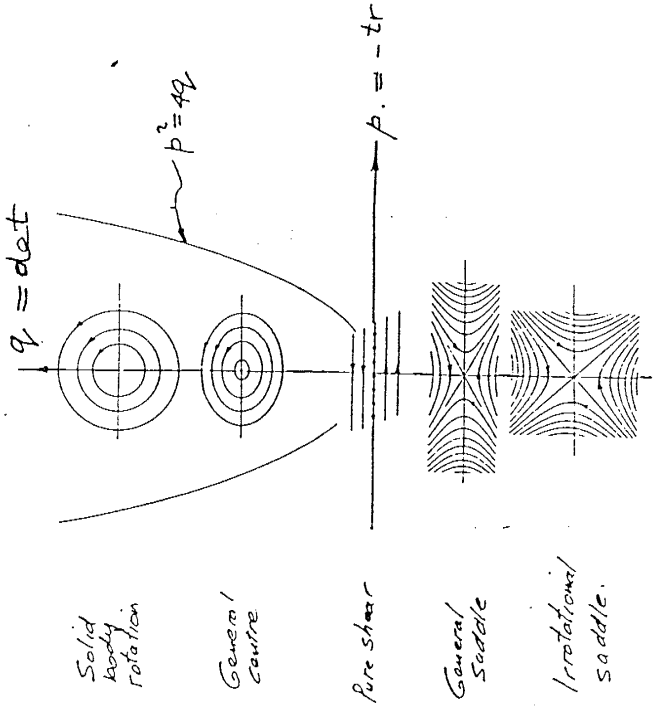

On the tr axis the node or saddle degenerates to a stagnation line:

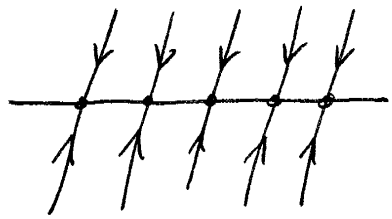

and that $\eta_y = 0$, so that $u(0, y, z) = 0$ can be satisfied. Also, the vorticity components η and ζ must be zero at $x = 0$, so that

$$\frac{\partial u}{\partial z} - \frac{\partial w}{\partial x} = 0 \quad \text{at} \quad x = 0$$

$$\frac{\partial v}{\partial x} - \frac{\partial u}{\partial y} = 0 \quad \text{at} \quad x = 0$$

giving $\xi_x = \eta_y = 0 = P_x$ ——— (12.16)

as the conditions for the (yz) plane to be a plane of symmetry.

Thus the symmetry plane is also a streamsurface and represents the second of the special planes. In this special plane determine the slope of the streamlines, by writing:

$$\left(\frac{dz}{dy}\right)_{SL} = \left(\frac{w}{v}\right)_{x=0} = \left(\frac{w/z}{v/z}\right)_{x=0} = \frac{(\xi_y - \eta_x)\, z/2}{\frac{P_y}{2\nu} z - \xi_y y} \quad \text{——— (12.17)}$$

At $z = y = 0$, the streamline direction again becomes undefined, so that $x = y = 0$ is a critical point in the symmetry plane also.

If we choose the elements of $\underset{\sim}{E}$ in such a way as to make the critical point in the symmetry plane a saddle point, and to make the critical point in the wall streamlines

a saddle also, then the sketch shows the

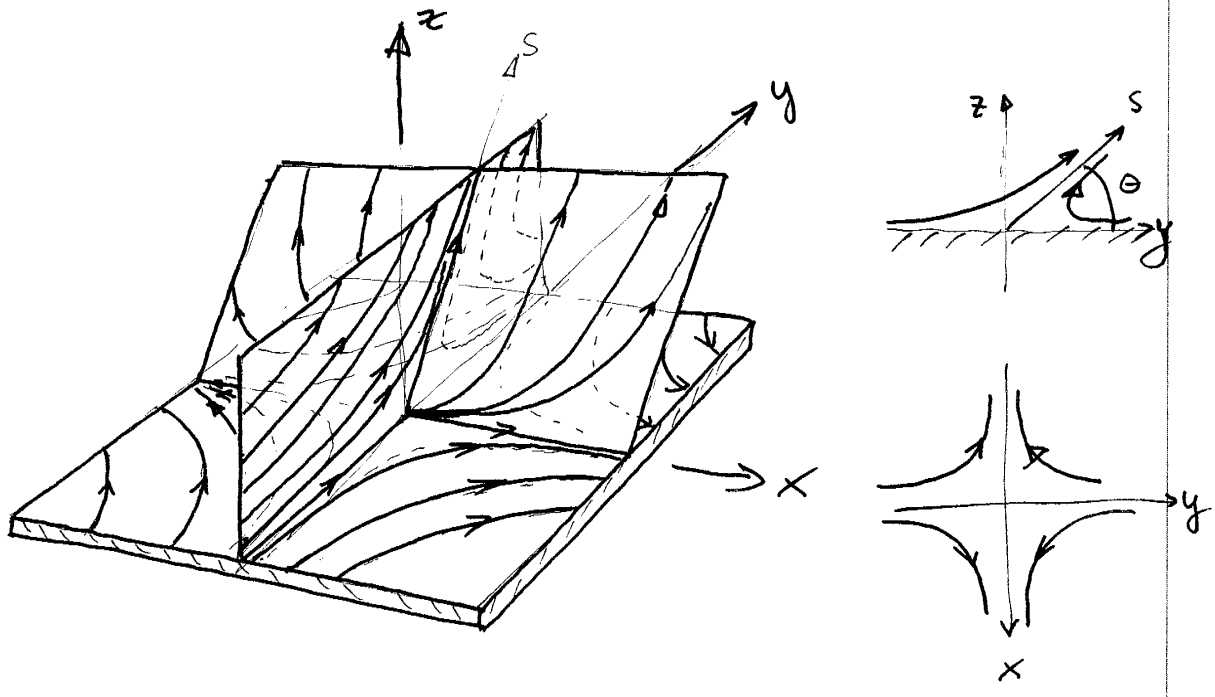

streamlines in the special planes. The (sx) plane defines the third special plane and in this plane the critical point $\underset{\sim}{x}=0$ is a node in the case chosen.

In general, the angles between the special planes need not be $\pi/2$, nor does the WSL-field have to be a saddle point. However, if $\underset{\approx}{F}$ has only real eigenvalues the critical point always appears as a saddle in two of the special planes and as a node in the third. The special planes appear here as planes and not as more general (curved) surfaces, because we have considered only the first term in the expansion $\underset{\sim}{u} = z\underset{\approx}{F}\underset{\sim}{x} + \ldots$

The properties of the critical point described by this set of values of the elements of $\underset{\approx}{F}$ corresponds to a particular form of a negative streamsurface bifurcation at a wall: the two wall streamsurfaces combine at the x-axis to form the streamsurface of the (sx) plane which leaves the wall. It is thus a generalization of separation into the third dimension. The direction of the separated sheet of the bifurcation is therefore very interesting. To determine θ, consider equation (12.17) as

$$\frac{dz}{dy} = \frac{(\xi_y - \eta_x)z}{\frac{P_y}{\nu}z - 2\xi_y y} = \frac{cz}{az-by}, \text{ say}$$

and determine

$$\frac{d^2z}{dy^2} = \frac{(az-by)c\frac{dz}{dy} - cz\left(a\frac{dz}{dy}-b\right)}{(az-by)^2} = 0,$$

defining the wall or the s-axis. This gives

$$(az-by)\frac{c^2z}{az-by} - cz\left(\frac{acz}{az-by} - b\right) = 0$$

or

$$az - (b+c)y = 0 \quad , \quad \text{or } z = 0$$

$$z = \frac{b+c}{a}y$$

or

$$z = \frac{3\xi_y - \eta_x}{P_v/\nu}y \qquad (12.18)$$

Thus, the angle θ at which the separating stream-surface leaves the wall at a symmetry plane is given by

$$\boxed{\tan\theta = \frac{3\xi_y - \eta_x}{P_y/\nu}} \qquad (12.19)$$

Consider this in the special case of plane flow, where $u \equiv 0$, so that $\eta_x = 0$, and

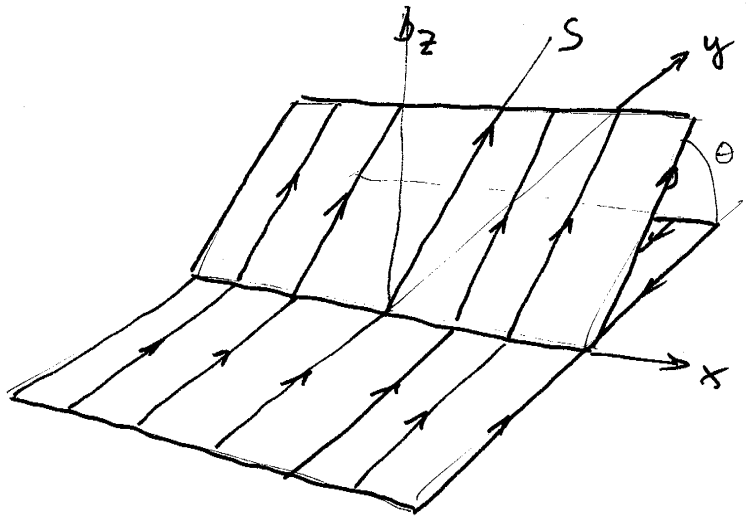

the degenerate case

$$\begin{bmatrix} \frac{v}{z} \\ \frac{w}{z} \end{bmatrix} = \begin{bmatrix} -\xi_y & P_y/2\nu \\ 0 & (\xi_y - \eta_x)/2 \end{bmatrix} \begin{bmatrix} y \\ z \end{bmatrix}$$

shown in the sketch results.

In this case,

$$\boxed{\tan\theta = 3\xi_y \nu / P_y} \qquad (12.20)$$

(12.19) is sometimes called the Oswatitsch relation, and (12.20) the Lighthill-relation.

In view of the fact that the angle of separation was shown before to be zero in the limit as $Re \to \infty$, it is now of interest to consider (12.20) in more detail.

Lorenzetti:

$$U^2 \frac{1}{\rho}\frac{dp}{dx} = O\left(\varepsilon\left(\frac{x}{L}\right)^{\frac{1}{2}}\right) = \varepsilon^{-2}$$

$$\frac{L}{\rho U^2}\frac{\partial \tau}{\partial z} = \frac{L}{\rho U^2}\frac{dp}{dx} = O\left(\varepsilon^{-2}\right)$$

$$\therefore \frac{L}{\rho U^2}\frac{\partial \tau}{\partial x} = O\left(\varepsilon^{-2}\right)\cdot\frac{z}{x} = O\left(\varepsilon^{-2}\right)\cdot\frac{\overbrace{\varepsilon^{\frac{1}{2}}\left(\frac{x}{L}\right)^{\frac{1}{4}}}^{\varepsilon^{\frac{3}{2}}}\overbrace{Re^{-\frac{1}{2}}}^{\varepsilon^{8}}}{\varepsilon^{6}}$$

$$= \varepsilon^{-2+4+8-6} = \varepsilon^{4}$$

$$S = 0.084\, Re^{-\frac{1}{16}}\left(\frac{x}{L}\right)^{3/2}$$

$$\frac{dS}{dx} = 0.126\, Re^{-\frac{1}{16}}\left(\frac{x}{L}\right)^{\frac{1}{2}}$$

$$\frac{x}{L} \sim O\left(Re^{-\frac{3}{8}}\right)$$

$$\frac{dS}{dx} = O\left(Re^{-\frac{1}{16}}\right)\cdot O\left(Re^{-\frac{3}{16}}\right)$$

$$= O\left(Re^{-\frac{1}{4}}\right)$$

$$\frac{dp}{dx} = O\left(Re^{-\frac{1}{16}}\right)\cdot O\left(\frac{Re}{L}\right)^{-\frac{1}{2}}$$

$$= O\left(Re^{-\frac{1}{16}}\right) O\left(Re^{\frac{3}{16}}\right) = O\left(Re^{\frac{1}{8}}\right)$$

Note that ξ_y may be related to the gradient of wall shear stress

$$\xi_y = -\frac{1}{\eta}\frac{\partial \tau_w}{\partial y}$$

so that $$\tan\theta = -\frac{3\,\partial\tau_w/\partial y}{\partial p/\partial y}.$$

In the context of the Sychev theory, the R.H.S. of this relation is $O(Re^{-\frac{1}{4}})$. It follows that

see opposite p 58

$$\tan\theta = O(Re^{-\frac{1}{4}})$$

and that the angle made by the separation streamline at the wall goes to zero as the Reynolds number becomes infinite.

e.g. $Re = 100{,}000$, $\Rightarrow \theta \approx 3^\circ$

Quasi two-dimensional separation

Now superimpose a uniform shear flow

$$u = kz$$

onto the plane separation of p. 102:
Note: no critical point any more!

$$\left.\begin{aligned} \frac{u}{z} &= k \\ \frac{v}{z} &= b_2 y + c_2 z \\ \frac{w}{z} &= -b_2 z/2 . \end{aligned}\right\} \qquad \begin{aligned} b_2 &= -\xi_y \\ c_2 &= \frac{P_y}{2\nu} \end{aligned}$$

This flow satisfies the Navier Stokes equations and the continuity equation, as well as the no-slip boundary condition at $z=0$.

Obtain the WSL from

$$\frac{v}{u} = \left(\frac{dy}{dx}\right)_{z=0} = \frac{b_2 y}{k}. \qquad (12.21)$$

This constitutes a differential equation for the wall streamlines. Along wall s.l. therefore

$$\boxed{y = y_0 \exp\left\{\frac{b_2}{k}(x - x_0)\right\}}, \qquad (12.22)$$

where y_0, x_0 is the point generating the streamline.

In the (xs) plane we may obtain the equation of the streamline by replacing z and y according to

$$z = s \sin\theta$$

$$y = s \cos\theta$$

and noting that the s-component of velocity, v_s is related to v and w by

$$w = v_s \sin\theta$$

$$v = v_s \cos\theta$$

Thus

$$\left(\frac{ds}{dx}\right)_{SL} = \frac{v_s}{u} = \frac{(b_2 s\cos\theta + c_2 s\sin\theta)\, s\tan\theta}{k s \sin\theta}$$

$$= \frac{s\,(b_2 + c_2\tan\theta)}{k}$$

Now $\tan\theta = -3b_2/2c_2$, so that

$$\left(\frac{ds}{dx}\right)_{SL} = -\frac{b_2 s}{2k}$$

and

$$\boxed{s = s_0 \exp\left\{-\frac{b_2}{2k}(x - x_0)\right\}} \qquad (12.23)$$

Equations (12.22) and (12.23) describe the shapes of the WSL and the separated sheet streamlines in the vicinity of a quasi two-dimensional separation, sketched here.

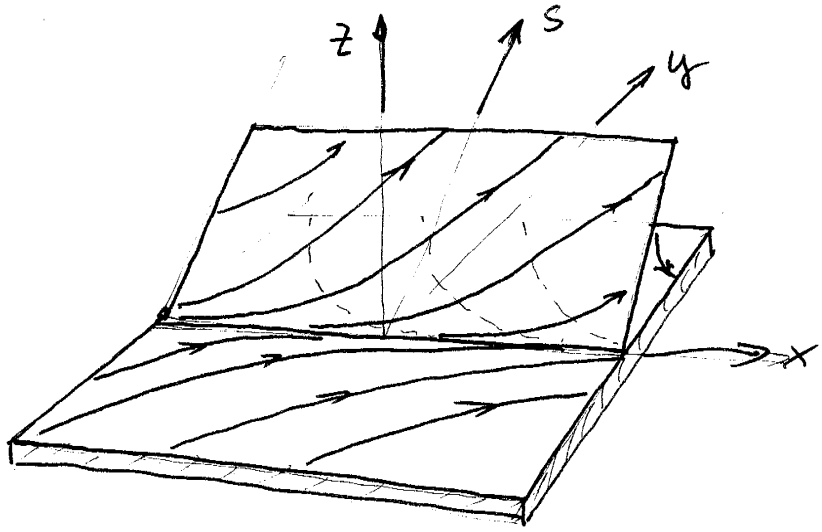

The WSL's converge asymptotically to the x-axis, but never reach it, the separating streamlines diverge asymptotically from the x-axis but have never been on it. In the sketch we have chosen the characteristic length k/b_2 to be negative in order to make the x-axis into a negative stream surface bifurcation line, i.e. a separation line. For positive SSB, put $k/b_2 > 0$, so that the arrowheads are reversed.

Comparing the sketches of p. 102 and p 105, we see that

<u>for 2-d separation</u>:

- a streamline leaves the wall
- reverse flow may be defined
- $\tau_w = 0$ at the separation point

<u>for quasi two-d separation</u>:

- no streamline leaves the wall
- "reverse flow" may not be defined
- τ_w is nowhere $= 0$.

In both cases fluid is carried away from the vicinity of the wall at the <u>same rate</u>. We conclude that in both cases the flow is separated, to a similar "degree".

It is clear from the above, that, along the SSB-line of p. 105, no <u>stream-line</u> bifurcation takes place, though a <u>stream surface</u> bifurcation does take place. This is the resolution of a controversy that arose as follows: WSL fields obtained from experiments show apparently, that WSL combine along a bifurcation line. A number of authors have been motivated from this observation to seek solutions of the Navier Stokes equations or of the b.l. equa-

tions which exhibit such cusp-like streamline behaviour. Only the b.l. equations have been shown to possess such solutions, and these are no longer valid in the vicinity of separation.

The nature of this difference may be illustrated by considering a line at a small distance z_1 from the wall that goes across the stream surface bifurcation line. Let this line be the generator of a stream surface. Now move the line a small distance toward the wall and let it generate another stream surface. Continuing this process a sequence of streamsurfaces is generated which envelop each other as shown. As $z_1 \to 0$, the point at which the streamsurface moves a significant distance away from the wall lies further and further downstream but remain self similar.

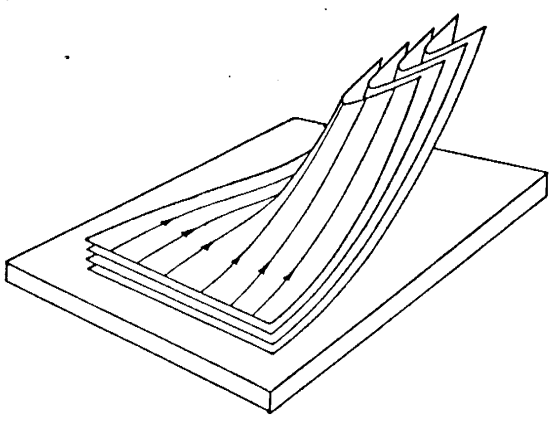

If a cusp-like SSB were possible, the shape of the streamsurface would change discontinuously as $z_1 \to 0$, eventually consisting only of the wall and the free sheet.

Complex eigenvalues of $\underset{\approx}{F}$

The eigenvalues of $\underset{\approx}{F}$ are either all real, or one is real and the two others are a complex conjugate pair. In the latter case, a wall critical point only has one special plane containing streamlines, namely the wall. The WSL's then form a vortical node at the critical point. The two other singular planes degenerate into a special direction along which a streamline leaves the wall or approaches it. The critical point of the WSL can therefore be a positive vortical node (unstable focus) from which the WSL's diverge, or a negative vortical node (stable focus) toward which they converge. Wherever a WSL pattern exhibits a vortical node the spatial structure of the flow exhibits a special direction along which a streamline leaves or enters the wall for negative or positive vortical node respectively.

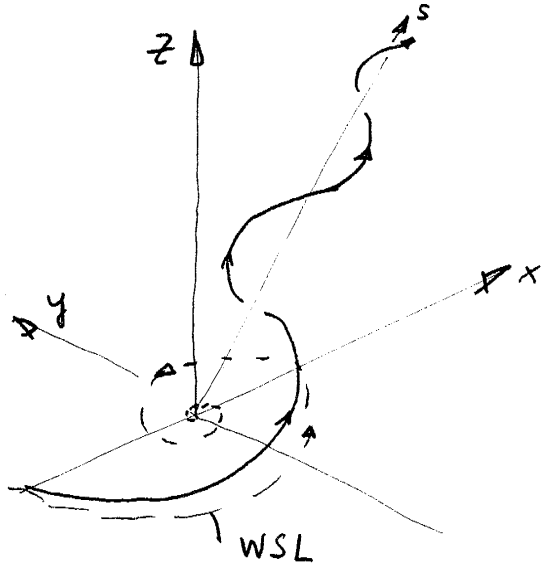

Free streamsurface bifurcation, free critical point.

Critical points also occur in the flow field at points that do not lie in the wall. In that case the expansion

$$u_i = A_i^1 + A_{ij}^2 x_j + \dots \qquad (12.1)$$

may be simplified only by omitting A_i^1 on the strength of the fact that $u_i = 0$ at $x_j = 0$. The no-slip condition, which previously allowed us to write

$$\frac{u_i}{z} = B_{ij}^2 x_j + \dots$$

may now not be used. Consequently, we write

$$\underset{\sim}{u} = \underset{\approx}{G}\, \underset{\sim}{x} + \dots \qquad (12.16)$$

and substitute the appropriate equations in the first approximation

$$\begin{bmatrix} u \\ v \\ w \end{bmatrix} = \begin{bmatrix} d_1 & e_1 & f_1 \\ d_2 & e_2 & f_2 \\ d_3 & e_3 & f_3 \end{bmatrix} \begin{bmatrix} x \\ y \\ z \end{bmatrix} \qquad (12.17)$$

in order to determine the elements of $\underset{\approx}{G}$.

The continuity equation yields

$$d_1 + e_2 + f_3 = 0 \qquad (12.18)$$

The vorticity components are

$$\left.\begin{aligned} \xi &= \frac{\partial w}{\partial y} - \frac{\partial v}{\partial z} = e_3 - f_2 \\ \eta &= \frac{\partial u}{\partial z} - \frac{\partial w}{\partial x} = f_1 - d_3 \\ \zeta &= \frac{\partial v}{\partial x} - \frac{\partial u}{\partial y} = d_2 - e_1 \end{aligned}\right\} \qquad (2.19)$$

<u>Note</u>: the vorticity is <u>constant</u> to this order.

The momentum equation yields:

$$\left.\begin{aligned} -P_{xx} &= d_1^2 + \cancel{e_1 d_2} + \cancel{f_1 d_3} \\ -P_{yy} &= \cancel{d_2 e_1} + e_2^2 + f_2 e_3 \\ -P_{zz} &= d_3 \cancel{f_1} + e_3 f_2 + f_3^2 \end{aligned}\right\} \qquad (12.20)$$

<u>Note</u>: The viscous terms enter only at higher order and the pressure has an extremum at the critical point.

To simplify matters, consider again the case when the (yz) plane is a plane of symmetry

I.e.

$$\left.\begin{aligned} u(0, y, z) &= 0 \\ \eta(0, y, z) &= 0 \\ \zeta(0, y, z) &= 0 \end{aligned}\right\} \qquad (12.21)$$

It follows that $\quad e_1 y + f_1 z = 0$ for all values of y and z

$$e_1 = f_1 = 0$$

$\eta = 0 \rightarrow \quad f_1 - d_3 = 0 \quad \Longrightarrow \quad d_3 = 0$

$\zeta = 0 \rightarrow \quad d_2 - e_1 = 0 \quad \Longrightarrow \quad d_2 = 0$

Thus

$$\left.\begin{aligned} -P_{xx} &= d_1^2 \\ -P_{yy} &= e_2^2 + f_2 e_3 \\ -P_{zz} &= e_3 f_2 + f_3^2 \end{aligned}\right\} \qquad (12.22)$$

$$\xi = e_3 - f_2 \qquad (12.23)$$

continuity $\quad f_3 = -(d_1 + e_2) \qquad (12.24)$

(12.22), 23) and 24) allow the elements to be determined in terms of the second derivatives of P and of ξ. The only non-zero components of $\underset{\sim}{G}$ are d_1, e_2, f_2, f_3 and e_3

The solutions are:

(12.25)

$$\left\{\begin{aligned} d_1 &= \sqrt{-P_{xx}} \\ e_2 &= -\frac{1}{2\sqrt{-P_{xx}}}\left\{P_{zz} - P_{yy} + P_{xx}\right\} \\ f_3 &= +\frac{1}{2\sqrt{-P_{xx}}}\left\{P_{zz} - P_{yy} - P_{xx}\right\} \\ f_2 &= \left\{\frac{1}{4}\xi^2 - \frac{1}{4P_{xx}}\left[P_{zz}^2 + P_{xx}^2 + P_{yy}^2 - 2P_{zz}P_{yy} + 2P_{xx}P_{yy} + 2P_{zz}P_{xx}\right]\right\}^{\frac{1}{2}} - \frac{1}{2}\xi \\ & \quad - \tfrac{1}{4}\left(-2P_{zz} + 2P_{yy} + 2P_{zz}\right) \\ e_3 &= \left\{ \qquad \right\}^{\frac{1}{2}} + \frac{1}{2}\xi \end{aligned}\right.$$

The matrix $\underline{\underline{G}}$ now is simply

$$\begin{bmatrix} u \\ v \\ w \end{bmatrix} = \begin{bmatrix} d_1 & 0 & 0 \\ 0 & -\frac{1}{2}d_1 & f_2 \\ 0 & f_2+\xi & -\frac{1}{2}d_1 \end{bmatrix} \begin{bmatrix} x \\ y \\ z \end{bmatrix} \qquad (12.26)$$

Using again the momentum equation and differentiation, obtain P_{xy} and set equal to P_{yx} similarly with $P_{xz} = P_{zx}$, $P_{yz} = P_{zy}$:

$$0 = 0$$

$$0 = 0$$

$$f_2 e_2 + f_3 f_2 = e_2 e_3 + e_3 f_3 \qquad (12.27)$$

or $$f_2 (e_2 + f_3) = e_3 (e_2 + f_3) \qquad (12.28)$$

(12.28) allows us to make an important decision: If $(e_2 + f_3) \neq 0$, then $f_2 = e_3$, so that, according to (12.23), $\xi = 0$. Since we want to study a critical point with finite vorticity, however, we take the other alternative, namely

$$e_2 = -f_3 \qquad (12.29)$$

Consequently (12.24) gives

$$d_1 = 0. \qquad (12.30)$$

This important result states that flow at a critical point away from a no-slip

boundary is always two-dimensional to the first approximation! Also, since $P_{xx} = 0$, the pressure does not vary along the vorticity direction! even to higher order than quadratic terms.

The problem thus reduces to

$$\begin{bmatrix} v \\ w \end{bmatrix} = \begin{bmatrix} e_2 & e_3 - \xi \\ e_3 & -e_2 \end{bmatrix} \begin{bmatrix} y \\ z \end{bmatrix} \qquad (12.31)$$

Since $P_{xx} = 0$, equation (12.25) shows that finite values of the elements of the coefficient matrix of (12.31) can only exist if $P_{zz} = P_{yy}$. Hence

$$P_{zz} = P_{yy} . \qquad (12.32)$$

The second of equations (12.22) together with (12.23) therefore give

$$e_3 (e_3 - \xi) = -P_{yy} - e_2^2$$

or

$$e_2 = \pm \sqrt{-P_{yy} - e_3 (e_3 - \xi)} \qquad (12.33)$$

So

$$\begin{bmatrix} v \\ w \end{bmatrix} = \begin{bmatrix} -\sqrt{-P_{yy} - e_3(e_3 - \xi)} & e_3 - \xi \\ e_3 & +\sqrt{-P_{yy} - e_3(e_3 - \xi)} \end{bmatrix} \begin{bmatrix} y \\ z \end{bmatrix} \qquad (12.34)$$

gives the solution to the velocity field in terms of the element e_3.

Now consider the eigenvalues of this matrix: The trace $tr = 0$, and the determinant $det = P_{yy}$. Thus we see that the eigenvalues are

$$\lambda_{1,2} = \pm\sqrt{-P_{yy}} \qquad (12.35)$$

independent of ξ!

and the only allowable critical points lie on the det axis, i.e. they must be saddles if $P_{yy} < 0$ and centers if $P_{yy} > 0$. A pressure maximum at $\underset{\sim}{u} = 0$ in a flow field always gives two-dimensional saddle point flow, a pressure minimum at $\underset{\sim}{u} = 0$ always a two-dimensional center.

If the critical point is a center ($P_{yy} > 0$) the eigenvalues are complex. The streamlines are then ellipses and their orientation is related to e_3. The ratio of the axes of the ellipses is

$$R = \sqrt{\frac{1+\varepsilon}{1-\varepsilon}}$$

with

$$\varepsilon = \sqrt{1 - \frac{4P_{yy}}{\xi^2}}.$$

Note that R is independent of e_3. Thus, we can adjust e_3 to rotate the streamline pattern about the x-axis without changing it.

If we wish to make the streamlines cut the y and z axes at right angles only, i.e. to make the symmetry axes of the streamline pattern coincide with the coordinates,

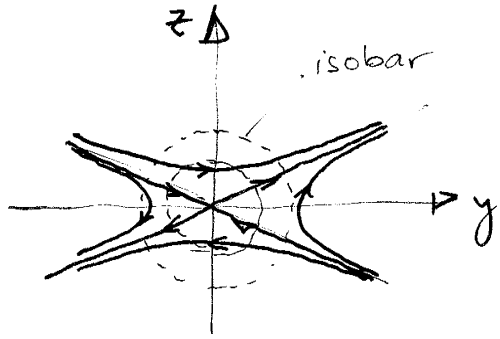

$P_{yy} < 0$

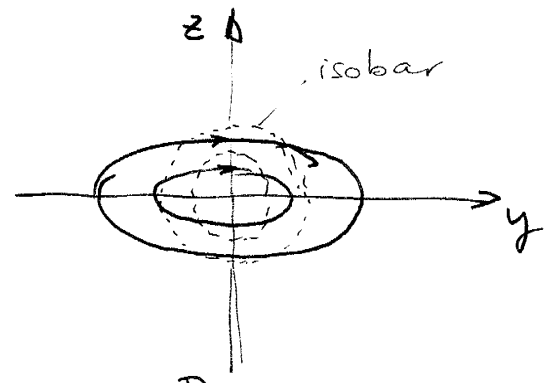

$P_{yy} > 0$.

then we have to choose e_3 such that

$$\sqrt{-P_{yy} - e_3(e_3 - \xi)} = 0 \qquad z = 0,\ v = 0 \text{ for all } y$$

or

$$e_3 = \frac{\xi \pm \sqrt{\xi^2 - 4P_{yy}}}{2}. \qquad (12.36)$$

Comparing with (12.34) we see that with this value of e_3,

$$\underset{\approx}{G} = \begin{bmatrix} 0 & e_3 - \xi \\ e_3 & 0 \end{bmatrix}.$$

Since e_3 is real,

$$4P_{yy} \leqslant \xi^2$$

so that the largest possible value of det is $\xi^2/4$.

Special cases

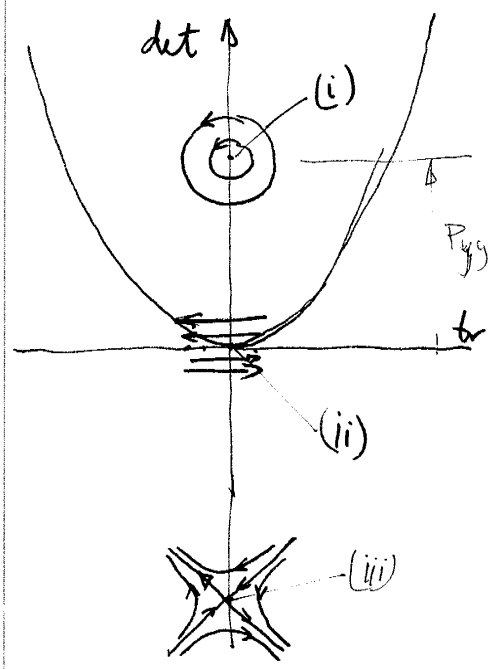

(i) $\underline{\xi^2 = 4P_{yy}}$

$$\underset{\approx}{G} = \begin{bmatrix} 0 & -\frac{\xi}{2} \\ \frac{\xi}{2} & 0 \end{bmatrix} \qquad \det = P_{yy}$$

solid body rotation with angular speed equal to $\xi/2$.

(ii) $\underline{P_{yy} = 0}$. In this case, $\det = \mathrm{tr} = 0$ and

$$\underset{\approx}{G} = \begin{bmatrix} 0 & -\xi \\ 0 & 0 \end{bmatrix} \qquad \begin{aligned} v &= -\xi z \\ w &= 0 \end{aligned}$$

so that the flow corresponds to simple shear

(iii) $\underline{|P_{yy}|/\xi^2 \to \infty, \quad P_{yy} < 0}$.

$$\det = +P_{yy}$$

$$\underset{\approx}{G} = \begin{bmatrix} 0 & -\sqrt{-P_{yy}} \\ -\sqrt{-P_{yy}} & 0 \end{bmatrix}$$

. This corresponds to an irrotational saddle with orthogonal eigenvectors.

All the flow patterns on the det axis may be decomposed into a linear combination of patterns (i) and (iii), i.e. into a combination of extensional strainrate and solid body rotation.

Summary of free slip critical points

At a free-slip critical point with finite vorticity along the x-direction:

- The second derivative of pressure with respect to x is zero: $P_{xx} = 0$
- The flow is two-dimensional and normal to x-axis.
- The second derivatives of pressure w.r.t y and z are equal ($P_{yy} = P_{zz}$) so that isobars are circular cylinders concentric with the x-axis
- The streamline pattern forms ellipses if $P_{yy} > 0$ and a saddle point if $P_{yy} < 0$. The excentricity of the ellipses is zero if $\xi^2 = P_{yy}$ and the eigenvectors of the saddle are orthogonal if $\xi^2/P_{yy} = 0$
- The flow can become locally three-dimensional only if $\xi = 0$. (Irrotational)

Free streamsurface bifurcation

The solution of the free-slip critical point now permits the determination of the flow in the vicinity of a free streamsurface bifurcation line, i.e. a bifurcation line that occurs away from a no-slip surface. To obtain this, rotate the saddle point flow pattern in the (y-z) plane about the x-axis by adjusting

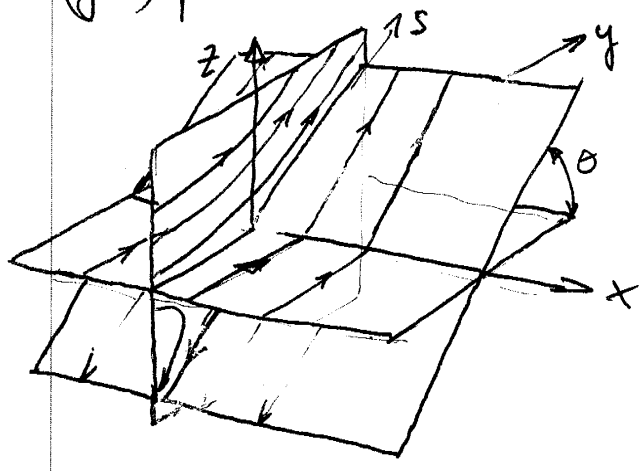

the element e_3 until one of the eigenvectors points in the y-direction. This requires that

$$w = e_3 y - e_2 z$$

be zero at $z = 0$, i.e. that $e_3 = 0$.

Hence

$$\begin{bmatrix} v \\ w \end{bmatrix} = \begin{bmatrix} -\sqrt{-P_{yy}} & -\xi \\ 0 & \sqrt{-P_{yy}} \end{bmatrix} \begin{bmatrix} y \\ z \end{bmatrix}.$$

Now superimpose a uniform velocity u_0 onto this flow. Though the equations are non-linear, so that superposition is not permissible in general, the superposition of a uniform velocity field corresponds to a Galilean transformation, which is o.k.

The equation for a streamline in the (xy) plane therefore becomes

$$\frac{dy}{dx} = \frac{v(x,y,0)}{u_0} = \frac{-\sqrt{-P_{yy}}}{u_0}\, y$$

or

$$\boxed{y = y_0 \exp\left\{-\frac{\sqrt{-P_{yy}}}{u_0}(x - x_0)\right\}} \qquad (12.37)$$

Indepdt of ξ!

As before we can obtain the equation to the streamlines in the (xs) plane as

$$\boxed{s = s_0 \exp\left\{+\frac{\sqrt{-P_{yy}}}{u_0}(x - x_0)\right\}}. \qquad (12.38)$$

The important difference between this <u>free</u> streamsurface bifurcation line and the <u>no-slip</u> bifurcation line of equations (12.22) and (12.23) is that the magnitude of the length scale of the exponential,

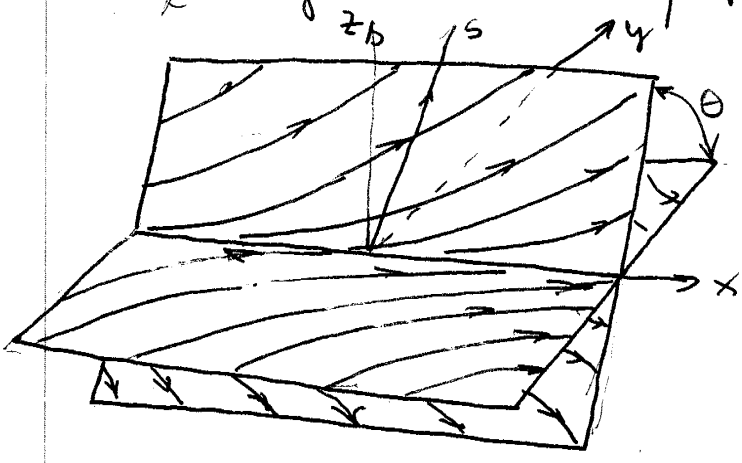

i.e. $\frac{u_0}{\sqrt{-P_{yy}}}$, is the same in each of the sheets, while the separating sheet had twice the scale of the wall sheet in the no-slip stream surface bifurcation. The angle θ may be obtained from

$$\boxed{\tan\theta = \frac{-2\sqrt{-P_{yy}}}{\xi}.} \qquad (12.39)$$

Thus, increasing the vorticity reduces θ and increasing the sharpness of the pressure maximum increases θ. Also, the direction of the vorticity must be aligned with the free streamsurface bifurcation line.

13 The topological structure of 3-d steady separated flows

The solutions obtained in the previous chapter, and the formalism and rules derived in conjunction with these, are able to provide the language needed for describing the topological structure of complex three dimensional flows. The configuration of streamsurface bifurcation lines and the streamsurfaces that form them define the topological features of such flows.

For example, an often observed wall streamline pattern involving a negative streamsurface bifurcation with a saddle and vortical node and a positive streamsurface bifurcation has the spatial structure shown. S_1 is the free sheet of the nega-

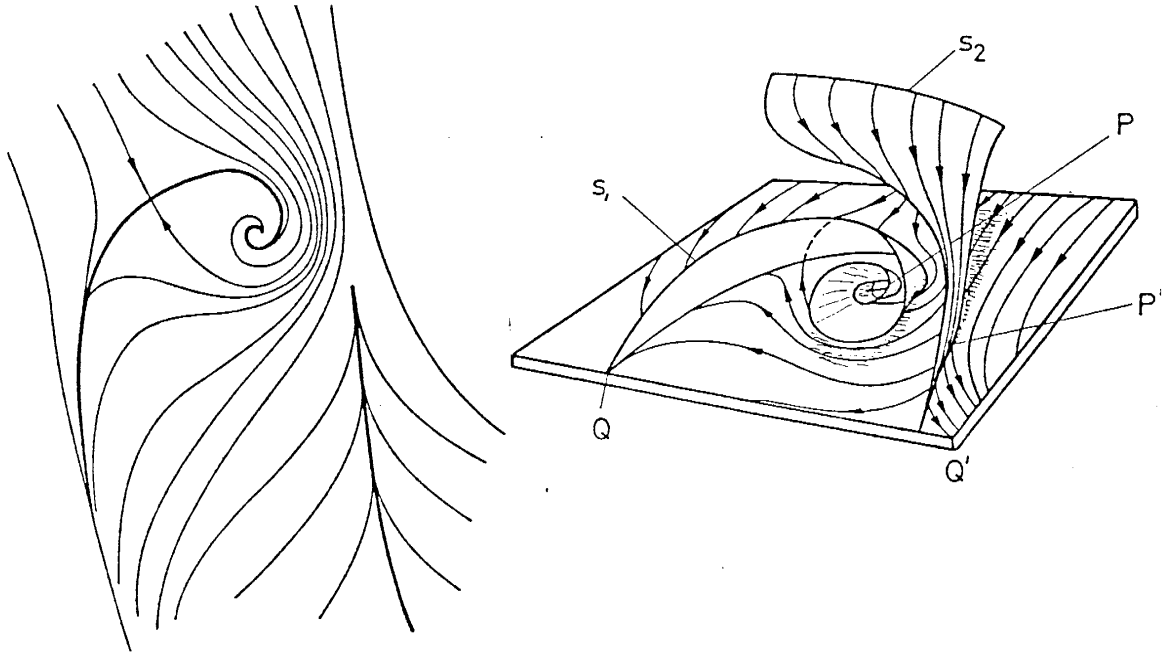

tive SSB (separating stream surface) and S_2 is the free sheet of the positive SSB (reattaching stream surface. The sheet S_1 generally rolls up to form a vortex. Note that in this configuration the reattachment line (positive SSB line) starts smoothly around ~~at~~ the point P' while the negative SSB terminates at a critical point. This need not be the case. E.g. the example shown below illustrates a case where a <u>negative</u> stream surface bifurcation line starts smoothly near the point P. Some authors argue that it is not possible for SSB lines to start smoothly (without a saddle point in the ~~VAS~~L pattern). Such open separations do, however, exist as will be shown later.

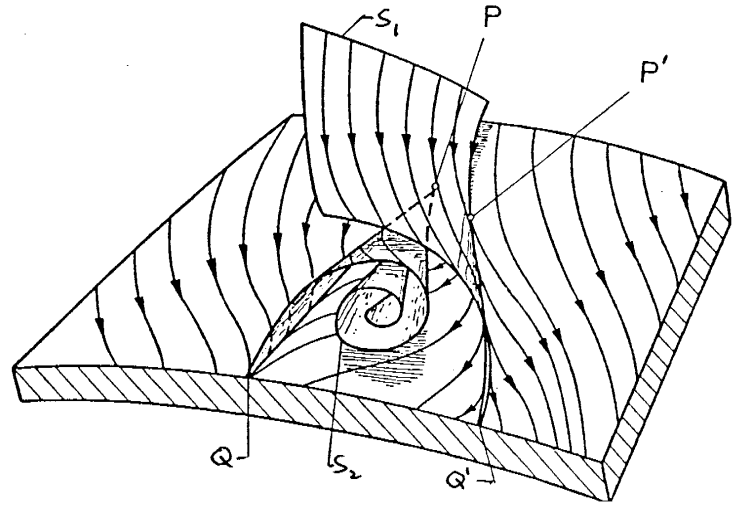

The sketch below illustrates the complexity that might occur in a configuration sometimes called simple U-shaped separation, for which half of the sketch shows the WSL-pattern.

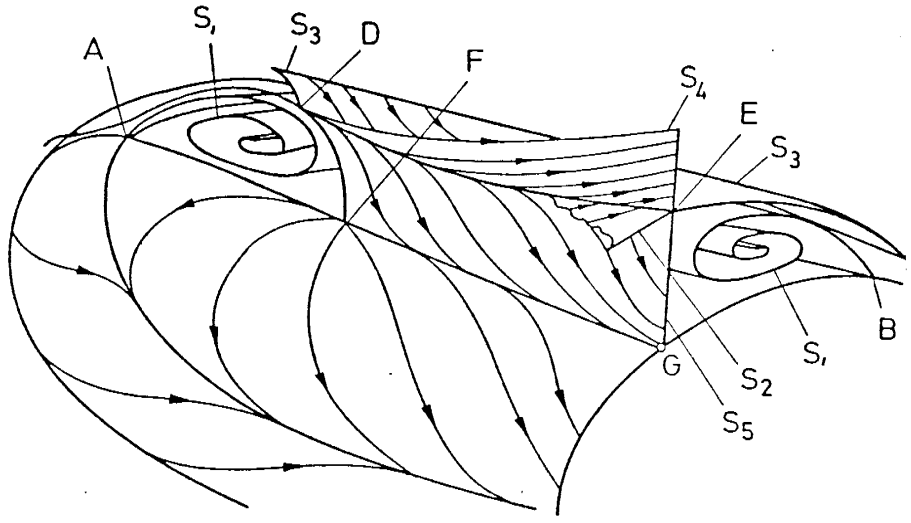

<u>The vortex skeleton model</u>.

As may be expected, more complicated separation configurations require unwieldy descriptions in terms of stream surface bifurcation lines. An example illustrates this well. The separation configuration at the junction of a slender ellipsoid with a sting support at zero angle of attack sometimes forms the pattern

sketched below. In this pattern, 18 free sheets associated with 12 SSB lines occur, and the description rapidly becomes hopelessly complicated.

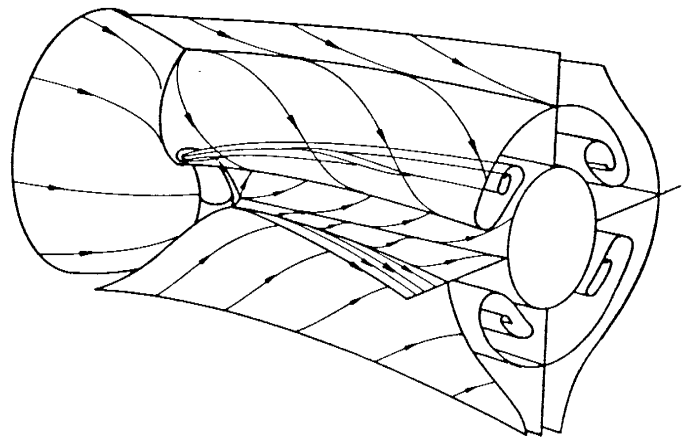

It turns out, however, that it is possible to describe such flows (slightly less unambiguously) in terms of the location and sign of the vortices that would be needed to produce a pattern of the same topological structure. To show this in the example, the sketch shows the "vortex skeleton" that would produce the above configuration of SSB lines (with suitable strengths of the vortices).

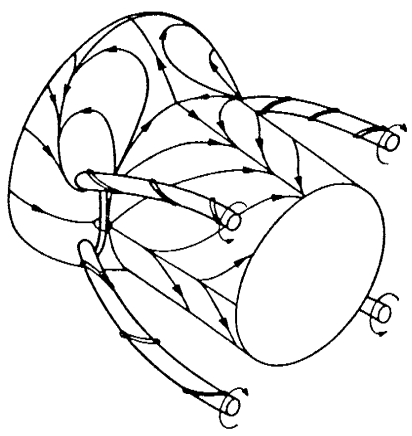

To demonstrate this in the WSL pattern Perry + Homsy set up an experiment with a magnetic field analogy: This is possible since, for the description of the topological structure of the flow a frictionless model in which the vorticity occurs only in concentrated form, is sufficient. The experiment uses a helical coil to produce a uniform magnetic field. This is analogous to a wind-tunnel. The "model" consists of an arrangement of current-carrying wires (vortices) and is inserted in the coil. In symmetry planes of this vortex configuration, the flow direction can be made visible by iron filings scattered on ~~the~~ a sheet of paper aligned with the symmetry plane. Many often-observed separation patterns were reproduced in this manner and a few examples are shown in the following pages. A rule about the minimum number of vortices required to generate a given WSL pattern could be established:

$$V \geq P + S$$

where V is the number of vortices, P is the

number of saddle-node pairs in the WSL pattern and S is the number of open separation lines (smoothly starting negative SSB lines)

A real flow will naturally be different from the "flow" generated by the electromagnetic analogy, because the three-dimensional boundary layer (not occurring in the e.m. analogy) is twisted. However, the b.l. can not produce any new topological features such as saddles, nodes in the WSL field without transporting vorticity away from the wall, i.e. without forming a new vortex. Hence the vortex skeleton <u>does</u> give the topological structure though not the exact geometrical shape

Open stream surface bifurcation

Oil flow visualization photographs often exhibit SSB lines that indicate smoothly increasing strength over a finite region, starting from zero. Strength is related to the rate of convergence of the wall streamlines (the inverse length scale of the exponential

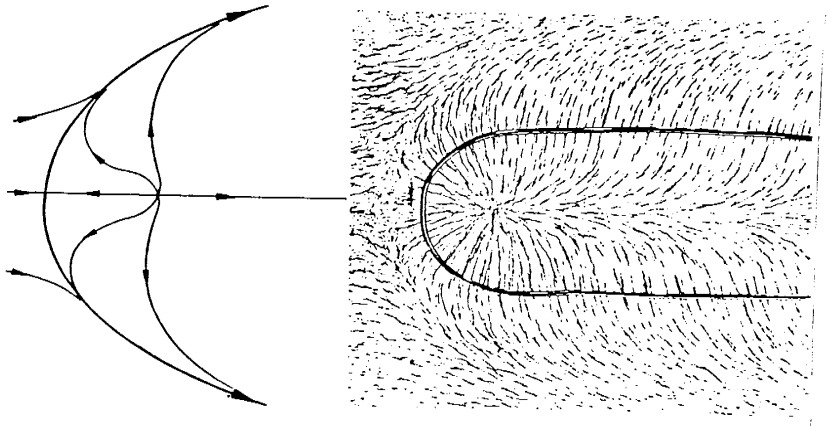

Fig.9a: Wall streamline pattern for simple U-shaped separation, sketch and electromagnetic simulation. One saddle-node pair occurs, all negative bifurcations start at saddles, i.e. P=1, S=0. Hence $V \geqslant 1$. One vortex only is needed in the skeleton.

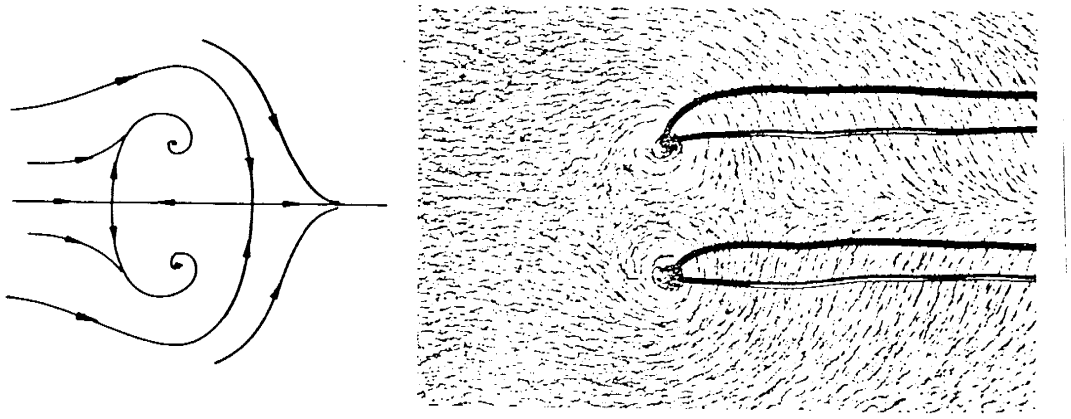

Fig.9b: Owl-face pattern of the first kind. P=2, S=0 so that $V \geqslant 2$. The two vortex-wires cast shadows onto the wall. Only two wires were used.

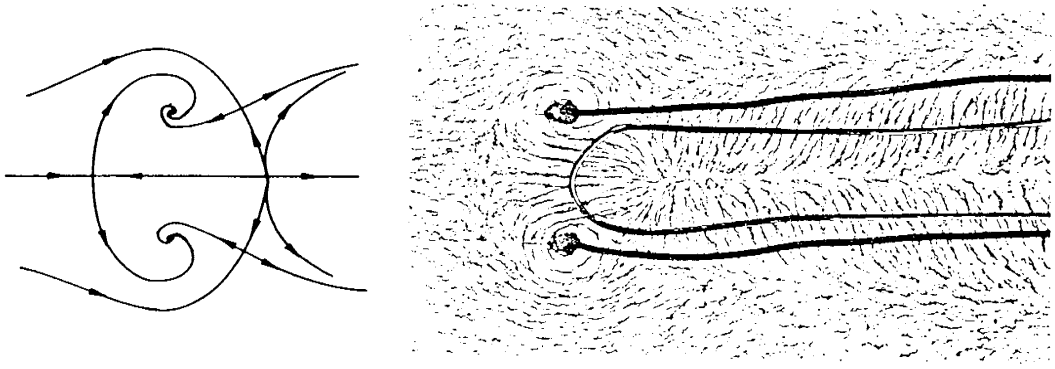

Fig.9c: Owl-face pattern of the second kind. P=3, S=0. so that $V \geqslant 3$.

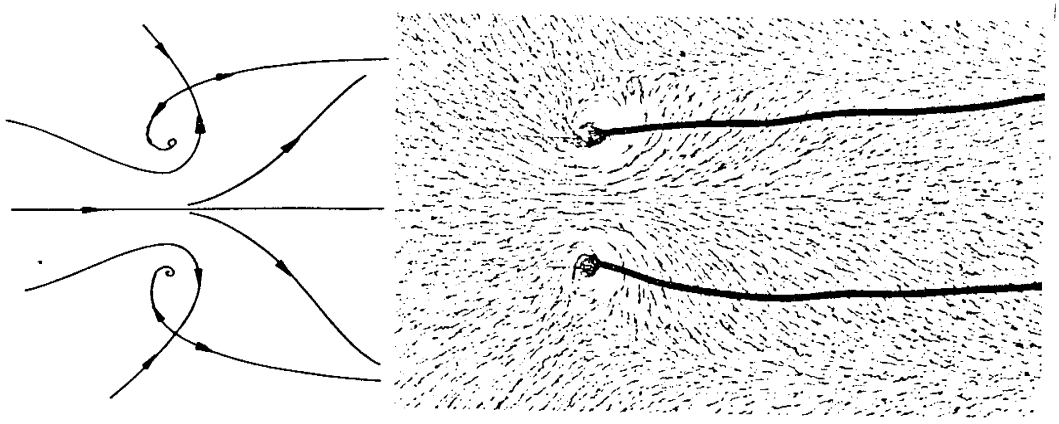

Fig.9d: Owl-face pattern of the third kind (Werlé-Legendre separation). P=2, S=0, so that V⩾2.

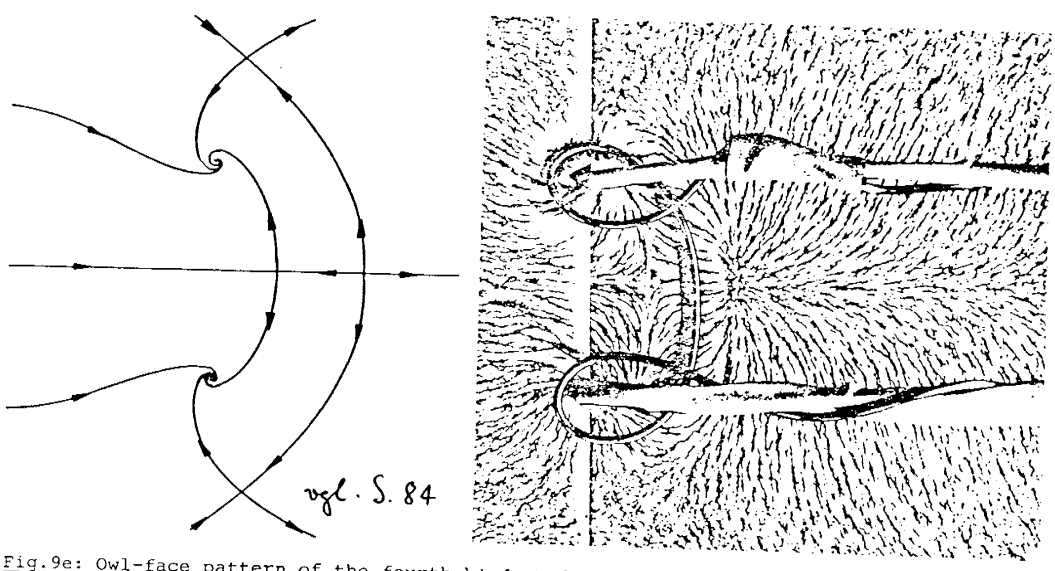

Fig.9e: Owl-face pattern of the fourth kind. P=3, S=0, so that V⩾3.

b_2/k (in equation (12.22)). An example is shown below. It is relatively simple to generate the vortex skeleton model for such a flow, since WSL's and vortex lines are orthogonal at a wall. In an open separation, the wall vortex lines bundle together to form a separated vortex. Hence the electromagnetic analogy involves two current carrying wires connected to each other by a copper plate close to and parallel to the wall.

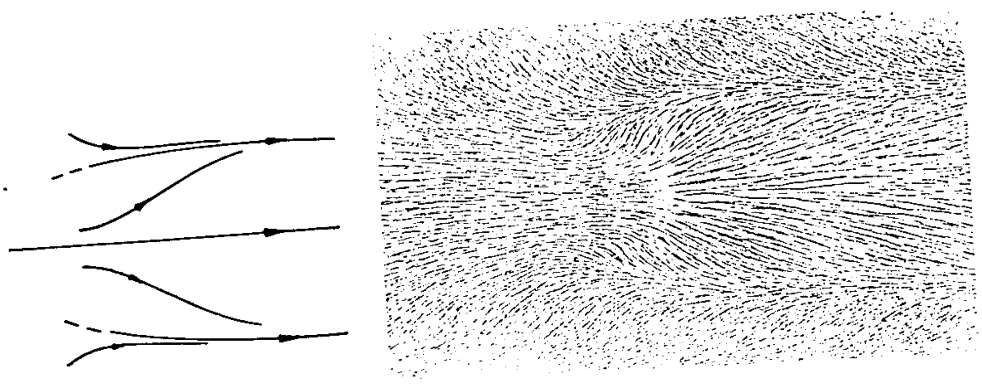

Fig.9f: Separation with two smoothly-beginning negative bifurcation lines. No critical points occur on the bifurcation lines. P=0, S=2, i.e. $V \geqslant 2$.

We now consider a succession of variants of this flow, by letting the node and saddle approach each other until the degenerate case occurs in which they coincide at a point where T has a minimum value = 0. Now project this process a little further. Extrapolation suggests the case d) which does not exhibit any zeros in T, i.e. no critical points in the wall streamline pattern. This is very well substantiated by experimental WS pattern (see e.g. p. 126).

Since some authors (even now) do not believe that such open separations exist, an attempt was made to obtain a local solution that exhibits the features of an open separation. To this end, an elegant fourth order solution by Perry 1982 for an almost two-dimensional separation provided the key. This is

$$\left.\begin{aligned}
\frac{u}{z} &= -exy^2 && + O(r^4)\\
\frac{v}{z} &= fy + gz + ex^2y && + O(r^4)\\
\frac{w}{z} &= -f\tfrac{z}{2} - ex^2\tfrac{z}{2} + ey^2\tfrac{z}{2} && + O(r^4)\\
\frac{p}{\nu} &= -ex^2z + ey^2z + 2gy - fz + \frac{p_0}{\nu} && + O(r^4)
\end{aligned}\right\} \quad (14.1)$$

14 Open threedimensional separation

To examine the question of the existence of open 3-d separation, imagine a negative SSB at a wall that involves a vortical node and a saddle in the WSL pattern as in the sketch p. 121. In the sketches below the negative SSB runs from a vortical node via a saddle to the right. Along this SSB line, plot the magnitude $T = |\tau_w|$ of the wall shear stress. At the node and saddle $T = 0$. The dashed line shows the background behaviour of T (parallel to the SSB line)

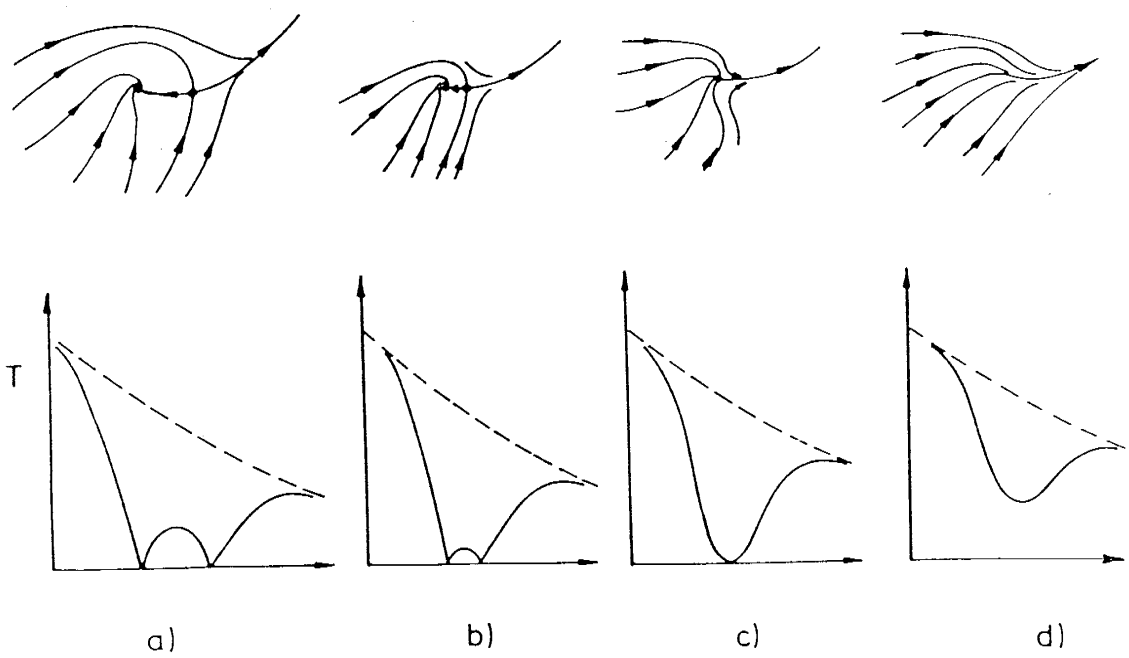

Fig.11: Bifurcation line starting from a saddle-node pair: As the distance between the saddle and node is reduced to zero (a-c) the degenerate case c) results, where the magnitude of the wall shear stress, T, just reaches zero. Fig.11d) shows that, when this process is extrapolated, the smoothly starting bifurcation line results, in which T does not reach zero any more

where e, f, g and p_0 are constants and $r = \sqrt{x^2+y^2+z^2}$. The sketch shows the pattern for $e>0$, $f<0$, $g=0$. Note that $e=0$ corresponds to the two-dimensional separation shown on p. 102.

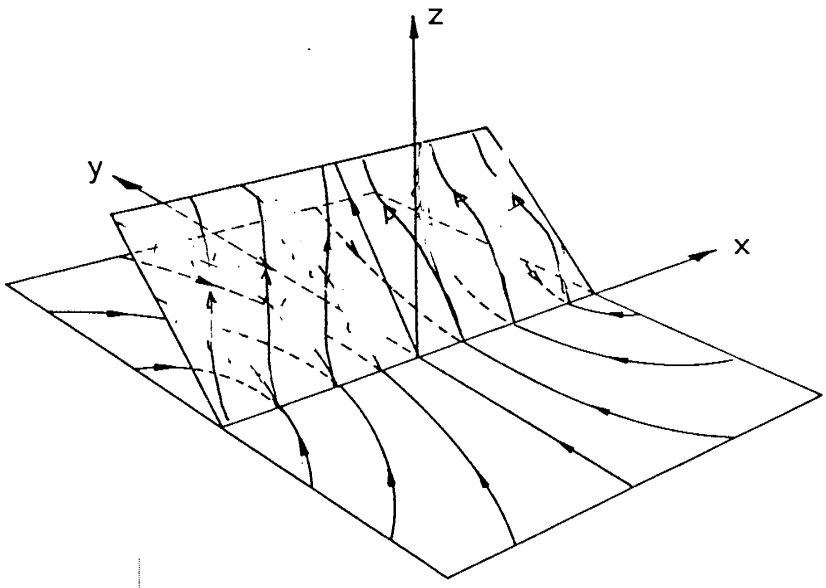

We now superimpose a simple shear flow $u = kz$ onto this flow, remembering that this will invalidate the solution since we have (at this order) a nonlinear differential equation. Substituting the solution into the Navier Stokes equation, it turns out that the resulting error may be corrected by adding a term in z^3 to u such that

$$\frac{u}{z} = -exy^2 + k - kfz^3/24\nu + O(r^4). \quad (14.2)$$

(14.1) with the first replaced by (14.2) is a local solution satisfying the Navier-Stokes and continuity equations to $O(r^3)$. It has a region of validity near the origin.

This solution has the character of an open SSB. Putting

$$g=0, \quad a^2 = -\frac{f}{e} > 0 \quad , \quad b^3 = \frac{k}{e} > 0 \qquad \text{——— (14.3)}$$

the WSL's may be obtained from

$$\left(\frac{dy}{dx}\right)_{WSL} = \frac{v}{u} = \frac{y\,(x^2-a^2)}{b^3 - xy^2} \qquad \text{——— (14.4)}$$

This WSL field has two critical points at

$$(x, y) = \left(a, \pm\sqrt{b^3/a}\right). \qquad \text{——— (14.5)}$$

They are either saddles or vortical nodes, depending on whether b^3/a^3 being greater or smaller than 16. They lie outside the region of validity of the solution. The diagram shows the WSL solution for $a=b=0.5$. Note that the WSL convergence rate increases smoothly from 0 at the left to larger values at the right, corresponding to open separation.

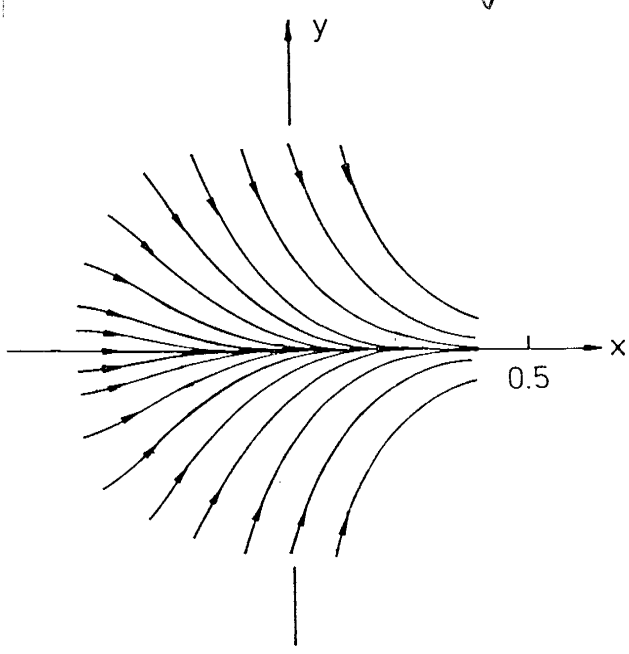

Wall streamlines near the beginning of a smoothly starting negative bifurcation line; numerical integration of equation (5) with a=0.5, b=0.5

When is a three-dimensional flow separated?

This question may be seen to become important in the light of the features of open separation. The degree of convergence of the wall streamlines (b_2/k) is clearly a measure of the ~~degree~~ of divergence ~~of the~~ from the wall of the streamlines in the separated sheet $\left(\frac{b_2}{2k}\right)$. A small value of b_2/k therefore merely corresponds to a small thickening of the boundary layer above the SSB line. Conversely, if b_2/k is large the distance to which vortical fluid is carried away from the wall becomes large. Hence one has to make some kind of a convention about the point at which a WSL convergence is to be called separation, and where it is agreed to be only a local thickening of the boundary layer.

A sensible definition appears to be one in which the length k/b_2 is compared to a characteristic length of the body, L. Thus, one might define a flow where

$$\frac{L b_2}{2k} \geq 1 \qquad (14.6)$$

as separated, while lower values correspond

to mere boundary layer thickening. The number on the right of (14.6) is arbitrary and a different value might be more suitable. A threshold of separation of this kind is necessary, however.

This difficulty of definition does not arise in two-dimensional flow, though, of course, it would be sensible to make the distinction there too. This is because small separation bubbles are unimportant in the global flow field (unless they lead to transition).

15. Higher-order solutions

Local solutions of the Navier-Stokes and continuity equations in terms of generalized Taylor series expansions have a limited range of validity. It is possible to increase the range of validity or to increase the degree of complexity of the flow that can be represented, by increasing the order. It is convenient for this purpose to use the tensor notation for the equations:

$$u_q \frac{\partial u_i}{\partial x_q} = -\frac{\partial P}{\partial x_i} + \nu \frac{\partial^2 u_i}{\partial x_q \partial x_q} \qquad (15.1)$$

$$\frac{\partial u_i}{\partial x_i} = 0 \qquad (15.2)$$

and to expand the velocity as

$$u_i = A_i + A_{ij} x_j + A_{ijk} x_j x_k + A_{ijkl} x_j x_k x_l + \dots \qquad (15.3)$$

(15.3) may now be substituted into (15.1) and (15.2) and coefficients of like powers of terms may be summed and equated to zero. This yields a large number of coefficient equations.

The properties of the equations are such as to make the coefficients symmetrical with respect to all the indices except the first.

I.e.:

$$A_{ijkl} = A_{ilkj} = A_{ikjl} \qquad (15.4)$$

etc. A consequence is that the expansion (15.3) may be written as

$$u_i = \sum_{n=0}^{N} R A_{i111\ldots,222\ldots,333\ldots} x_1^a x_2^b x_3^c \qquad (15.5)$$

where $(a+b+c) = n$ in all possible permutations, with a, b, c non-negative integers. R is the number of possible permutations of the indices in $(111\ldots, 222\ldots, 333\ldots)$ 1 being repeated a times, 2 b times, 3 c times.

Possible combinations of powers	Possible permutations of powers	Terms generated
3	003	$A_{i333}\, x_1^0 x_2^0 x_3^3$
	030	$A_{i222}\, x_1^0 x_2^3 x_3^0$
	300	$A_{i111}\, x_1^3 x_2^0 x_3^0$
12	012	$\left.\begin{array}{l} A_{i233}\, x_1^0 x_2^1 x_3^2 \\ + A_{i323}\, x_1^0 x_2^1 x_3^2 \\ + A_{i332}\, x_1^0 x_2^1 x_3^2 \end{array}\right\} = 3A_{i233}\, x_1^0 x_2^1 x_3^2$
	021	$\left.\begin{array}{l} A_{i223}\, x_1^0 x_2^2 x_3^1 \\ + A_{i232}\, x_1^0 x_2^2 x_3^1 \\ + A_{i322}\, x_1^0 x_2^2 x_3^1 \end{array}\right\} = 3A_{i223}\, x_1^0 x_2^2 x_3^1$
	102	$\left.\begin{array}{l} A_{i133}\, x_1^1 x_2^0 x_3^2 \\ + A_{i313}\, x_1^1 x_2^0 x_3^2 \\ + A_{i331}\, x_1^1 x_2^0 x_3^2 \end{array}\right\} = 3A_{i133}\, x_1^1 x_2^0 x_3^2$
	120	$\left.\begin{array}{l} A_{i122}\, x_1^1 x_2^2 x_3^0 \\ + A_{i212}\, x_1^1 x_2^2 x_3^0 \\ + A_{i221}\, x_1^1 x_2^2 x_3^0 \end{array}\right\} = 3A_{i122}\, x_1^1 x_2^2 x_3^0$
	201	$\left.\begin{array}{l} A_{i113}\, x_1^2 x_2^0 x_3^1 \\ + A_{i131}\, x_1^2 x_2^0 x_3^1 \\ + A_{i311}\, x_1^2 x_2^0 x_3^1 \end{array}\right\} = 3A_{i113}\, x_1^2 x_2^0 x_3^1$
111	111	$\left.\begin{array}{l} A_{i123}\, x_1^1 x_2^1 x_3^1 \\ + A_{i132}\, x_1^1 x_2^1 x_3^1 \\ + A_{i213}\, x_1^1 x_2^1 x_3^1 \\ + A_{i231}\, x_1^1 x_2^1 x_3^1 \\ + A_{i312}\, x_1^1 x_2^1 x_3^1 \\ + A_{i321}\, x_1^1 x_2^1 x_3^1 \end{array}\right\} = 6A_{i123}\, x_1^1 x_2^1 x_3^1$

To illustrate this, with $n=3$, $a+b+c=3$ the scheme to the left shows the possible terms at order $n=3$. Thus the contribution from $n=3$ may be written as

$$u_i[3] = A_{i333}(003) + A_{i222}(030) + A_{i111}(300) + 3\{A_{i233}(012) + A_{i223}(021) + A_{i133}(102) + A_{i122}(120) + A_{i113}(201)\} + 6A_{i123}(111) \qquad (15.6)$$

Chong showed that, generally,

$$R = (a+b+c)!/(a!\,b!\,c!) \qquad (15.7)$$

The number of unknown + distinct coefficients at order n, say c_n, generated by the nth order term in u_i : i.e. by $u_i[n]$ is

$$c_n = 1, 3, 6, 10, 15, 21 \ldots \qquad (15.8)$$

for $n = 1 \ldots 5$, for each value of i.

<u>Continuity</u>:

Differentiating (15.3) w.r.t. x_i,

$$\frac{\partial u_i}{\partial x_i} = A_{ii} + (A_{iji}x_j + A_{ijk}x_k)$$
$$+ (A_{iikl}x_k x_l + A_{ijil}x_j x_l + A_{ijki}x_j x_k)$$
$$+ \ldots = 0 \quad \text{by continuity.} \qquad (15.9)$$

Since each of the powers of the coordinates must separately vanish as $r \to 0$, each of the brackets in (15.9) may separately be equated to zero. Also, since the indices that are repeated between the coefficients and the coordinates are dummy indices, sums such as

$$A_{ii\alpha\beta} + A_{i\alpha i\beta} + A_{i\alpha\beta i} = 0 \qquad (15.10)$$

may be set $= 0$. Writing this out long-hand,

$$A_{11\alpha\beta} + A_{22\alpha\beta} + A_{33\alpha\beta} + A_{1\alpha1\beta} + A_{2\alpha2\beta} + A_{3\alpha3\beta}$$
$$+ A_{1\alpha\beta1} + A_{2\alpha\beta2} + A_{3\alpha\beta3} = 0. \qquad (15.11)$$

The symmetry properties of A_{ijkl} finally gives

$$3A_{11\alpha\beta} + 3A_{22\alpha\beta} + 3A_{33\alpha\beta} = 0 \qquad (15.12)$$

(15.9) ~~(220)~~ generates 9 equations 3 of which are redundant because of the symmetry properties.

In general

n	no of "continuity eqns".
0	0
1	1
2	3
3	6
4	10
⋮	⋮

In a similar way, the substitution of u_i into the Navier-Stokes equation and summing of powers of like order gives a large number of coefficient equations. The analysis is omitted here. The following table indicates the manner in which the no. of coefficients

and the no. of equations increases with the order included.

N	N_c	E_c	E_{NS}	E_{NSp}	E_E
1	12	1	3	—	3
2	30	4	3	3	3
3	60	10	3	11	11
4	105	20	11	26	26
5	168	35	26	50	50
6	252	56	50	85	85
7	360	84	85	133	133

$N =$ order of expansion.

$N_c =$ no. of distinct unknown coefficients

$E_c =$ no of coefficient equations from (C)

$N_{NS} =$ no. of coeff. eqns. from Navier Stokes

$N_{NSp} =$ no of coeff. equations from potl. flow NS

$E_E =$ no. of ~~Euler equations~~ coefficient eqns gen. from Euler

<u>Unsteady terms</u>

Since the partial derivative w.r.t time of u_i

$$\frac{\partial u_i}{\partial t} = \dot{A}_i + \dot{A}_{ij} x_j + \dot{A}_{ijk} x_j x_k + \dots \qquad (15.73)$$

may be used in the equations of motion, and the A's may be considered to be

functions of time $A_{\cdots} = A_{\cdots}(t)$, it is possible to obtain the coefficient equations not as simply algebraic equations but as first order differential equations w.r.t. time. This allows time-dependence to be included in such flow patterns as may be analysed by local methods.

The remainder of this chapter will now be devoted to examples obtained by Perry and his colleagues and students by just stating the results.

<u>Inviscid vortical flow with unsteady stretching</u>

(First order)
Stretching along x_3

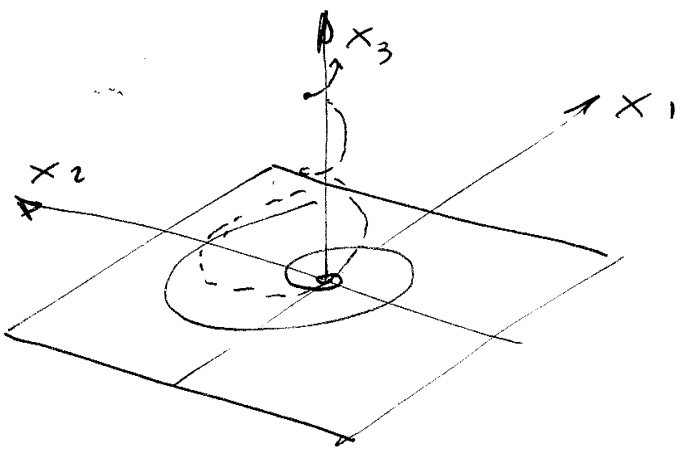

$$\begin{bmatrix} u_1 \\ u_2 \\ u_3 \end{bmatrix} = \begin{bmatrix} -A & -ke^{2At} & 0 \\ ke^{2At} & -A & 0 \\ 0 & 0 & 2A \end{bmatrix} \begin{bmatrix} x_1 \\ x_2 \\ x_3 \end{bmatrix} \quad (15.14)$$

This is stretching along the direction of the vorticity, such that the vorticity increases exponentially. A consequence of ~~[illegible]~~ constant strain rate.

Stretched viscous vortex

$$\begin{bmatrix} u_1 \\ u_2 \\ u_3 \end{bmatrix} = \begin{bmatrix} -a & -b & 0 \\ b & -a & 0 \\ 0 & 0 & 2a \end{bmatrix} \begin{bmatrix} x_1 \\ x_2 \\ x_3 \end{bmatrix} + \frac{ab}{4\nu} \begin{bmatrix} x_1^2 x_2 + x_2^3 \\ -(x_1^3 + x_2^2 x_1) \\ 0 \end{bmatrix} \qquad (15.15)$$

This is a steady flow. The stretching along the x_3 axis which, in inviscid flow, would increase the vorticity, is balanced by a diffusion of vorticity away from the x_3 axis. I.e. the vorticity varies with $\sqrt{x_1^2 + x_2^2}$. The x_3 component of vorticity is the only non-zero component.

Open stream surface bifurcation

$$\begin{bmatrix} u_1 \\ u_2 \\ u_3 \end{bmatrix} = z \begin{bmatrix} -exy^2 + k - kfz^3/24\nu \\ fy + ex^2 y \\ -f\frac{z}{2} - ex^2\frac{z}{2} + ey^2\frac{z}{2} \end{bmatrix} \qquad (15.16)$$

See last chapter.

These and many more have been obtained by Perry and Chong, who also made movies of solutions that are time-depen

dent, thus solving the problem of three-dimensional unsteady separated flow. (see steady solns in diagrams)

The prospect offered by patching

It is clear that such local solutions to higher order may also be regarded as the building blocks of a numerical scheme in a similar fashion as the simple first order expansion term is usually used in a linear approximation of finite difference equation. This has so far not been done, though the success of a similar attempt in an experimental fit is highly successful: A coflowing wake measured by Perry and Tan (see next page) shows this effectively.

Literature:

Oswatitsch K. IUTAM Symp. Freiburg 1957
Perry A.E. DFVLR-FB 84-36, 1984
Hornung AGARD CP 342 1983
Perry + Tan J Fluid Mech 141 (1984)
Lighthill (see Rosenhead, Laminar b.l.'s)
Horing + Perry ZFW 8 1984 pp. 77-87, 155-160
Ladyzhenskaya Ann Rev FM 7 1975
Perry A.E. DFVLR FB 84-34 1984

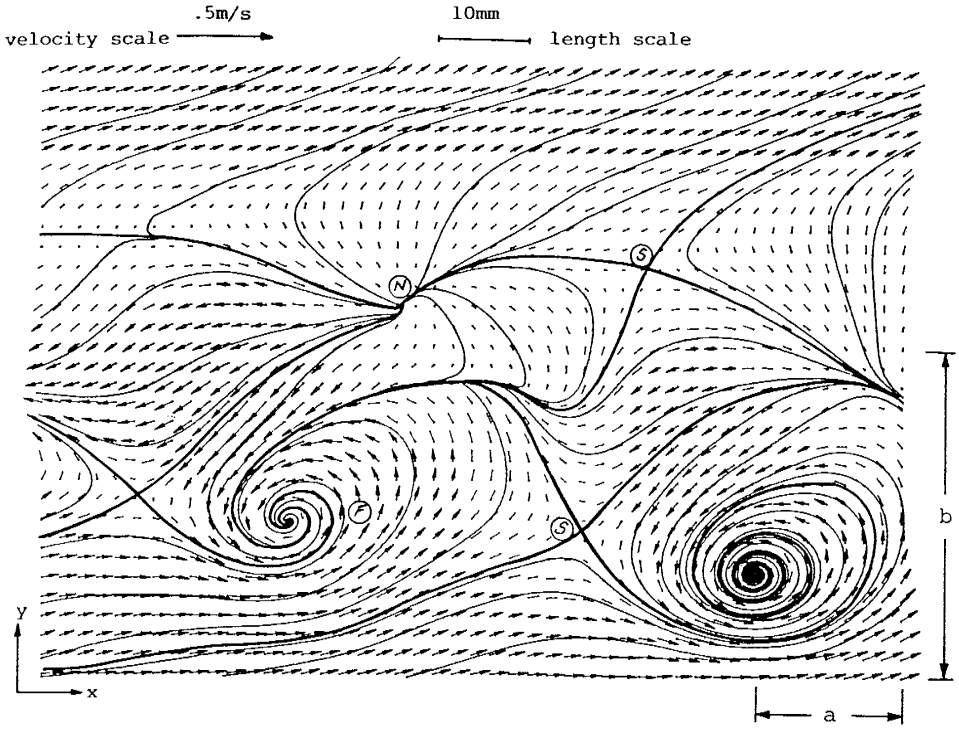

Fig. 1 Coflowing wake structures of Perry and Tan [4]. Instantaneous vector field determined by experiment is shown. Streamlines were determined by integrating a two-dimensional 5th order Taylor series expansion fit to the data in overlapping tiles dimensioned a×b. Pattern is as seen by an observer moving with the eddies.

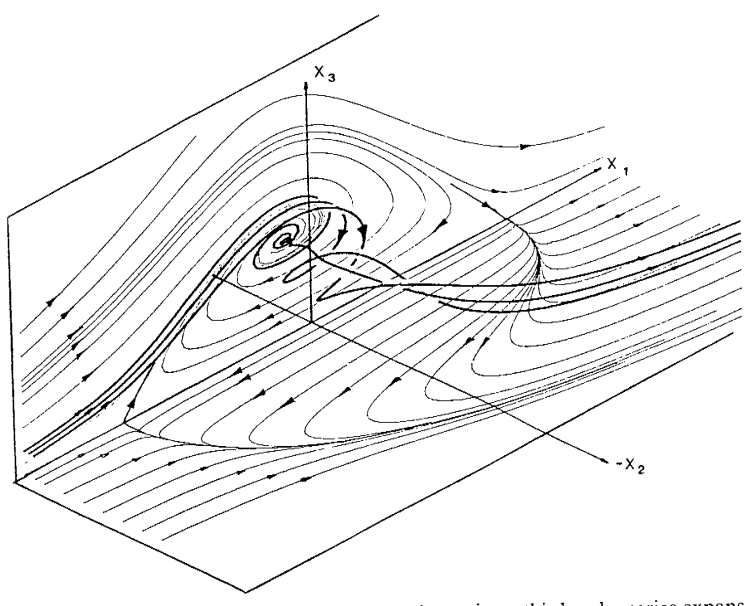

Figure 23 A computed simple U-shaped separation using a third-order series expansion.

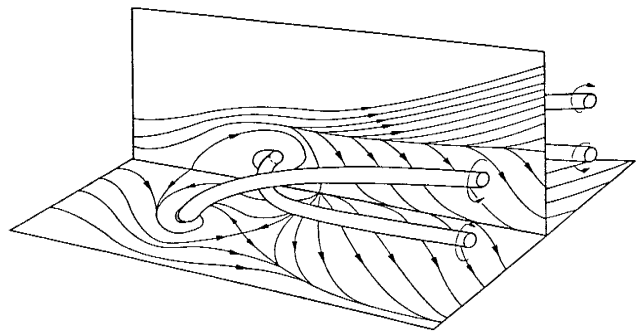

Figure 22 One possible vortex skeleton for an owl-face of the second kind. Image vortices under the horizontal surface are not shown.

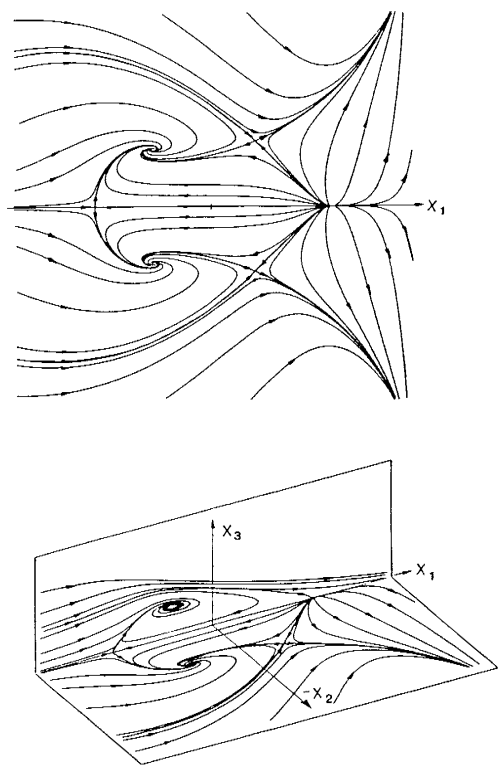

Figure 24 A computed owl-face of the second kind using a fourth-order series expansion. (*top*) Limiting streamlines on the surface, i.e. x_1x_2 plane. (*bottom*) Oblique view of the pattern.

16 Shock wave boundary layer interaction

Many features of incompressible flow boundary layer theory carry over into compressible flow boundary layers. A proper treatment would require a discussion of compressible flow boundary layers but this is omitted here for time limitation reasons. The most important new effect due to compressibility is that caused by the almost infinite pressure gradient experienced by a boundary layer when it has to negotiate a shock wave. An example is the termination of the supersonic region of a transonic flow over a wing by a shock that intersects the boundary layer on the wing.

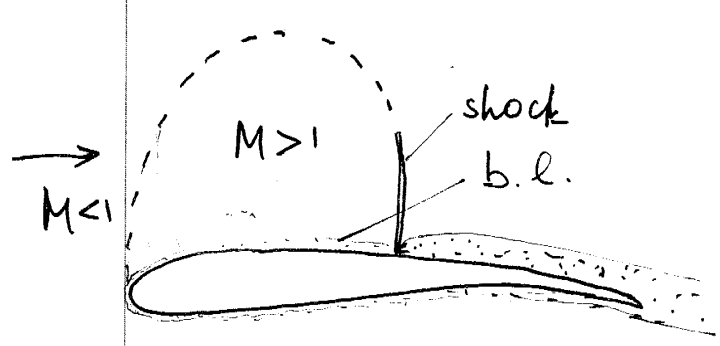

Another example is that of a concave corner in supersonic flow. When the shock wave in either of these two cases is sufficiently strong, it causes the boundary layer to separate.

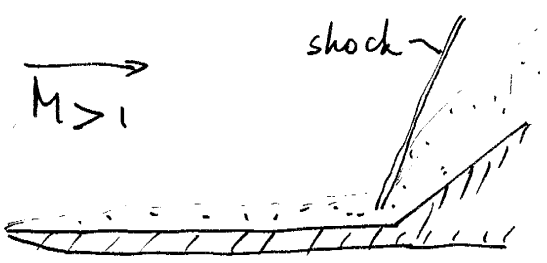

Without going into details of the vast literature of shock boundary layer interaction, this chapter gives a somewhat unorthodox and superficial treatment.

To introduce this, consider the upstream influence of a concave corner in supersonic flow. Outside the b.l. the flow is supersonic and upstream influence is not possible unless it occurs via the subsonic part of the boundary layer flow. Idealize the flow

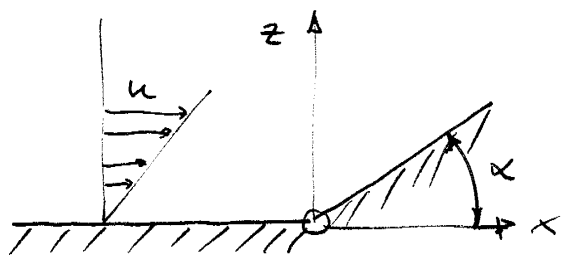

in the immediate vicinity of the corner as a simple shear flow with $\frac{\partial u}{\partial z} = \omega$ and introduce $P_x = \frac{1}{\rho}\frac{\partial p}{\partial x}$. $\left[\frac{L}{T^2}\right]$

This depends on the variables

$$P_x = P_x(\omega, \alpha, x).$$

Dimensional analysis gives

$$\frac{P_x}{\omega^2 x} = f(\alpha).$$

For fixed α, this integrates to

$$P = P_0 - k\omega^2 x^2 \qquad (1.1)$$

where $k = -f(\alpha)$ is a constant.

Thus the pressure has a parabolic maximum at the corner. This gives the characteristic length of the upstream influence as

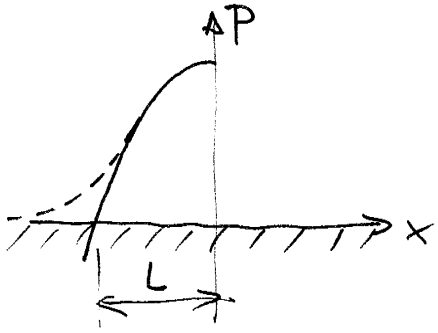

$$L = \frac{\sqrt{P_0}}{\omega} \doteq \frac{\sqrt{p_0/\rho}}{\omega} \sim \frac{a}{\omega} \qquad (16.2)$$

where a is the local speed of sound. Rewriting this in terms of the usual dimensionless numbers,

$$L \sim \frac{a}{\omega} = \frac{a}{\partial u/\partial z} = \frac{\rho a \nu}{\tau_w} = \frac{\rho a \nu}{\frac{1}{2}\rho U^2 C_f} = \frac{2\nu}{U M C_f} \qquad (16.3)$$

or

$$\boxed{\frac{LU}{\nu} \sim \frac{1}{M C_f}} \qquad (16.4)$$

The Reynolds number based on the characteristic length of the upstream influence is related to the Mach number of the flow and the skin friction coefficient of the arriving boundary layer. This crude argument gives a surprisingly useful rule of thumb. For example, the upstream influence in laminar boundary layers extends to approximately 10 b.l. thicknesses, while L is approximately equal to the

b.l. thickness of a turbulent layer. Also, for a given Mach number expect the C_f-Re relation to translate into a (LU/ν)-Re relation as shown.

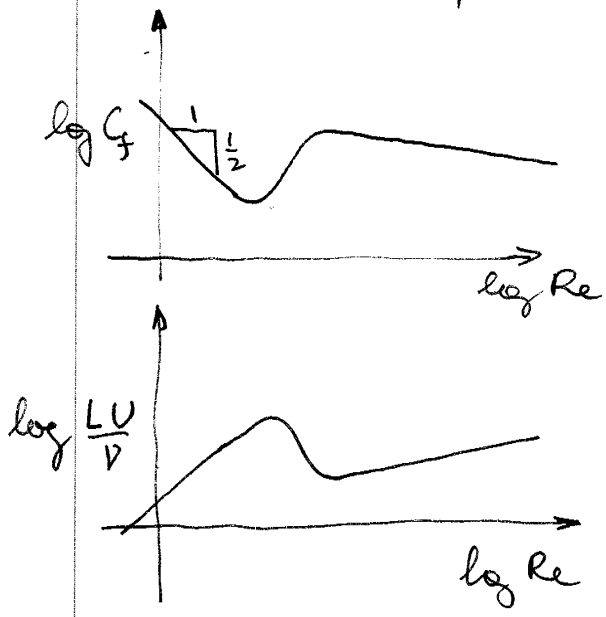

Shock induced separation

For the definition of some concepts consider the qualitative behaviour of the pressure distribution with increasing α.

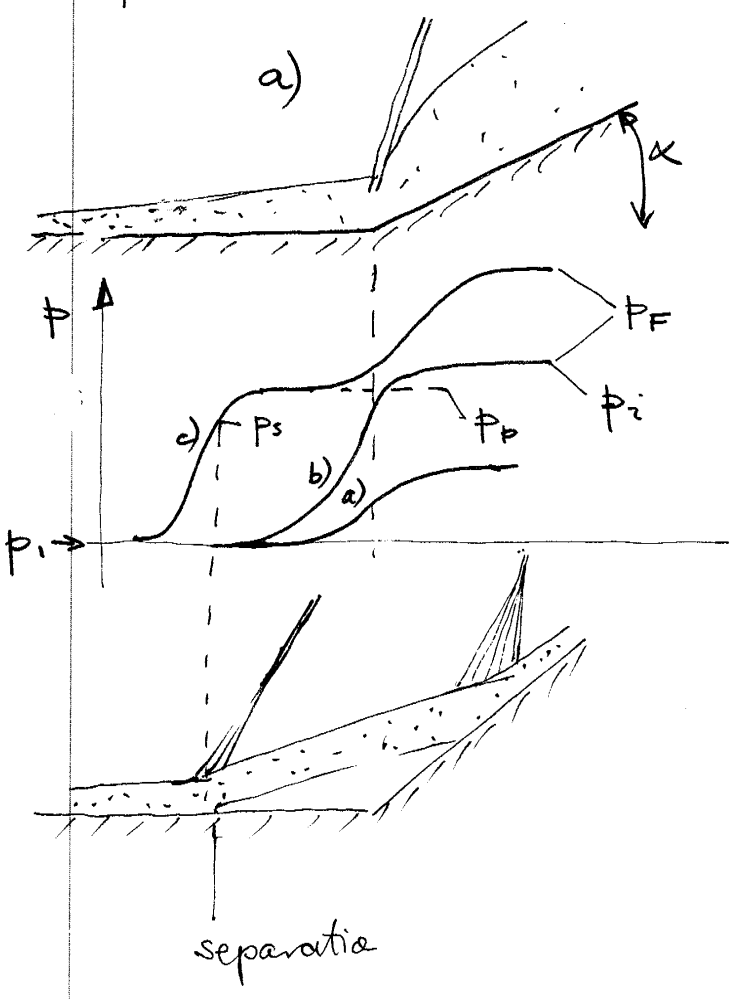

At small α the b.l. remains attached, but the pressure rises upstream of the corner (a). As α is increased, the incipient separation b) is reached, where the pressure rise is just insufficient to cause separation. Further increase of α causes a sepa-

ration bubble to appear, with an associated pressure plateau p_P, see c). This is accompanied by the appearance of a second shock wave at the reattachment point.

An approximate analysis of Chapman Kuehn and Larson also leads to C_f as a key quantity in shock boundary layer interaction: If the deflection angle at the separation point is sufficiently small, the linear theory should apply and

$$\frac{p - p_1}{\frac{1}{2}\rho_1 U_1^2} = \frac{2}{\sqrt{M_1^2 - 1}} \frac{d\delta^*}{dx} \qquad (16.5)$$

where δ^* is the displacement thickness of the b.l. Assume the upstream influence range to be L. Thus the order of magnitude of the pressure rise to separation is

$$\frac{p_s - p_1}{\frac{1}{2}\rho_1 U_1^2} \doteq \frac{2}{\sqrt{M_1^2 - 1}} \frac{\delta^*}{L}$$

Also, since $\frac{dp}{dx} = \left(\frac{\partial \tau}{\partial z}\right)_w$ or $\frac{p_s - p_1}{L} \doteq \frac{\tau_w}{\delta^*}$

$$\boxed{\frac{p_s - p_1}{\frac{1}{2}\rho_1 U_1^2} \sim \frac{\sqrt{C_f}}{(M_1^2 - 1)^{\frac{1}{4}}}} \qquad (16.6)$$

Note that this result gives

$$\frac{L}{\delta^*} \sim \frac{1}{\sqrt{C_f M_1}} \quad . \quad \text{for large } M_1$$

Experimental correlations by Roshko and Thomke also show that it is best to use C_f and M as independent variables in the correlation of shock b.l. interaction phenomena.

The separated length also decreases when the flow is turbulent. Needham's correlation shows this best and exhibits a remarkable similarity to the sketch on p. 148.

$$\frac{L_{sep} M_1^3}{x_0 \left(\frac{p_3}{p_2}\right)^2}$$

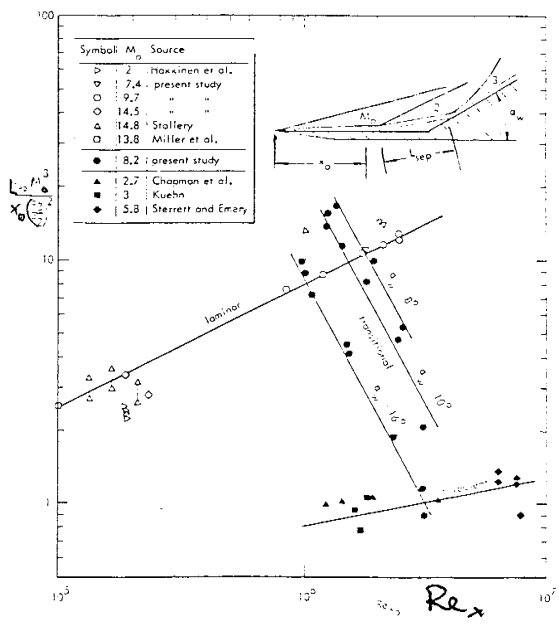

Clearly, $1/C_f$ is a dominant characteristic in this upstream influence range, and bridges the question of laminar or turbulent boundary layer.

The characteristics of the flow pattern

for laminar and turbulent b.l. do differ however. This is illustrated in the sketches.

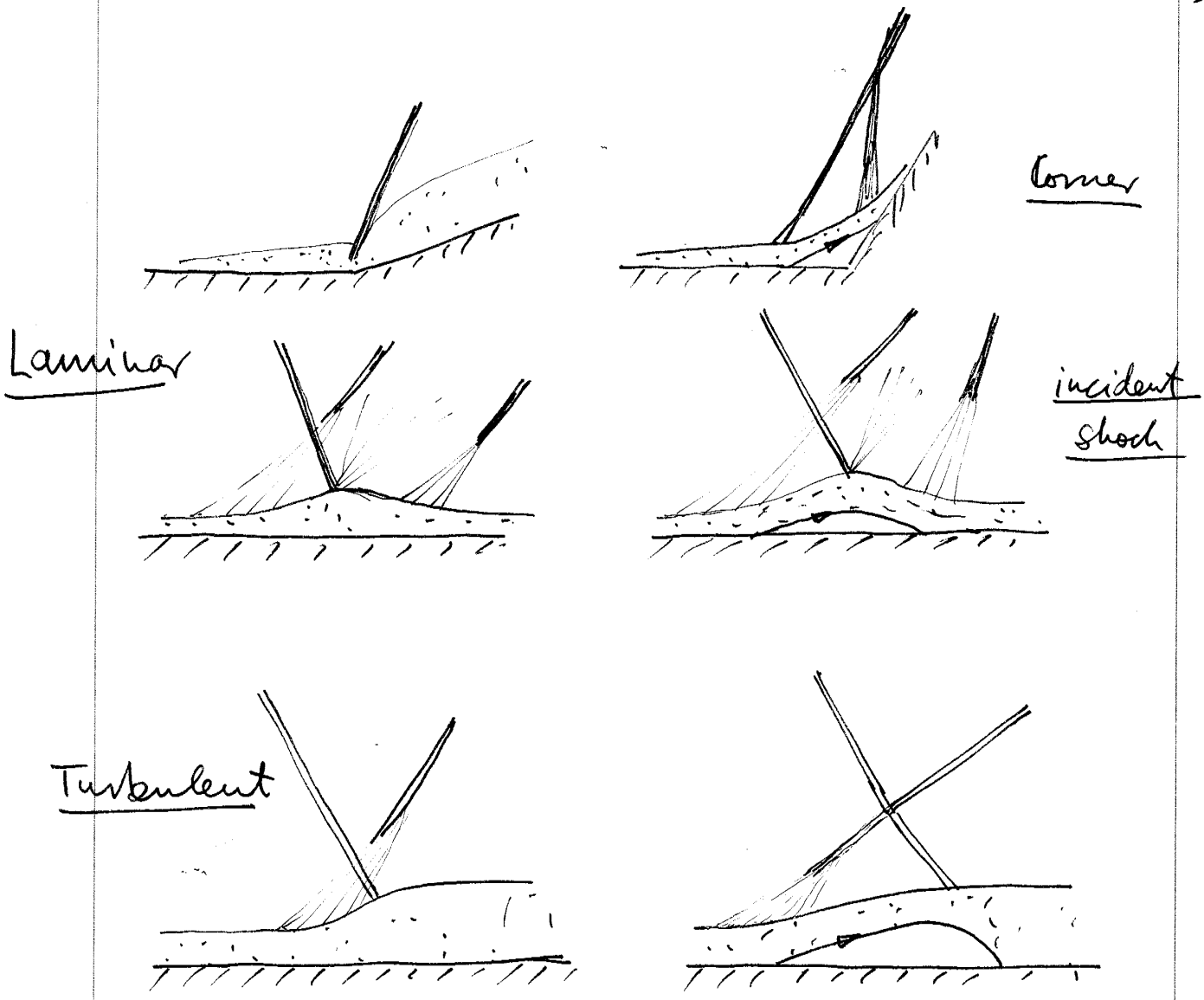

In laminar shock induced separation two reflected shocks can usually be easily resolved. In turbulent shock induced separation only one reflected shock occurs, because the separated region remains short.

1. Show that the two forms of the energy equation

$$\rho \frac{Dh_0}{Dt} = \frac{\partial p}{\partial t} + \operatorname{div}\left(\underset{\approx}{T}\,\underset{\sim}{u}\right) + \rho\left(\underset{\sim}{u}\cdot\underset{\sim}{f}\right) - \operatorname{div}\underset{\sim}{q}$$

and $\rho T \dfrac{Ds}{Dt} = \operatorname{tr}\left(\underset{\approx}{T}\,\underset{\approx}{D}\right) - \operatorname{div}\underset{\sim}{q}$

are equivalent.

2. Show that in simple shear flow the frictional stress is spatially uniform for all fluids. Does this include turbulent flow? Discuss.

3. Show that a fluid can only be at rest in a conservative force field.

In two-dimensional steady separated flow a half-saddle point in the streamline configuration is of fundamental importance. In general, this half-saddle point is not symmetrical, i.e. the separation streamline may leave the wall at an angle different from $\pi/2$.

a) Show that, in potential flow, the separatrices of a simple half-saddle are normal to each other, and that the angles between separatrices are equal in a higher-order half-saddle.

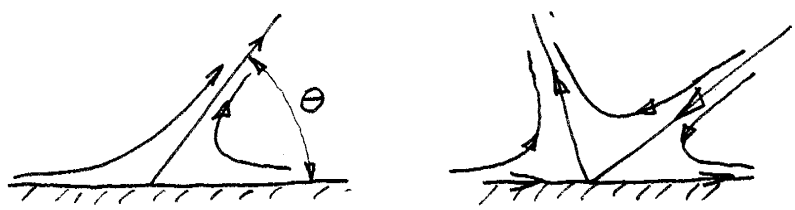

simple higher order

b) Determine the conditions under which the angle θ (see a)) is not $\pi/2$. Derive a relation between θ and the magnitude of the quantity that needs to be introduced.

c) Show that the pressure reaches a maximum at a half-saddle point.

1. Consider a smooth 90° bend of a two-dimensional channel. Let the flow through this bend be incompressible and at constant density as well as steady. Consider the pressure field on the outside wall and on the inside wall. Deduce where separated flow might be encountered and sketch the pressure distributions with and without separation. Give careful arguments for your results. How do you expect the ratio of channel width to curvature radius to affect the flow pattern? Why? Discuss the effect of Reynolds number.

2. Find the angle between the eigenvectors of critical points in the wall streamline field as functions of tr and det. Relate these two quantities to the components of the wall shear stress vector and their space derivatives. Find the points in (tr, det) space where
   - a symmetrical saddle
   - a symmetrical centre

   occurs.

3. Equation (12.4) represents an expansion

suitable for the velocity field near a critical point at which the no-slip condition applies in the (x,y) plane. This allows some of the third-order terms to be introduced in terms of the expansion in equation (12.1). Which ones are these? At which order of equation (12.5) will the non-linear terms of the Navier-Stokes equation begin to play a part?

4. Discuss how the removal of the no-slip condition would influence the form of the expansion near a critical point [Applies to critical point away from the wall]. Determine the meaning of the elements of the coefficient matrix of the first term in the expansion in that case. Determine the eigenvalues of the coefficient matrix and classify the critical points according to their location in the corresponding (tr, det)-space.

Analyse the problem of irrotational critical points for which the second alternative of the two possibilities available after eqn. (12.28) has to be taken.

Discuss the possible flow patterns that are available, by delineating forbidden regions of the (tr, det) space for the special planes.